ELSEVIER

Physica B 270 (1999) 172–220

PHYSICA B

Magnetopolarons in quasi-one-dimensional quantum-well wires

L. Wendler*

Anna-Siemsen-Straße 66, D-07745 Jena, Germany

Received 19 May 1998; received in revised form 7 October 1998; accepted 22 December 1998

Abstract

The interaction of quasi-one-dimensional electrons and longitudinal-optical (LO) phonons in the presense of a quantizing magnetic field is calculated. Results are detailed presented for the polaron correction to the subband energies, the polaron cyclotron mass and the polaron effective mass. The calculations are done by using different approaches, Rayleigh–Schrödinger perturbation theory, Wigner–Brillouin perturbation theory, improved Wigner–Brillouin perturbation theory and Green's function technique. In the framework of a diagrammatic approach a modified Hartree–Fock approximation is developed, which allows the calculation of the quasi-particle properties of lower-dimensional semiconductor nanostructures in the subband space. It is shown that the Rayleigh–Schrödinger perturbation theory, improved Wigner–Brillouin perturbation theory and the modified Hartree–Fock approximation well describe the ground-state renormalization, but only the improved Wigner–Brillouin perturbation theory and the modified Hartree–Fock approximation well describe the bend-over and pinning behaviour of the subbands at the boundary of the phonon continuum. Rayleigh–Schrödinger and Wigner–Brillouin perturbation theories fail for the calculation of the renormalization of the excited subband energies in quantum-well wires with strong confining potential even for vanishing magnetic field and polaron momentum. In addition to the symmetric scattering processes, which are the only processes involved in the self-energy of the old-fashioned perturbation theories, Green's function technique allows also to calculate the contribution of all asymmetric scattering processes of two electrons by exchanging an optical phonon.

PACS: 71.38. + i; 71.50; 71.70

Keywords: Electron–phonon interaction; Polaronic self-energy; Quasi-one-dimensional electron system; Many-particle Green's function technique

1. Introduction

The rapid growth of the science of nanostructures is having a considerable impact on physics, because these structures exhibit qualitatively new phenomena, and on electrical engineering, because they have

* Tel.: + 49-3641-608757.
E-mail address: wendler@pinet.uni-jena.de (L. Wendler)

0921-4526/99/$ - see front matter
PII: S0921-4526(99)00074-5

applications to the electronic devices of the future. This developement was made possible by the availability of semiconducting materials of unprecedented purity and crystalline perfection. Such multilayered systems can be structured to contain a thin layer of highly mobile electrons. Motion perpendicular to this layer is quantized, so that the electrons are constrained to move in a plane parallel to the heterointerfaces. Such *quasi-two-dimensional* (Q2D) *systems* are typified by an energy spectrum consisting of discrete levels in growth direction, the electric *subbands*, with typical energy separations of $\Delta\mathscr{E} \approx 20$–$200$ meV for electrons, and a free motion dispersion parallel to the heterointerfaces. This *quasi-two-dimensional electron gas* (Q2DEG) combines a number of desirable properties. Typically the Fermi wavelength is comparable to the dimension of the structures and the elastic mean free path can be quite large, exceeding the typical length scale of the samples. Thus, the electrons behave ballistical and size-quantization effects become important.

One of the challenging topics of the current interest involves systems of further reduced dimensionality. Among them, Q1D *quantum-well wires* (QWWs) play an important role. QWWs have been prepared by starting from Q2D heterosystems employing nanometer techniques or directly by molecular-beam epitaxy, using macrosteps on semiconductor surfaces.

Many of the currently studied semiconductor structures are based on III–V compounds that are weakly polar. Electrons moving through such crystals polarize its surroundings and hence, couple to this self-induced polarization field. This dielectric polarization field is connected with the vibration of the solid in an optical mode. Because only long-wavelength optical phonons are accompanied by large electric dipole moments, only these phonons interact with the electrons. In polar 3D bulk semiconductors the electrons only interact with the *longitudinal-optical* (LO) phonons. The *electron–phonon interaction* (EPI) has the following effect on the electrons: A quasi-particle, called *polaron* is formed [1–7], consisting of an electron and its surrounding phonon cloud (lattice distortion). Polarons behave quite differently from conduction-band electrons. The polaron concept was introduced firstly by Landau [1]. Subsequently, Landau and Pekar [3–5] investigated the physical properties of polarons. In the today's terminology these first studies were all devoted to the *strong-coupling theory*. The standard field-theoretical Hamiltonian describing the interaction of electrons with the long-wavelength optical phonons was firstly derived by Fröhlich, who showed the need for a *weak-coupling theory*. This theory was provided by Fröhlich and co-workers [6,7]. The most natural approach of the Fröhlich polaron theory is to treat the interaction as a small perturbation. For $\alpha_p \ll 1$, with α_p the dimensionless 3D polaron coupling constant, this leads to (for reviews of the earlier work see e.g. [8,9]):

1. A *shift in the energy*: $\mathscr{E}_{3D}(\boldsymbol{k}) = \hbar^2\boldsymbol{k}^2/(2m_e) \to E_{3D}(\boldsymbol{k}) = \mathscr{E}_{3D}(\boldsymbol{k}) + \Delta E_{3D}(\boldsymbol{k})$, where for the ground-state renormalization $\Delta E_{3D}(0) = -\alpha_p\hbar\omega_L$ is valid, with $\hbar\omega_L$ the energy of the LO phonon [7].
2. A *mass renormalization*: $m_e^*/m_e = (1 - \alpha_p/6)^{-1}$, where m_e is the effective conduction-band-edge mass and m_e^* is the polaron mass [7].
3. A *polaron induced nonparabolicity*: $\frac{3}{40}\frac{\alpha_p}{\hbar\omega_L}(\frac{\hbar^2\boldsymbol{k}^2}{2m_e})^2$ for small 3D wave vectors $\boldsymbol{k} = (k_x, k_y, k_z)$ [7].
4. The energy–momentum relation $E_{3D}(\boldsymbol{k})$ is a single-valued continuous function for all $\boldsymbol{k}$, which *bends over* if the polaron kinetic energy approaches the LO phonon energy above the correct ground-state, i.e. $E_{3D}(\boldsymbol{k})$ exists above and below this line but shows a discontinuous derivative at $E_{3D}(\boldsymbol{k}) = E_{3D}(0) + \hbar\omega_L$ [10,11].

Cyclotron resonance (CR) is the mostly used standard technique for the determination of the mass of electrons and holes in solids. Thus, polarons are observed and studied experimentally in magnetic fields. *Polarons* ($B = 0$) and *magnetopolarons* ($B \neq 0$) have been studied extensively both theoretically and experimentally in 3D bulk systems [8,9]. The applied magnetic field quantizes the carrier motion in the plane perpendicular to the magnetic field into Landau levels $\mathscr{E}_N^{3D}(k_z) = \hbar\omega_c(N + 1/2) + \hbar^2k_z^2/(2m_e)$; $N = 0,1,2,\ldots$, separated by $\hbar\omega_c$, where $\omega_c = eB/m_e$ is the cyclotron frequency. In the presence of a magnetic field the quasi-particle *magnetopolaron* is formed with the following properties:

1. In the case of *weak magnetic fields*, i.e. if $\omega_c \ll \omega_L$ is valid and assuming $\alpha_p \ll 1$, to first order in α_p the energy shift is [12] $\Delta E_N^{3D} \equiv \Delta E_N^{3D}(0) = -\alpha_p \hbar\omega_L[1 + \frac{2N+1}{12}\frac{\omega_c}{\omega_L} + \frac{18N^2+18N-1}{240}(\frac{\omega_c}{\omega_L})^2 + \cdots]$ and the mass renormalization becomes [13] $m_c^*/m_e = [1 - \frac{\alpha_p}{6}(1 + \frac{9}{10}\frac{\omega_c}{\omega_L} + \frac{47}{84}(\frac{\omega_c}{\omega_L})^2 + \cdots)]^{-1}$, with m_c^* the *polaron cyclotron mass*, implying that the separation between the Landau levels becomes renormalized: $\omega_c^* = eB/m_c^* = (E_N^{3D} - E_{N-1}^{3D})/\hbar$, which gives $m_c^* = e\hbar B/(E_N^{3D} - E_{N-1}^{3D})$ and usually one detects the transition $E_0^{3D} \to E_1^{3D}$.
2. When $\omega_c \approx \omega_L$, i.e. for a *resonant magnetic field* $B_L \equiv m_e\omega_L/e$, the phenomena of level crossing would appear in the absence of EPI: the first excited Landau level with the energy $\mathscr{E}_1^{3D}(0) = \frac{3}{2}\hbar\omega_c$ becomes degenerate with the lowest Landau level plus one LO phonon with the energy $\frac{1}{2}\hbar\omega_c + \hbar\omega_L$. Due to the EPI these two levels split into two non-crossing levels $E_1^{3D\pm}$. This phenomenon is called *resonant magnetopolaron level coupling* (RMPLC) and the resulting quasi-particle is called *resonant magnetopolaron*. The renormalization of the lower level at the resonance calculated with degenerate perturbation theory, e.g. Wigner–Brillouin perturbation theory, is $\Delta E_1^{3D-} = -(\alpha_p/2)^{2/3}\hbar\omega_L$ in leading order of α_p [14,15]. The upper level E_1^{3D+} lies in the phonon continuum, which is above the threshold energy $E_{th} = \mathscr{E}_0^{3D}(0) + \Delta E_0^{3D} + \hbar\omega_L$, where even for $T = 0$ real LO phonons are present. The continuum of states exists because the optical phonon can take up any amount of momentum. In the lowest order of α_p the renormalization of the upper level at the resonance, calculated with Wigner–Brillouin perturbation theory, is $\Delta E_1^{3D+} = \sqrt{\pi}\frac{\alpha_p}{2}\hbar\omega_L$ [15]. Note that in the so-called *resonance approximation* [13] the splitting of all resonance-split levels becomes symmetrical around the unperturbed result [12,14]: $\Delta E_N^{3D\pm} = \pm[\alpha_p/(2N)]^{2/3}\hbar\omega_L$. Due to the presence of two branches one can define two different polaron cyclotron masses. When $B < B_L$ the transtion $E_0^{3D} \to E_1^{3D-}$ has the most oscillator strength in cyclotron resonance, which leads to a mass $m_c^{*-} > m_e$, which becomes m_e^* for $B = 0$. For $B > B_L$ most of the oscillator strength is transferred to the transition $E_0^{3D} \to E_1^{3D+}$, whose polaron cyclotron mass is $m_c^{*+} < m_e$ and approaches asymptotically m_e for $B \to \infty$. Right at the resonance ($\omega_c = \omega_L$) both masses are given by $m_c^{*\pm}/m_e = 1 \mp (\alpha_p/2)^{2/3}$ in the resonance approximation [12].
3. In the strong magnetic field limit, i.e. for $\omega_c \gg \omega_L$, the lower energy levels are pinned at the energy E_{th}. This result is only obtained with *improved* versions of the Wigner–Brillouin perturbation theory. Standard Wigner–Brillouin perturbation theory itselfs gives $E_N^{3D}(0) = \mathscr{E}_0^{3D}(0) + \hbar\omega_L - \frac{\alpha_p\hbar\omega_L}{4N^4}(\frac{\omega_L}{\omega_c})^2$, i.e. pinning at the unrenormalized lowest Landau level plus one LO phonon [12].
4. The energy–momentum relation $E_N^{3D}(k_z)$ bends over at E_{th} when calculated beyond Wigner–Brillouin perturbation theory. In difference to the case $B = 0$, for a non-vanishing magnetic field, the curve $E_N^{3D}(k_z)$ becomes pinned at this line having a *finite gap* for finite k_z [16], i.e. this branch has the property $E_N^{3D}(k_z) < E_{th}$ for finite k_z.

In general, polaronic effects in 3D bulk semiconductors are well described by one-polaron theories. This is valid because in undoped 3D bulk semiconductors the electron density is usually relatively small ($n_0 \approx 10^{13}\text{cm}^{-3}$ in GaAs) which leads to a Fermi energy $E_F \ll k_B T$, where k_B is the Boltzmann constant and the electrons satisfy Boltzmann statistics. The quantum confinement of the electrons in semiconductor nanostructures changes these properties considerably both quantitative and qualitative (see e.g. for 2D and Q2D systems [12,15,17–25], for Q1D systems [26–36] and for Q0D systems [37]). It is shown [37] that the polaronic effects increase as the dimensionality of the structure is reduced. For example in the case of a strict 2D electron system synthesized in a weakly polar semiconductor ($\alpha_p \ll 1$) the EPI leads to:

1. For weak magnetic fields applied perpendicular to the electron sheet the energy shift of each Landau level $\mathscr{E}_N^{2D} = \hbar\omega_c(N + \frac{1}{2})$ is $\Delta E_N^{2D} = -\alpha_p\hbar\omega_L\frac{\pi}{2}(1 + \frac{2N+1}{8}\frac{\omega_c}{\omega_L} + \frac{18N(N+1)+1}{128}(\frac{\omega_c}{\omega_L})^2 + \cdots)$ and the mass renormalization becomes $m_c^*/m_e = [1 - \alpha_p\frac{\pi}{8}(1 + \frac{9}{8}\frac{\omega_c}{\omega_L} + \frac{145}{128}(\frac{\omega_c}{\omega_L})^2 + \cdots)]^{-1}$ to first order in α_p [12,38,39].

2. For resonant magnetic fields the energy correction in the resonance approximation is $\Delta E_N^{2D\pm} = \pm \alpha_p^{1/2}\hbar\omega_L[(\pi/N)^{1/2}(2N-1)!!/(2^{N+1}N!)]^{1/2}$, where $(2N-1)!! = 1\cdot 3\cdot \cdots \cdot(2N-1) = (2N)!/2^N N!$; $(-1)!! = 1$ [12,17,39]. For strictly 2D systems in perpendicular magnetic fields the phonon continuum is absent because there is no dispersion in the problem. Near the resonance the polaron cyclotron masses of both branches are $m_c^{*\pm}/m_e = 1 \mp [\alpha_p(\pi^{1/2}/8)]^{1/2} + (\omega_L - \omega_c)/(2\omega_c)$ in the resonance approximation [39]. As in the 3D case when applying an improved version of Wigner–Brillouin perturbation theory the splitting is not symmetric [15,40].
3. For strong magnetic fields improved versions of Wigner–Brillouin perturbation theory give that the Landau levels become pinned at the line $E_0^{2D} + \hbar\omega_L$, whereas Wigner–Brillouin perturbation theory gives the wrong pinning at $\mathscr{E}_0^{2D} + \hbar\omega_L$ for $B \to \infty$: $E_N^{2D} = \mathscr{E}_0^{2D} + \hbar\omega_L - \alpha_p\hbar\omega_L \frac{\sqrt{\pi}(2N-1)!!}{2^{N+1}N!}\sqrt{\frac{\omega_L}{\omega_c}}$ [12].
4. For vanishing magnetic field, where $\mathscr{E}_{2D} = \mathscr{E}_{2D}(\boldsymbol{k}_{||}) = \hbar^2\boldsymbol{k}_{||}^2/(2m_e)$ is valid, the polaron induced non-parabolicity is $\frac{9\pi}{128}\frac{\alpha_p}{\hbar\omega_L}(\frac{\hbar^2\boldsymbol{k}_{||}^2}{2m_e})^2$ for small 2D wave vectors $\boldsymbol{k}_{||} = (k_x, k_y)$ [41].
5. For vanishing magnetic field the energy–momentum relation $E_{2D}(\boldsymbol{k}_{||}) = \mathscr{E}_{2D}(\boldsymbol{k}_{||}) + \Delta E_{2D}(\boldsymbol{k}_{||})$ calculated within an improved version of Wigner–Brillouin perturbation theory bends over at the line $E_{2D}(0) + \hbar\omega_L$ with $|\Delta E_{2D}(\boldsymbol{k}_{||})| \to \infty$ if $E_{2D}(\boldsymbol{k}_{||}) \to E_{2D}(0) + \hbar\omega_L$ [42]. Consequently, the line $E_{2D}(0) + \hbar\omega_L$ cannot be reached for finite values of $\boldsymbol{k}_{||}$ and thus $E_{2D}(\boldsymbol{k}_{||}) < E_{2D}(0) + \hbar\omega_L$ for finite $\boldsymbol{k}_{||}$. For $k_{||} = |\boldsymbol{k}_{||}| > k_L \equiv \sqrt{2m_e\omega_L/\hbar}$ there is another branch in the region $E_{2D}(\boldsymbol{k}_{||}) > E_{2D}(0) + \hbar\omega_L$ showing a back-bended curvature, so that $E_{2D}(\boldsymbol{k}_{||})$ is a three-valued function of $\boldsymbol{k}_{||}$ [42].

For true Q2D systems (see e.g. [15,21–23]) and Q1D systems (see e.g. [29,31,32]) the final results become more complex due to the subband structure. For Q1D magnetopolarons it depends on the ratio of the confinement energy to the phonon energy, whether a resonant magnetopolaron case is possible or not [29]. In general, in lower-dimensional semiconductor nanostructures the polaron theories become more complicated by many reasons. Whereas the electrons in 3D bulk systems only interact with LO phonons, in layered systems of polar materials the electrons interact with *modified* LO and *interface* phonons [43]. Both types of phonons are also present in QWWs [44–50]. The principal difficulty in calculating the optical phonons in QWWs is that the equation of motion and the boundary conditions for the phonons do not separate in general in these geometries. This is only the case for cylindrical QWWs [45,50]. In the case of QWWs with rectangular cross sections mostly ad hoc approximations have been used. It is shown [49,50] that for an electron, quantum confined in a cylindrical QWW, the total polaronic energy shift and scattering rate of modified LO and interface phonons is nearly the same as that for 3D bulk LO phonons if the width of the QWW is larger than 20 nm. Thus, the approximation of using 3D bulk LO phonons instead of the modified optical phonon spectrum provides good results for the todays typical QWWs if the effect of the EPI on the interested physical quantity occurs as the sum over all phonon states. Further, in most QWWs the lateral confinement of the electrons is realized by an electrostatic potential, created by a grating-type gate on top of the sample (field-effect devices). In these nanostructures there is no influence of interfaces in lateral direction on the spectrum of optical phonons and thus, one has the Q1D confined electron coupling to the optical phonons of stratified media [43]. In that what follows we apply this widely used approach of using 3D bulk LO phonons instead of using the modified spectrum of optical phonons [26–32].

The aim of the present paper is to calculate the influence of the magnetic field on the energy-momentum relations for polarons, quantum confined in QWW's. The theory of the dispersion relation of 3D bulk polarons has been given by Whitfield and Puff [10] and by Larsen [11]. Here, we use different approaches, Rayleigh-Schrödinger, Wigner-Brillouin and a modified improved Wigner-Brillouin perturbation theory of conventional quantum-mechanics, the Tamm-Dancoff approximation and a modified Hartree-Fock approximation of many-particle Green's function technique to calculate the magnetopolaron self-energy. The different results are analyzed and compared in detail.

2. Magnetopolaron Hamiltonian

The unperturbed system, a single electron in the presence of a quantizing perpendicular magnetic field is described in the effective-mass approximation by the Hamiltonian

$$H_e = \frac{\boldsymbol{\pi}_e^2}{2m_e} + V(\boldsymbol{x}) + \frac{g^*}{2}\mu_B \boldsymbol{B}\cdot\boldsymbol{\sigma}, \tag{1}$$

where

$$\boldsymbol{\pi}_e = \boldsymbol{p}_e + e\boldsymbol{A}(\boldsymbol{x}) \tag{2}$$

is the quasi-(or mechanical) momentum operator, which satisfies the commutation relations $[\pi_{e_x}, \pi_{e_y}] = (e\hbar/i)B_z(\boldsymbol{x})$, $[\pi_{e_y}, \pi_{e_z}] = (e\hbar/i)B_x(\boldsymbol{x})$, $[\pi_{e_z}, \pi_{e_x}] = (e\hbar/i)B_y(\boldsymbol{x})$; $[\pi_{e_x}, x] = [\pi_{e_y}, y] = [\pi_{e_z}, z] = (\hbar/i)$ and the other commutators between components of $\boldsymbol{\pi}_e$ and $\boldsymbol{x}$ are zero. Further, $\boldsymbol{p}_e = (\hbar/i)\nabla$ is the momentum operator of the electron with charge $-e$, which satisfies $[\boldsymbol{p}_e, \boldsymbol{A}(\boldsymbol{x})] = (\hbar/i)\nabla\cdot\boldsymbol{A}(\boldsymbol{x})$, where $\boldsymbol{A}(\boldsymbol{x})$ is the vector potential of the static magnetic field $\boldsymbol{B} = \nabla\times\boldsymbol{A}(\boldsymbol{x})$, m_e is the effective conduction-band-edge mass, $\mu_B = e\hbar/(2m_0)$ denotes Bohr's magneton with m_0 the free (bare) electron mass, g^* is the effective spin-splitting factor and $\boldsymbol{\sigma} = (\sigma_x, \sigma_y, \sigma_z)$ stands for the Pauli spin (vector) operator ($\boldsymbol{s} = (\hbar/2)\boldsymbol{\sigma}$ is the spin operator), where the components of $\boldsymbol{\sigma}$ are the Pauli matrices

$$\sigma_x = \begin{pmatrix} 0 & 1 \\ 1 & 0 \end{pmatrix}, \tag{3}$$

$$\sigma_y = \begin{pmatrix} 0 & -i \\ i & 0 \end{pmatrix}, \tag{4}$$

$$\sigma_z = \begin{pmatrix} 1 & 0 \\ 0 & -1 \end{pmatrix}. \tag{5}$$

Assuming the Landau gauge for the vector potential $\boldsymbol{A}(\boldsymbol{x}) = (-yB, 0, 0)$ of the homogeneous DC magnetic field and a parabolic confining potential in y direction, $V(\boldsymbol{x}) = m_e\Omega^2 y^2/2 + V(z)$, where Ω is the confining frequency, we have

$$H_e = \frac{\boldsymbol{p}_e^2}{2m_e} - \omega_c y p_{e_x} + \frac{m_e}{2}\tilde{\omega}_c^2 y^2 + V(z) + \frac{g^*}{2}\mu_B B\sigma_z. \tag{6}$$

Herein, $\omega_c = eB/m_e$ is the cyclotron frequency and $\tilde{\omega}_c = (\omega_c^2 + \Omega^2)^{1/2}$ is the hybrid frequency. Because the x component of the momentum operator p_{e_x} along the wire axis commutes with H_e, one can diagonalize p_{e_x} and H_e simultaneously. For each eigenvalue $\hbar k_x$ (k_x: x component of the electron wave vector) of p_{e_x}, the Hamiltonian has a discrete spectrum of energy eigenvalues, resulting from the electron motion in the y–z plane. The eigenvalue problem of H_e in the y–z plane becomes equivalent to two separate equations, one for the size quantization in the z direction and one for the mixed size and magnetic quantization in y direction. With the ansatz

$$\langle \boldsymbol{x}, \sigma | N, k_x, m_s\rangle = \Psi_{Nk_xm_s}(\boldsymbol{x}, \sigma) = \frac{1}{\sqrt{L_x}} e^{ik_x x}\Phi_N(y - Y_{k_x})\ \varphi(z)\ \chi_{m_s}(\sigma) \tag{7}$$

for the single-particle wave function, where $\boldsymbol{x}$ is the spatial and σ the spin coordinate, L_x is the (unit) length of the sample in x direction and $\{N, k_x, m_s\}$ is the relevant set of quantum numbers, the Schrödinger equation

for the orbital part of the electron motion in the y direction separates in the absence of spin–orbit coupling from the spin part. It reads [51]

$$\left(\frac{\hbar^2 k_x^2}{2\tilde{m}_e} - \frac{\hbar^2}{2m_e}\frac{d^2}{dy^2} + \frac{m_e}{2}\tilde{\omega}_c^2(y - Y_{k_x})\right)\Phi_N(y - Y_{k_x}) = \mathscr{E}_N(k_x)\ \Phi_N(y - Y_{k_x}) \tag{8}$$

with $\tilde{m}_e = m_e(\tilde{\omega}_c/\Omega)^2$ the magnetic-field-dependent effective mass. We assume that the electron is confined in a zero-thickness x–y plane along the z direction at $z = 0$. Hence, $|\varphi(z)|^2 = \delta(z)$ is valid. The solution of Eq. (8) is a shifted harmonic-oscillator wavefunction

$$\Phi_N(y - Y_{k_x}) = \frac{1}{\sqrt{2^N N!\pi^{1/2}\tilde{l}_0}}\exp\left(-\frac{1}{2\tilde{l}_0}(y - Y_{k_x})\right)H_N\left(\frac{1}{\tilde{l}_0}(y - Y_{k_x})\right), \tag{9}$$

with the center coordinate $Y_{k_x} = \gamma\tilde{l}_0^2\ k_x$, $\tilde{l}_0 = [\hbar/(m_e\tilde{\omega}_c)]^{1/2}$ is the typical width of the wave function in the y direction, $\gamma = \omega_c/\tilde{\omega}_c$, and $H_N(\xi)$ is Hermite's polynomial. For vanishing confining potential ($\Omega = 0$), $\tilde{l}_0$ results in the magnetic length $l_0 = [\hbar/(eB_0)]^{1/2}$. The spin function in Eq. (7) has the property $\chi_{m_s}(\sigma) = \delta_{\sigma m_s}$ and thus, $\chi_{m_s}(\sigma)$ is the σth component of the eigenspinor $[\chi]_{m_s} = \begin{pmatrix}\chi_{m_s}(\sigma = +\frac{1}{2})\\ \chi_{m_s}(\sigma = -\frac{1}{2})\end{pmatrix}$ of the operator $\sigma_z/2$ with spin quantum numbers $m_s = \pm\frac{1}{2}$; ($s_z = \hbar m_s$ is the spin eigenvalue), where σ is the spin coordinate for spin up ($\sigma = +\frac{1}{2} \equiv \uparrow$) and spin down ($\sigma = -\frac{1}{2} \equiv \downarrow$) electrons. The associated eigenvalues are

$$\mathscr{E}_{Nm_s}(k_x) = \mathscr{E}_{Nm_s} + \frac{\hbar^2 k_x^2}{2\tilde{m}_e}, \tag{10}$$

where the subband bottoms $\mathscr{E}_{Nm_s} = \mathscr{E}_N + \mathscr{E}_{m_s}$ are given by

$$\mathscr{E}_{Nm_s} = \hbar\tilde{\omega}_c(N + \tfrac{1}{2}) + g^*\mu_B B m_s, \quad N = 0,1,2,\ldots,\ m_s = \pm\tfrac{1}{2}. \tag{11}$$

The corresponding *density of states* (DOS) in the absence of impurity scattering, surface and interface roughness is given by

$$\rho_{Q1D}(\mathscr{E}) = \frac{L_x}{\pi}\sum_{N,m_s}\left(\frac{d\mathscr{E}_{Nm_s}(k_x)}{dk_x}\right)^{-1} = \frac{L_x}{\pi\hbar}\sqrt{\frac{\tilde{m}_e}{2}}\sum_{N,m_s}\frac{\Theta(\mathscr{E} - \mathscr{E}_{Nm_s})}{(\mathscr{E} - \mathscr{E}_{Nm_s})^{1/2}}, \tag{12}$$

where $\Theta(x)$ is the Heaviside unit step function, $\Theta(x) = 1$ for $x > 1$ and $\Theta(x) = 0$ for $x < 0$. In general, due to the broken time-reversal symmetry the DOS is different for $+k_x$ and $-k_x$: $\rho_{Q1D}(\mathscr{E}) = \rho^+_{Q1D}(\mathscr{E}) + \rho^-_{Q1D}(\mathscr{E})$. However, for the parabolic confining potential we have $\mathscr{E}_{Nm_s}(k_x) = \mathscr{E}_{Nm_s}(-k_x)$, which guarantees the identical DOS for electrons travelling in opposite directions: $\rho_{Q1D}(\mathscr{E}) = 2\rho^+_{Q1D}(\mathscr{E}) = 2\rho^-_{Q1D}(\mathscr{E})$. Compared with the 3D and Q2D case, the degeneracy of the energy levels has been lifted by the lateral confining potential in y direction. In a quasi-classical picture, the term $\hbar^2 k_x^2/(2\tilde{m}_e)$ arises from the electrons on *skipping orbits* on the two edges of the wire due to the lateral confining potential and the Lorentz force; i.e. this term describes the *edge states*. For large magnetic fields the kinetic-energy term vanishes and thus, the 2D limit is realized with degenerate spin-split Landau levels $\mathscr{E}_{Nm_s}$.

The energy levels of an electron are shifted by the interaction of the electron with the long-wavelength optical phonons. These phonons are well described by the *dielectric continuum model*, the basic model of the *Fröhlich or polar type* of the EPI [7]. This type of EPI describes the coupling of the macroscopic electric field with the charge of the electron. The Hamiltonian of the polaron is

$$H_p = H_e + H_{ph} + H_{ep}, \tag{13}$$

where H_e is given by Eq. (6). The Hamiltonian of the unperturbed phonon system is described by

$$H_{ph} = \sum_{\boldsymbol{q}} \hbar\omega_L \left(a_L^\dagger(\boldsymbol{q}) a_L(\boldsymbol{q}) + \frac{1}{2} \right). \tag{14}$$

This Hamiltonian has the eigenvalue equation

$$H_{ph} |\{n_{\boldsymbol{q}}\}\rangle = \left[\sum_{\boldsymbol{q}} \hbar\omega_L \left(n_{\boldsymbol{q}} + \frac{1}{2} \right) \right] |\{n_{\boldsymbol{q}}\}\rangle, \tag{15}$$

where the state vector of the LO phonons is

$$|\{n_{\boldsymbol{q}}\}\rangle = \prod_{\boldsymbol{q}} \frac{1}{\sqrt{n_{\boldsymbol{q}}}} (a_L^\dagger(\boldsymbol{q}))^{n_{\boldsymbol{q}}} |\{0_{\boldsymbol{q}}\}\rangle, \tag{16}$$

with $|\{0_{\boldsymbol{q}}\}\rangle$ the state vector of the phonon vacuum and $n_{\boldsymbol{q}}$ is the number of LO phonons with momentum $\hbar\boldsymbol{q}$ and energy $\hbar\omega_L$:

$$a_L^\dagger(\boldsymbol{q}) a_L(\boldsymbol{q}) |\{n_{\boldsymbol{q}}\}\rangle = n_{\boldsymbol{q}} |\{n_{\boldsymbol{q}}\}\rangle, \quad n_{\boldsymbol{q}} = 0, 1, 2, \ldots . \tag{17}$$

The operators $a_L(\boldsymbol{q})$ and $a_L^\dagger(\boldsymbol{q})$ are the phonon destruction and creation operators, respectively, satisfying

$$\begin{aligned} &[a_L(\boldsymbol{q}), a_L^\dagger(\boldsymbol{q}')] = \delta_{\boldsymbol{q}\boldsymbol{q}'}, \\ &[a_L^\dagger(\boldsymbol{q}), a_L^\dagger(\boldsymbol{q}')] = [a_L(\boldsymbol{q}), a_L(\boldsymbol{q}')] = 0 \end{aligned} \tag{18}$$

and $\boldsymbol{q} = (q_x, q_y, q_z)$ is the 3D wave vector of the 3D bulk LO phonons. H_{ep} is the standard Fröhlich Hamiltonian of the EPI [7]

$$H_{ep} = \sum_{\boldsymbol{q}} e^{i\boldsymbol{q}\cdot\boldsymbol{x}} \, V(\boldsymbol{q}) \, (a_L(\boldsymbol{q}) + a_L^\dagger(-\boldsymbol{q})), \tag{19}$$

where

$$V(\boldsymbol{q}) = \frac{M(\boldsymbol{q})}{V_G^{1/2}} = \frac{1}{V_G^{1/2}} \frac{M_0}{|\boldsymbol{q}|}, \tag{20}$$

and

$$M_0 = \left(\frac{e^2 \hbar\omega_L}{2\varepsilon_0} \left(\frac{1}{\varepsilon_\infty} - \frac{1}{\varepsilon_s} \right) \right)^{1/2} = \sqrt{4\pi\alpha_p r_p (\hbar\omega_L)^2}. \tag{21}$$

The dimensionless 3D polaron coupling constant is

$$\alpha_p = \frac{1}{2} \frac{e^2}{4\pi\varepsilon_0 r_p} \left(\frac{1}{\varepsilon_\infty} - \frac{1}{\varepsilon_s} \right) \frac{1}{\hbar\omega_L} \tag{22}$$

and the corresponding 3D polaron radius reads

$$r_p = \left(\frac{\hbar}{2 m_e \omega_L} \right)^{1/2}. \tag{23}$$

Herein, ε_∞ and ε_s are the high-frequency (optical) and the static dielectric constant, respectively, of the semiconductor containing the electron, ε_0 is the permittivity in vacuum and $V_G = L_x L_y L_z$ is the (unit) volume of the sample.

3. Perturbation theories

The energy levels of an electron $\mathscr{E}_{Nm_s}(k_x)$ are shifted about $\Delta E_{Nm_s}(k_x)$ by the interaction with the LO phonons:

$$E_{Nm_s}(k_x) = \mathscr{E}_{Nm_s}(k_x) + \Delta E_{Nm_s}(k_x). \tag{24}$$

In the weak-coupling limits i.e. if $\alpha_p \ll 1$ is valid, which is well fulfilled for the typical semiconductors used to form QWWs, the EPI is a small perturbation and thus, in most cases it is sufficient to consider perturbed states that contain not more than one LO phonon. Hence, second-order perturbation theory can be used. Then, the energy shift $\Delta E_{Nm_s}(k_x)$ of the subband energy, the so-called *polaron self-energy*, is given by

$$\Delta E_{Nm_s}(k_x) = -\sum_{N'=0}^{\infty} \sum_{k'_x} \sum_{m'_s=\pm\frac{1}{2}} \sum_{\boldsymbol{q}} \times \frac{|\langle N', k'_x, m'_s; 1_{\boldsymbol{q}}|H_{ep}|N, k_x, m_s; 0_{\boldsymbol{q}}\rangle|^2}{\hbar\omega_L + \hbar\tilde{\omega}(N'-N) + (\hbar^2/(2m_e))(k'^2_x - k^2_x) + g^*\mu_B B(m'_s - m_s) - \Delta_{Nm_s}(k_x)}. \tag{25}$$

The ket $|N, k_x, m_s; \{n_{\boldsymbol{q}}\}\rangle = |N, k_x, m_s\rangle \otimes |\{n_{\boldsymbol{q}}\}\rangle$ describes an eigenstate of the *unperturbed* electron–phonon system, i.e. of $H_0 = H_e + H_{ph}$, composed of an electron in subband N with momentum $\hbar k_x$, spin $s_z = \hbar m_s$ and energy $\mathscr{E}_{Nm_s}(k_x)$, and $\{n_{\boldsymbol{q}}\}$ LO phonons with momenta $\{\hbar\boldsymbol{q}\}$ and energy $\hbar\omega_L$: $H_e|N, k_x, m_s\rangle = \mathscr{E}_{Nm_s}(k_x)|N, k_x, m_s\rangle$ and $H_{ph}|\{n_{\boldsymbol{q}}\}\rangle = (\sum_{\boldsymbol{q}} \hbar\omega_L n_{\boldsymbol{q}})|\{n_{\boldsymbol{q}}\}\rangle$ ignoring the zero-point energy. Because the x component of the total momentum operator of the coupled electron–phonon system $\boldsymbol{P}_{pol} = \boldsymbol{p}_e + \sum_{\boldsymbol{q}} \hbar\boldsymbol{q} a^\dagger_L(\boldsymbol{q}) a_L(\boldsymbol{q})$ commutes with the Hamiltonian, $[H_p, P^{pol}_x] = [H_{ep}, P^{pol}_x] = 0$, reflecting the translational symmetry along the wire axis, it is useful to rewrite $k_x = k^{pol}_x - \sum_{\boldsymbol{q}} q_x n_{\boldsymbol{q}}$ in the state vector of the unperturbed system: $|N, k^{pol}_x, m_s; \{n_{\boldsymbol{q}}\}\rangle$. The associated level we call *n-phonon unperturbed level*, as opposed to the *renormalized* level, the *n-phonon magnetopolaron level*, discussed below. Then, the n-phonon unperturbed level has the energy

$$\mathscr{E}_{Nm_s;n_{\boldsymbol{q}}}(k^{pol}_x) = \mathscr{E}_{Nm_s} + \frac{\hbar^2}{2\tilde{m}_e}\left(k^{pol}_x - \sum_{\boldsymbol{q}} q_x n_{\boldsymbol{q}}\right)^2 + \sum_{\boldsymbol{q}} \hbar\omega_L n_{\boldsymbol{q}}. \tag{26}$$

In Eq. (25) only zero-phonon states $|N, k^{pol}_x = k_x, m_s; 0_{\boldsymbol{q}}\rangle$ and one-phonon states $|N, k^{pol}_x = k_x + q_x, m_s; 1_{\boldsymbol{q}}\rangle$ occur.

Because H_{ep} does not contain the spin operator, the matrix element is diagonal in the spin indices and thus, $\Delta E_{Nm_s}(k_x) \equiv \Delta E_N(k_x)$ is independent of the spin. With

$$\langle N', k'_x, m'_s; 1_{\boldsymbol{q}}|H_{ep}|N, k_x m_s; 0_{\boldsymbol{q}}\rangle = \delta_{m'_s m_s}\delta_{k'_x, k_x - q_x} M_{\substack{N' \\ k_x - q_x}\ \substack{N \\ k_x}}(-\boldsymbol{q}) \tag{27}$$

it follows[1]

$$\Delta E_N(k_x) = -\sum_{N'=0}^{\infty} \sum_{\boldsymbol{q}} \frac{|M_{\substack{N' \\ k_x - q_x}\ \substack{N \\ k_x}}(-\boldsymbol{q})|^2}{D_{N'N}(k_x, q_x)} \tag{28}$$

and thus, spin up and down electrons are independent. The Zeeman energy is only a energy shift which scales the energy. Thus, in cyclotron resonance experiments on QWWs the spin direction of the electrons is

[1] Please note that contrary to our earlier work [29] here we use the abbreviation $M_{\substack{N' \\ k_x - q_x}\ \substack{N \\ k_x}}(-\boldsymbol{q}) \equiv M_{N'N}(\boldsymbol{q})$ because this definition fits better with the formulation used in Green's function technique, developed in Section 4.

conserved. This is true as long as in the absence of EPI the subbands are parabolic. All the further considerations are performed for the orbital part only. The spin may be included when necessary in the final equations:

$$E_{Nm_s}(k_x) = \mathscr{E}_N(k_x) + \Delta E_N(k_x) + g^*\mu_B B m_s \tag{29}$$

with $\mathscr{E}_N(k_x) = \mathscr{E}_N + \mathscr{E}(k_x)$,

$$\mathscr{E}_N(k_x) = \hbar\tilde{\omega}_c\left(N + \frac{1}{2}\right) + \frac{\hbar^2 k_x^2}{2\tilde{m}_e}. \tag{30}$$

The energy denominator in Eq. (28) is given by

$$D_{N'N}(k_x, q_x) = \hbar\omega_L + \hbar\tilde{\omega}_c(N' - N) + \frac{\hbar^2 q_x^2}{2\tilde{m}_e} - \frac{\hbar^2}{\tilde{m}_e} k_x q_x - \Delta_N(k_x), \tag{31}$$

where the value of $\Delta_N(k_x)$ depends on the type of perturbation theory used [52]:

1. $\Delta_N(k_x) = 0$ leads to the *Rayleigh–Schrödinger perturbation theory* (RSPT),
2. $\Delta_N(k_x) = \Delta E_N(k_x)$ results in the *Wigner–Brillouin perturbation theory* (WBPT) and
3. $\Delta_N(k_x) = \Delta E_N(k_x) - \Delta E_0^{\mathrm{RSPT}}(0)$ gives a *modified improved Wigner–Brillouin perturbation theory* (IWBPT) [29,31].

For the ground state $\Delta E_0^{\mathrm{IWBPT}}(0) = \Delta E_0^{\mathrm{RSPT}}(0)$ is valid for all magnetic fields. Expanding $E_N(k_x)$ in a power series of k_x^2:

$$E_N(k_x) = \mathscr{E}_N(k_x) + \Delta E_N(0) + \frac{\mathrm{d}}{\mathrm{d}(k_x^2)}\Delta E_N(k_x)\bigg|_{k_x^2=0} k_x^2 + \frac{1}{2}\frac{\mathrm{d}^2}{\mathrm{d}(k_x^2)^2}\Delta E_N(k_x)\bigg|_{k_x^2=0} k_x^4 + \cdots \tag{32}$$

the *magnetopolaron effective mass* $\tilde{m}_N^*$ for the magnetopolaron motion in x direction near the bottom of the Nth subband is

$$\frac{\tilde{m}_e}{\tilde{m}_N^*} = 1 + \frac{\tilde{m}_e}{k_x\hbar^2}\frac{\mathrm{d}}{\mathrm{d}k_x}\Delta E_N(k_x)\bigg|_{k_x=0}. \tag{33}$$

When performing the derivative care must given in the case of WBPT and IWBPT because $\Delta E_N(k_x)$ depends self-consistently on $\Delta E_N(k_x)$. In an optical experiment, analogeous as in cyclotron resonance experiments on 3D samples, one excites the optical transition $E_{N-1} \to E_N$. Thus, the polaron hybrid frequency $\tilde{\omega}_c^* = (E_N - E_{N-1})/\hbar$ defines a Q1D *polaron cyclotron mass* [29]

$$\frac{m_c^*}{m_e} = \frac{\hbar\omega_c}{\sqrt{(E_N - E_{N-1})^2 - (\hbar\Omega)^2}}. \tag{34}$$

Usually, one detects the transition $E_0 \to E_1$ in the experiment. Note that WBPT and IWBPT make Eq. (28) self-consistent with the result that higher powers of α_p occur in $\Delta E_N(k_x)$, m_N^* and m_c^*.

Considering for the moment the energy–momentum relation for the n-phonon unperturbed states $\mathscr{E}_{N;n_q}(k_x^{\mathrm{pol}})$, it is obvious that below the energy of the one-phonon unperturbed state, $\mathscr{E}_0(0) + \hbar\omega_L$, there is only a *finite* number of subbands resulting from zero-phonon unperturbed states. However, above $\mathscr{E}_0(0) + \hbar\omega_L$ there is a quasi-continuum of states, called *phonon continuum*. The physical reason for this continuum is as follows. For the one-phonon unperturbed state the wave vector is a sum of the electron and phonon wave vector $k_x^{\mathrm{pol}} = k_x + q_x$ and hence, the energy is

$$\mathscr{E}_{N;1_q}(k_x^{\mathrm{pol}}) = \hbar\tilde{\omega}_c\left(N + \frac{1}{2}\right) + \frac{\hbar^2}{2\tilde{m}_e}(k_x^{\mathrm{pol}} - q_x)^2 + \hbar\omega_L. \tag{35}$$

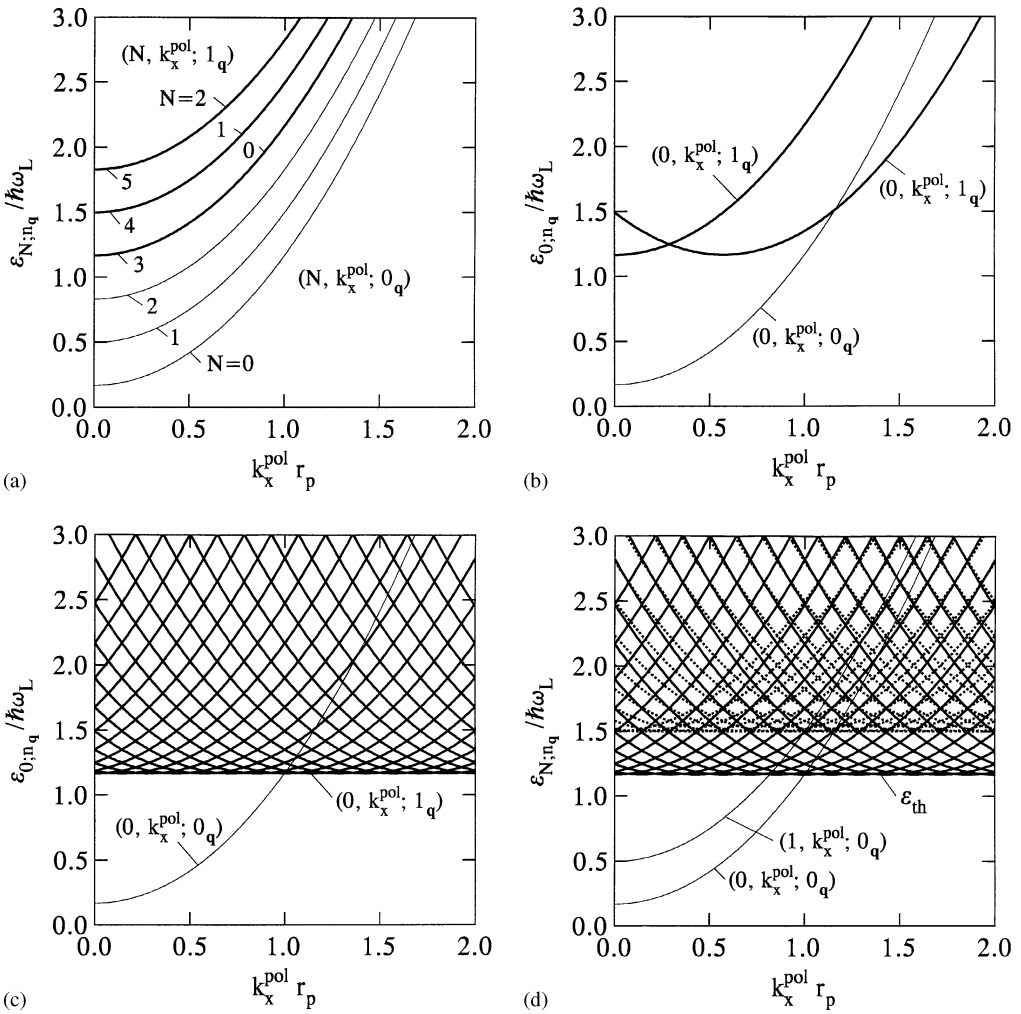

Fig. 1. Energy–momentum relation for Q1D magnetopolarons in unperturbed states $\mathscr{E}_{N;n_q}(k_x^{pol})$ for vanishing magnetic field: (a) some of the dispersion relations $\mathscr{E}_{N;0_q}(k_x^{pol})$ (thin solid lines) and $\mathscr{E}_{N;1_q}(k_x^{pol})$ (heavy solid lines) calculated for $q_x = 0$; (b) the dispersion relation $\mathscr{E}_{0;0_q}(k_x^{pol})$ and two of the dispersion curves $\mathscr{E}_{0;1_q}(k_x^{pol})$ arising for two different phonon wave vector components q_x; (c) the dispersion relation $\mathscr{E}_{0;0_q}(k_x^{pol})$ and some dispersion curves forming the associated one-phonon continuum $\mathscr{E}_{0;1_q}(k_x^{pol})$; (d) the dispersion relations $\mathscr{E}_{0;0_q}(k_x^{pol})$ and $\mathscr{E}_{1;0_q}(k_x^{pol})$ and some dispersion relations $\mathscr{E}_{0;1_q}(k_x^{pol})$ and $\mathscr{E}_{1;1_q}(k_x^{pol})$ forming the (unperturbed) one-phonon continua of subbands $N = 0$ and $N = 1$, respectively, lying above the threshold energy $\mathscr{E}_{th}$.

The resulting dispersion curves are shown as a function of the wave vector in Fig. 1 for $B = 0$. The numerical calculations are performed with the parameters: $m_e = 0.06624\, m_0$ and $\hbar\omega_L = 36.17$ meV valid for GaAs. If not indicated explicitely in the figure caption, we use $\hbar\Omega = 12$ meV for the confinement energy of the lateral potential. The energies $\mathscr{E}_{N;0_q}(k_x^{pol}) = \mathscr{E}_N(k_x)$ and $\mathscr{E}_{N;1_q}(k_x^{pol}) = \mathscr{E}_N(k_x + q_x) + \hbar\omega_L$, denoted by $(N, k_x^{pol}; n_q)$, are plotted in Fig. 1(a) as a function of the wave vector k_x^{pol} for $q_x = 0$. For the used material parameters the difference between $\mathscr{E}_{N+3;0_q}$ and $\mathscr{E}_{N;1_q}$ is not to be drawn. Whereas only one dispersion curve $\mathscr{E}_{N;0_q}(k_x^{pol})$ is present, an quasi-infinite number of dispersion curves of $\mathscr{E}_{N;1_q}(k_x^{pol})$ results due to the different

$q_x = 2\pi n_x/L_x$; $n_x = 0, \pm 1, \pm 2, \ldots$ forming the *one-phonon continuum* of subband N. In Fig 1(b) we show two dispersion curves $\mathscr{E}_{0;1_q}(k_x^{\rm pol})$ resulting for two different phonon wave vectors q_x and in Fig. 1(c) the level $\mathscr{E}_{0;0_q}(k_x^{\rm pol})$ and the resulting one-phonon continuum, formed by $\mathscr{E}_{0;1_q}(k_x^{\rm pol})$, is plotted. Each level, $N = 0, 1, 2, \ldots$, is accompanied by the corresponding phonon continuum. The second level $\mathscr{E}_{1;0_q}(k_x^{\rm pol})$ and the associated one-phonon continuum resulting from $\mathscr{E}_{1;1_q}(k_x^{\rm pol})$ is plotted in Fig. 1(d) in addition to the energies $\mathscr{E}_{0;0_q}(k_x^{\rm pol})$ and $\mathscr{E}_{0;1_q}(k_x^{\rm pol})$. Hence, above the threshold $\mathscr{E}_{\rm th} \equiv \mathscr{E}_{\rm th}(B) = \mathscr{E}_{0;1_q}(0; B) = \hbar\tilde{\omega}_{\rm c}/2 + \hbar\omega_{\rm L}$ exists the one-phonon continuum of all the subbands (Fig. 1(d)). It is seen that with increasing wave vector all the zero-phonon states with bottoms below the phonon continuum, i.e. if $N\tilde{\omega}_{\rm c} < \omega_{\rm L}$, cross the lower boundary $\mathscr{E}_{\rm th}$ of the one-phonon continuum at $\mathscr{E}_N(k_x) = \mathscr{E}_{\rm th}$. The energy–momentum relations cross this line at $k_x = k_{\rm L}^{(N)} = [(2\tilde{m}_{\rm e}/\hbar)(\omega_{\rm L} - N\tilde{\omega}_{\rm c})]^{1/2}$, which gives $B = 0$: $k_{\rm L}^{(N)} = [(2m_{\rm e}/\hbar)(\omega_{\rm L} - N\Omega)]^{1/2}$. The threshold energy of the phonon continuum is independent of the wave vector, but depends on the magnetic field. The dependence of the subbands on the magnetic field is plotted in Fig. 2 for $k_x = 0$. Fig. 2(a) shows the zero- and one-phonon states for $k_x^{\rm pol} = 0$. In Figs. 2(b) and 2(c) some of the dispersion curves, which are the origin of the one-phonon continuum, are plotted for two different confinement energies, $\hbar\Omega = 12$ and 2 meV, respectively, and $k_x = 0$. The first two levels and some dispersion curves forming the associated one-phonon continua are plotted in Fig. 2(d). It becomes obvious that the zero-phonon unperturbed states with $N > 0$ and with bottoms below $\mathscr{E}_{\rm th}$, i.e. if $N\Omega < \omega_{\rm L}$ is valid, cross for $k_x = 0$ and with increasing magnetic field the lower boundary of the one-phonon continuum at $\omega_{\rm c} = \omega_{\rm c}^{(N)} = [(\omega_{\rm L}/N)^2 - \Omega^2]^{1/2}$. If $k_x \neq 0$ the corresponding crossings are at $\omega_{\rm c} = \omega_{\rm c}^{(N)} = [((1/N)(\omega_{\rm c} - \hbar k_x^2/2\tilde{m}_{\rm e}))^2 - \Omega^2]^{1/2}$ for $N > 0$. In this case also the unshifted level $\mathscr{E}_{0;0_q}(k_x; B)$ crosses $\mathscr{E}_{\rm th}$ at $\omega_{\rm c} = \omega_{\rm c}^{(0)} = \Omega[(k_x r_{\rm p})^2 - 1]^{1/2}$, but only if $k_x r_{\rm p} \geqslant 1$. For levels $\mathscr{E}_{N;0_q}(0; B)$ with $\omega_{\rm L} \leqslant N\Omega$ there is no crossing with the line $\mathscr{E}_{\rm th}$ with increasing magnetic field and for $\omega_{\rm L} \leqslant N\tilde{\omega}_{\rm c}$ the same is true for increasing wave vector. Thus, there are *two different ways* to cross the lower boundary $\mathscr{E}_{\rm th}$ of the one-phonon continuum: one with increasing magnetic field and the other one with increasing kinetic energy. As mentioned above, in 3D and strict 2D systems the magnetopolaron behaviour is quite different on the two ways. Hence, with increasing magnetic field and wave vector the zero-phonon levels with bottoms below the threshold energy, $\mathscr{E}_{N;0_q}(0; 0) < \mathscr{E}_{\rm th}$, become degenerate with the continuous states inside the one-phonon continuum. At these resonances the denominator of Eq. (28) vanishes for RSPT and thus, $\Delta E_N(k_x)$ diverges negatively. Henceforth, RSPT requires $k_x < k_{\rm L}^{(N)}$ for all levels and $\omega_{\rm c} < \omega_{\rm c}^{(N)}$ for states with $N > 0$ in order to exclude degeneracy with the real phonon states of the phonon continuum. This is the reason why different perturbation theories are necessary to describe correctly the states for different situation. To see this explicitely we shortly review the basic equations of the perturbation theory.

If the Hamiltonian H, which satisfies $H|\psi_n\rangle = E_n|\psi_n\rangle$, is the sum of the unperturbed part H_0, with $H_0|\psi_n^{(0)}\rangle = E_n^{(0)}|\psi_n^{(0)}\rangle$, and the time-independent perturbation H_1, the energy renormalization is $\Delta E_n \equiv E_n - E_n^{(0)} = \langle\psi_n^{(0)}|H_1|\psi_n\rangle$. The different types of perturbation theories then follows with different expansions of $|\psi_n\rangle$. RSPT is obtained with

$$\Delta E_n^{\rm RSPT} = \langle\psi_n^{(0)}|H_1 \sum_{k=0}^{\infty} \left(\sum_{m\neq n} \frac{|\psi_m^{(0)}\rangle\langle\psi_m^{(0)}|}{E_n^{(0)} - E_m^{(0)}} (H_1 - \Delta E_n^{\rm RSPT}) \right)^k |\psi_n^{(0)}\rangle, \tag{36}$$

which gives in second order the well-known result

$$\Delta E_n^{\rm RSPT} = \sum_{m\neq n} \frac{|\langle\psi_m^{(0)}|H_1|\psi_n^{(0)}\rangle|^2}{E_n^{(0)} - E_m^{(0)}}. \tag{37}$$

Resonances occur at the zeros of the denominator: $E_n^{(0)} = E_m^{(0)}$. In terms of the relevant Hilbert state of a QWW in the presence of a magnetic field, taking into account the property of the one-phonon continuum, the energetically lowest resonances occur at $\mathscr{E}_N(k_x) = \mathscr{E}_0(0) + \hbar\omega_{\rm L}$. Thus, RSPT describes the energy correction $\Delta E_0(k_x)$ quite well for the ground state if $k_x \ll k_{\rm L}^{(0)}$, but it fails near the resonances, where the energy shift

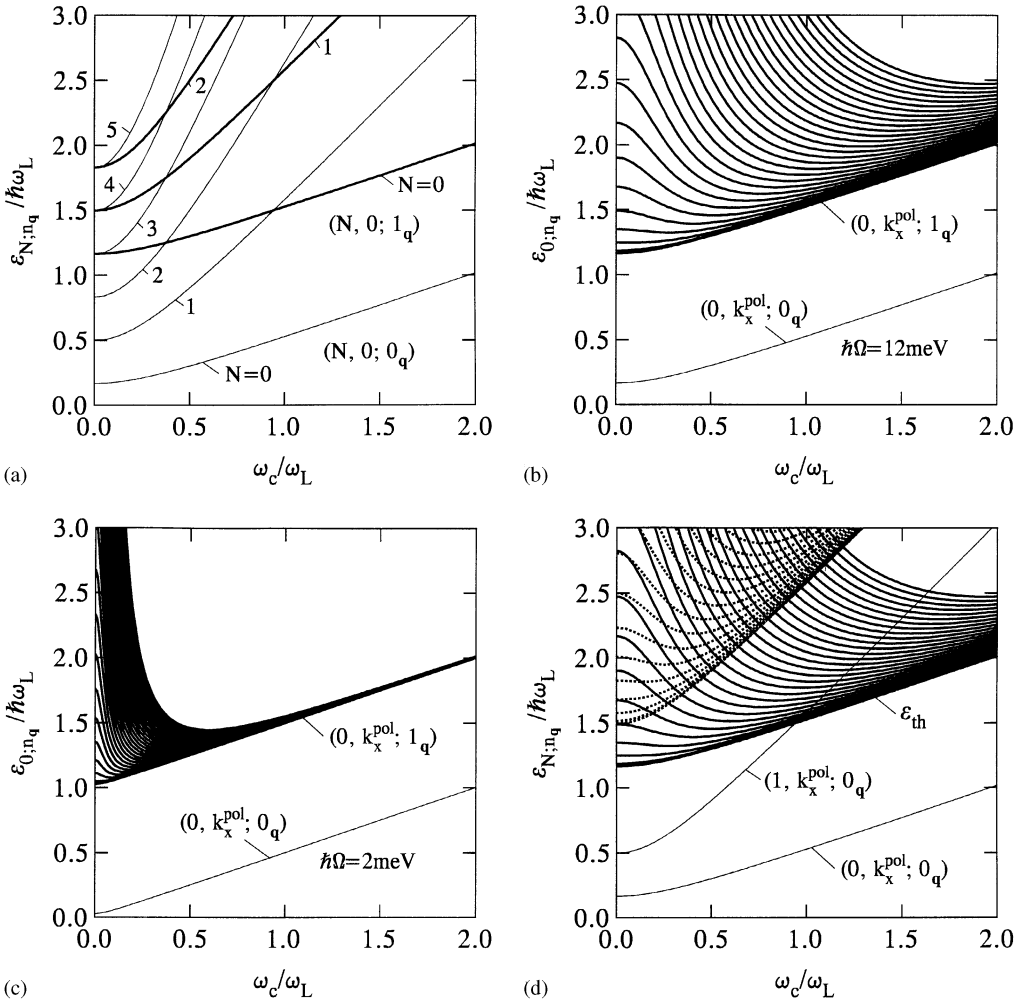

Fig. 2. The dispersion relations of unperturbed states in dependence on the magnetic field: (a) $\mathscr{E}_{N;0_q}(k_x^{pol})$ (thin solid lines), $N = 0, 1, 2, 3, 4, 5$ and $\mathscr{E}_{N;1_q}(k_x^{pol})$ (heavy solid lines), $N = 0, 1, 2$ for $k_x^{pol} = 0$; (b) $\mathscr{E}_{0;0_q}(k_x^{pol})$ and some of $\mathscr{E}_{0;1_q}(k_x^{pol})$, calculated for $k_x = 0$ and $\hbar\Omega = 12$ meV and for $\hbar\Omega = 2$ meV (c); (d) the dispersion relations $\mathscr{E}_{0;0_q}(k_x^{pol})$ and $\mathscr{E}_{1;0_q}(k_x^{pol})$ and some dispersion relations $\mathscr{E}_{0;1_q}(k_x^{pol})$ and $\mathscr{E}_{1;1_q}(k_x^{pol})$ forming the (unperturbed) one-phonon continua of subbands $N = 0$ and $N = 1$, respectively, lying above the threshold energy $\mathscr{E}_{th}$.

$\Delta E_0(k_x)$ diverges negatively. The same is true for states with $N > 0$ if $k_x \ll k_L^{(N)}$ and $\omega_c \ll \omega_c^{(N)}$. Hence, degenerate perturbation theory is needed. Unfortunately, degenerate RSPT would result in an infinite dimensional secular equation because the degeneracy is between one discrete state and a continuum of states. Thus, only self-consistent perturbation theories are profitable. The EPI couples the degenerate states, leading to a *splitting* at the resonance into an upper and lower branch with *anticrossing* behaviour. This effect is called *resonant (magneto) polaron level coupling* (R(M)PLC) and the associated quasi-particle state is called *resonant (magneto) polaron*. The upper branch is above the boundary of the phonon continuum, but the lower-energetic branch is below the line $\mathscr{E}_{th}$. Hence, all states $|N, k_x; 0_q\rangle$ lying below the energy $\mathscr{E}_{th}$ must bend over

if their energies approach, with increasing momentum and magnetic field, the near vicinity of the phonon continuum, because of the anticrossing repulsion of the levels due to the von Neumann non-crossing theorem. For larger momenta and/or magnetic fields these states are then pinned at this line. Exactly this is described by WBPT. This type of perturbation theory follows in the above form by

$$\Delta E_n^{\mathrm{WBPT}} = \langle\psi_n^{(0)}|H_1 \sum_{k=0}^{\infty} \left(\sum_{m\neq n} \frac{|\psi_m^{(0)}\rangle\langle\psi_m^{(0)}|}{E_n - E_m^{(0)}} H_1 \right)^k |\psi_n^{(0)}\rangle, \tag{38}$$

which is evidently self-consistent because $E_n = E_n^0 + \Delta E_n^{\mathrm{WBPT}}$ contains the energy renormalization. Because of this self-consistency no divergencies occur at the resonances in WBPT. The second order term reads

$$\Delta E_n^{\mathrm{WBPT}} = \sum_{m\neq n} \frac{|\langle\psi_m^{(0)}|H_1|\psi_n^{(0)}\rangle|^2}{E_n - E_m^{(0)}}, \tag{39}$$

which has resonances at $E_n = E_m^{(0)}$, i.e. at $E_N(k_x) = \mathscr{E}_0(0) + \hbar\omega_{\mathrm{L}}$. From this it follows that WBPT well describes the splitting of the levels, but gives the pinning at the wrong energy, i.e. at the one-phonon energy $\hbar\omega_{\mathrm{L}}$ above the *unrenormalized*, i.e. *unshifted*, ground state $\mathscr{E}_0(0)$. This is true because WBPT uses the one-phonon approximation (for details see Section 4) and following describes the energy renormalization due to electron transitions between unperturbed states. The single electron which is present then renormalizes the final state only. If this would be the physical reality, the magnetopolarons in the bend-over region would not have any physical sense because they would decay into a free phonon, which is available for these energies, and to a magnetopolaron with $N = 0$ and $k_x = 0$.

Because the EPI renormalizes all energy levels, the accurate dispersion curves of all subbands with bottoms below $\mathscr{E}_{\mathrm{th}}$ must bend over at $E_{\mathrm{th}} = \min\{\mathscr{E}_0(k_x + q_x) + \hbar\omega_{\mathrm{L}} + \Delta E_0(k_x + q_x)\} = \mathscr{E}_0(0) + \hbar\omega_{\mathrm{L}} + \Delta E_0(0)$, i.e. at the minimum energy of the one-phonon magnetopolaron energy. Thus, the threshold energy is at the one-phonon energy $\hbar\omega_{\mathrm{L}}$ above the *shifted*, i.e. *renormalized*, ground state $E_0(0)$ of the system. Because a single electron is considered, this single electron will not modify the phonon system and thus, the phonon frequency is unchanged. In order to get the energies $E_N(k_x)$ of each subband with the correct bend-over and pinning behaviour, improvements on the WBPT must be made. From the discussion above it becomes obvious that at least perturbation theories which include two phonons are necessary. One possibility would be the ad hoc substitution of $E_m^{(0)}$ by E_m in Eq. (39). This corresponds to the so-called *Hartree–Fock approximation* (HFA), derived and discussed in detail in Section 4.4. Unfortunately, this would result in a very complicated system of self-consistend equations, which could be solved in principle if one includes only a very small number of subbands. Fortunately, a suitable approximation is not to use E_m, but to set $E_m \to E_m^{(0)} + \Delta E_0^{\mathrm{RSPT}}$. Obviously, in this simplifying approach, as the starting-point of the self-consistent calculation, it is assumed that the renormalization of all levels is the same. This approach has the big advantage over WBPT to give the pinning for all levels at the *correct* energy $E_N(k_x) = \mathscr{E}_0(0) + \Delta E_0^{\mathrm{RSPT}}(0) + \hbar\omega_{\mathrm{L}}$ and is compared with the HFA computationally much simpler and highly efficient. This approach *modifies* the IWBPT of Lindemann et al. [52] to the case of magnetopolarons in QWWs. The IWBPT was firstly proposed in Ref. [53] but originally developed in detail in Ref. [52] for 3D bulk magnetopolarons. Thus, we start from the "unperturbed" energy $\mathscr{E}_N + \Delta E_0^{\mathrm{RSPT}}(0)$ and take this level as the reference level for the excited states, which is equivalently to the decomposing of H_{p} as $H_{\mathrm{p}} = [H_0 + \Delta E_0^{\mathrm{RSPT}}(0)] + [H_{\mathrm{ep}} - \Delta E_0^{\mathrm{RSPT}}(0)]$. This obviously results in $\Delta_N(k_x) = \Delta E_N(k_x) - \Delta E_0^{\mathrm{RSPT}}(0)$ in Eq. (31). It was shown recently [31] that this modification of the IWBPT gives the correct bend-over and pinning behaviour for all polaron levels. The self-consistency of WBPT and IWBPT induces corrections of higher order in α_{p}. It is known from 3D magnetopolarons that WBPT [13] and IWBPT [54] give relatively large spurious contributions to the polaron energy in the order α_{p}^2 for $\omega_{\mathrm{c}} \gg \omega_{\mathrm{L}}$ and lead to an α_{p}^2 correction of the polaron cyclotron mass, which has even for $\omega_{\mathrm{c}} = 0$ the wrong sign [54].

Thus, WBPT gives the correct splitting at the resonance and IWBPT the correct energy-momentum relation for small polaron coupling constants $\alpha_p < 0.1$, but it still underestimates the polaron effects [55]. The physcial reason for this underestimation of the polaron effects will become clear from the discussion in Section 4.4. Similar properties are expected for Q1D magnetopolarons calculated with WBPT and modified IWBPT.

In dependence on the magnetic field the levels are then pinned at the lower boundary of the one-phonon continuum. This behaviour of the branches below E_{th} is true for all dimensionalities, i.e. from 3D to Q0D. It should be noted that only for bulk 3D and Q1D systems a phonon continuum exists above E_{th}, which is absent for Q2D systems if $B \neq 0$ and Q0D systems due to the lack of dispersion. The upper split branch, existing in the region $E > E_{th}$, behaves quite different for the different dimensionalities, e.g. it only exists in 3D systems for magnetic fields, larger than a certain stop-point [13], but exists for all magnetic fields in lower-dimensional systems (see e.g. [22,40]).

Quite different is the behaviour if the energy of the levels with bottoms below E_{th} approaching this line with increasing wave vector. The energy-momentum relation of 3D systems is a *single valued continuous function* for all wave vectors existing below and above E_{th} in the absence of a magnetic field [10,11] with a discontinuous derivative at $E(\boldsymbol{k}) = E(0) + \hbar\omega_L$, while for 2D systems if $B = 0$ [42], Q1D systems [31] and 3D systems if $B \neq 0$ [16] the dispersion relations have a branch which is below E_{th} for all finite wave vectors, i.e. the dispersion relation exhibits a *non-zero gap* at the resonance.

Difficulties arise with the levels above $E_0(0; B) + \hbar\omega_L$. Whereas the energy renormalization below the phonon continuum results from *virtual* emission and absorption processes of LO phonons, inside the phonon continuum (or above $E_0(0; B) + \hbar\omega_L$ if there is no phonon continuum like in 2D and Q0D systems) the magnetopolaron state has enough energy to emit a *real* LO phonon and then relaxes to the subband minimum. The relaxation results in a *damping* of the magnetopolaron state and thus, the energy levels have a *non-zero width.* Above the threshold energy E_{th} the denominator $D_{N'N}(k_x, q_x)$ of $\Delta E_N(k_x)$ has a zero and the standard quantum-mechanical perturbation theories do not give an unique way to calculate $\Delta E_N(k_x)$ in this case. The above mentioned results for levels above E_{th} were obtained by interpreting the integral over the phonon wave vector $\boldsymbol{q}$ as a principal value integral without any deeper justification. But, unfortunately due to the relaxation processes above the boundary of the one-phonon continuum in general the quasi-particle picture is no more valid. Thus, one possible way to solve this problem is to use rigorous many-particle Green's function technique as discussed in Section 4 below.

Because the electron–phonon interaction is spin independent, there exist *two different threshold energies*, one for spin up (↑) and one for spin down (↓) electrons: $E_{th}^{(m_s)} = \mathscr{E}_0(0) + \hbar\omega_L + \Delta E_0(0) + g^*\mu_B B m_s$. This gives the following picture. At the energetically lowest threshold energy $E_{th}^{(m_s)} = \mathscr{E}_0(0) + \hbar\omega_L + \Delta E_0(0) - |g^*\mu_B B m_s|$ the electrons with spin quantum number m_s have energy-momentum relations which bend over and become pinned for larger magnetic fields, while those with $-m_s$ cross this line and bend over at $E_{th}^{(-m_s)} = \mathscr{E}_0(0) + \hbar\omega_L + \Delta E_0(0) + |g^*\mu_B B m_s|$. In the further consideration of this section only the branches below the phonon continuum are of interest.

To calculate the energy correction $\Delta E_N(k_x)$ we first perform the matrix element in Eq. (28). For the matrix element we have

$$M_{\substack{k_x - q_x \\ k_x}}^{\substack{N' \\ N}}(-\boldsymbol{q}) = \frac{1}{V_G^{1/2}} \frac{M_0}{|\boldsymbol{q}|} g_{\substack{k_x - q_x \\ k_x}}^{\substack{N' \\ N}}(-q_y) \equiv \frac{1}{\sqrt{L_x}} \bar{M}_{\substack{k_x - q_x \\ k_x}}^{\substack{N' \\ N}}(-\boldsymbol{q}), \tag{40}$$

where

$$g_{\substack{k_x - q_x \\ k_x}}^{\substack{N' \\ N}}(-q_y) \equiv \langle N' | e^{-iq_y y} | N \rangle = \int_{-\infty}^{\infty} dy\, \Phi_{N'}^*(y - Y_{k_x - q_x})\, e^{-iq_y y} \Phi_N(y - Y_{k_x}). \tag{41}$$

Note that the lower indices on $M_{k_x-q_x\ N'\ k_x\ N}(-\boldsymbol{q})$ and $g_{k_x-q_x\ N'\ k_x\ N}(-q_y)$ denote the wave vector component of the center coordinate. The last integral can be evaluated with the help of Ref. [56] to be

$$g_{k_x-q_x\ N'\ k_x\ N}(-q_y)=\exp\left(\frac{1}{4\tilde{l}_0^2}(Y_{q_x}^2+\tilde{l}_0^4q_y^2)\right)\exp\left(-\mathrm{i}q_y\left(Y_{k_x}-\frac{Y_{q_x}}{2}\right)\right)$$

$$\times\begin{cases}\sqrt{\dfrac{N'!}{N!}}\,2^{\frac{N-N'}{2}}\left(\dfrac{1}{2\tilde{l}_0}[-Y_{q_x}-\mathrm{i}\tilde{l}_0^2q_y]\right)^{N-N'}L_{N'}^{N-N'}\left(\dfrac{1}{2\tilde{l}_0^2}[Y_{q_x}^2+\tilde{l}_0^4q_y^2]\right), & \text{if } N'<N,\\ \sqrt{\dfrac{N'!}{N!}}\,2^{\frac{N'-N}{2}}\left(\dfrac{1}{2\tilde{l}_0}[Y_{q_x}-\mathrm{i}\tilde{l}_0^2q_y]\right)^{N'-N}L_{N'}^{N'-N}\left(\dfrac{1}{2\tilde{l}_0^2}[Y_{q_x}^2+\tilde{l}_0^4q_y^2]\right), & \text{if } N'\geqslant N,\end{cases}\quad(42)$$

where $L_N^{N'}(\xi)$ is the associated Laguerre polynomial. Because of

$$\left|M_{k_x-q_x\ N'\ k_x\ N}(-\boldsymbol{q})\right|^2=M_{k_x\ N\ k_x-q_x\ N'}(\boldsymbol{q})M_{k_x-q_x\ N'\ k_x\ N}(-\boldsymbol{q})\quad(43)$$

we can calculate Eq. (28) as

$$\Delta E_N(k_x)=-\frac{1}{L_x}\sum_{q_x}\sum_{N'}\frac{f^{\mathrm{LO}}_{k_x\ N\ k_x-q_x\ N'\ k_x-q_x\ N'\ k_x\ N}(q_x)}{D_{N'N}(k_x,\,q_x)},\quad(44)$$

where

$$f^{\mathrm{LO}}_{k_x\ N\ k_x-q_x\ N'\ k_x-q_x\ N'\ k_x\ N}(q_x)=\sum_{q_y,q_z}\bar{M}_{k_x\ N\ k_x-q_x\ N'}(\boldsymbol{q})\bar{M}_{k_x-q_x\ N'\ k_x\ N}(-\boldsymbol{q}),\quad(45)$$

$$=\alpha_{\mathrm{p}}r_{\mathrm{p}}(\hbar\omega_{\mathrm{L}})^2\int_{-\infty}^{\infty}\mathrm{d}q_y\frac{g_{k_x\ N\ k_x-q_x\ N'}(q_y)\ g_{k_x-q_x\ N'\ k_x\ N}(-q_y)}{\sqrt{q_x^2+q_y^2}},\quad(46)$$

$$\equiv 2\alpha_{\mathrm{p}}r_{\mathrm{p}}(\hbar\omega_{\mathrm{L}})^2f^{\mathrm{C}}_{k_x\ N\ k_x-q_x\ N'\ k_x-q_x\ N'\ k_x\ N}(q_x).\quad(47)$$

In Eq. (46) we have converted the sum over the phonon momentum into an integral according $\sum_{\boldsymbol{q}}\to L_xL_yL_z/(2\pi)^3\int\mathrm{d}^3q$ and have performed the integral over q_z. With Eq. (41) the form factor is given by

$$f^{\mathrm{C}}_{k_x\ N\ k_x-q_x\ N'\ k_x-q_x\ N'\ k_x\ N}(q_x)=\frac{1}{2}\int_{-\infty}^{\infty}\mathrm{d}q_y\frac{1}{\sqrt{q_x^2+q_y^2}}\int_{-\infty}^{\infty}\mathrm{d}y\int_{-\infty}^{\infty}\mathrm{d}y'\Phi_N^*(y-Y_{k_x})\Phi_{N'}(y-Y_{k_x-q_x})$$

$$\times\mathrm{e}^{\mathrm{i}q_x(y-y')}\Phi_{N'}^*(y'-Y_{k_x-q_x})\Phi_N(y'-Y_{k_x}),\quad(48)$$

which can be transformed with Ref. [57] in the form

$$f^{\mathrm{C}}_{k_x\ N\ k_x-q_x\ N'\ k_x-q_x\ N'\ k_x\ N}(q_x)=\int_{-\infty}^{\infty}\mathrm{d}y\int_{-\infty}^{\infty}\mathrm{d}y'\Phi_N^*(y-Y_{k_x})\Phi_{N'}(y-Y_{k_x-q_x})K_0(|q_x(y-y')|)$$

$$\times\Phi_{N'}^*(y'-Y_{k_x-q_x})\Phi_N(y'-Y_{k_x}),\quad(49)$$

where $K_0(|q_x(y-y')|)$ is the modified Bessel function of zeroth order. From Eq. (48) with Eq. (42) it follows

$$f^{\mathrm{C}}_{\substack{N \\ k_x}\ \substack{N' \\ k_x-q_x}\ \substack{N' \\ k_x-q_x}\ \substack{N \\ k_x}}(q_x) = \frac{1}{2}\int_{-\infty}^{\infty} \mathrm{d}q_y \frac{\mathrm{e}^{-a} a^{N_1-N_2}}{\sqrt{q_x^2+q_y^2}} \frac{N_2!}{N_1!}[L_{N_2}^{N_1-N_2}(a)]^2, \tag{50}$$

where $a = \frac{1}{2\tilde{l}_0}(Y_{q_x}^2 + \tilde{l}_0^4 q_y^2) = \frac{\tilde{l}_0^2}{2}(\gamma^2 q_x^2 + q_y^2)$, $N_1 = \max(N,N')$ and $N_2 = \min(N, N')$. From Eq. (50) it becomes obvious that the form factor is independent of the wave vector component k_x.

For vanishing magnetic field ($B = 0$ corresponding to $\gamma = 0$), the integral over q_y can be performed analytically. It is calculated in Ref. [58] with the result

$$f^{\mathrm{C}}_{N_1N_2N_3N_4}(q_x) = (-1)^{N_1+N_2}\delta_{N_1+N_2+N_3+N_4,2n}\sqrt{N_1!N_2!N_3!N_4!}\sum_{m_2=0}^{N_2}\sum_{m_4=0}^{N_4}\sum_{\nu=0}^{\kappa} \mathrm{e}^b(-1)^\nu \times \frac{b^\kappa C_\nu^\kappa (2\kappa-1)!!K_\nu(b)}{m_2!m_4!(N_2-m_2)!(N_4-m_4)!(N_1-N_2+m_2)!(N_3-N_4+m_4)!(\kappa-\nu)!}, \tag{51}$$

where $n = 0, 1, 2, \ldots$, $b = (q_x l_\Omega/2)^2$, $\kappa = m_2 + m_4 + (N_1 - N_2 + N_3 - N_4)/2$, $N_1 \geqslant N_2$, $N_3 \geqslant N_4$ and

$$C_\nu^\kappa = \begin{cases} \dfrac{1}{(\kappa+1)\cdot \ldots \cdot(\kappa+\nu)} & \text{if } \nu \neq 0, \\ \dfrac{1}{2} & \text{if } \nu = 0. \end{cases} \tag{52}$$

Introducing in Eq. (44) 3D polaron units, i.e. energies are measured in units of $\hbar\omega_{\mathrm{L}}$ and lengths are measured in units of r_p, so that e.g. $\mathscr{E}_N(k_x) = (1-\gamma^2)k_x^2 + \lambda^2(N+1/2)$ is valid, and introducing cylindrical coordinates in the $q_x - q_y$ plane: $q_x = q_{||}\cos\varphi$, $q_y = q_{||}\sin\varphi$, $q_{||} = \sqrt{q_x^2+q_y^2}$, we obtain

$$\Delta E_N(k_x) = -\frac{\alpha_p}{2\pi}\int_0^\infty \mathrm{d}q_{||}\int_{-\pi}^{\pi}\mathrm{d}\varphi\,\mathrm{e}^{-a}\sum_{N'=0}^{\infty}\frac{N_1!}{N_2!}a^{N1-N2} \times \frac{[L_{N_2}^{N_1-N_2}(a)]^2}{1+\lambda^2(N'-N)+q_{||}^2(1-\gamma^2)\cos^2\varphi - 2k_x q_{||}(1-\gamma^2)\cos\varphi - \Delta_N(k_x)}, \tag{53}$$

where $a = (q_{||}^2/\lambda^2)\,[1-(1-\gamma^2)\cos^2\varphi]$ and $\lambda^2 = \tilde{\omega}_{\mathrm{c}}/\omega_{\mathrm{L}}$.

The goal of the present paper is to consider the Q1D magnetopolaron levels and energy–momentum relations below the phonon continuum and compare the results of the orthodox perturbation theories with that of Green's function technique. The resonant magnetopolaron effect, i.e. the resonance of the lowest one-phonon magnetopolaron level with the first excited zero-phonon magnetopolaron level for the case of zero momentum is analyzed in detail in Ref. [29]. The mostly used method for the calculation of the energy shifts at the resonance is the so-called *resonance approximation* (see e.g. [13,17]). Within this approach one only include the main contributing term to the sum over N' in Eq. (53) which is the term $N' = 0$. It is known that the resonance approximation leads to a slight up to a considerable overestimation of the energy shift (e.g. for strict 2D systems an overestimation of the level splitting of about 48% was found in Ref. [40] for $\alpha_{\mathrm{p}} = 0.07$ and $\omega_{\mathrm{c}} = \omega_{\mathrm{L}}$) and gives an upper limit for the correct value at the resonance. If applied for small magnetic fields unrealistic results for the polaronic corrections follow. Thus, in general one has to be very cautions in cutting the sum over N'. Unfortunately, here this approach is unsufficient because to calculate the energy–momentum relation we need $\Delta E_N(k_x)$ for all momenta and not only at the resonance. Fortunately, this calculation can be performed successfully. Below the phonon continuum $D_{N'N}(k_x, q_x) > 0$ is valid and

thus, it is possible to convert the denominator in Eq. (53) by the integral [59]

$$\frac{1}{D_{N'N}(k_x,\, q_x)} = \int_0^\infty \mathrm{d}t \exp[-D_{N'N}(k_x,\, q_x)t], \tag{54}$$

with the result

$$\Delta E_N(k_x) = -\frac{\alpha_\mathrm{p}}{2\pi}\int_0^\infty \mathrm{d}q_{||}\int_{-\pi}^{\pi}\mathrm{d}\varphi\, \mathrm{e}^{-a}\int_0^\infty \mathrm{d}t \exp\{-[1-\lambda^2 N + (1-\gamma^2)q_{||}^2\cos^2\varphi - 2(1-\gamma^2)k_x q_{||}\cos\varphi - \Delta_N(k_x)]t\}\sum_{N'=0}^{\infty}\frac{N_2!}{N_1!}a^{N_1-N_2}[L_{N_2}^{N_1-N_2}(a)]^2\mathrm{e}^{-\lambda^2 N' t}. \tag{55}$$

The sum over N' and the integral over $q_{||}$ can be performed analytically, e.g. for the lowest subband one obtains with the help of Ref. [60]

$$\Delta E_0(k_x) = -\alpha_\mathrm{p}\frac{\lambda}{\sqrt{\pi}}\int_0^{\pi/2}\mathrm{d}\varphi\int_0^\infty \mathrm{d}t\, \mathrm{e}^{-(1-\Delta_0(k_x))t} \times \frac{\exp\{\lambda^2 t^2 k_x^2(1-\gamma^2)^2\cos^2\varphi/[1-\mathrm{e}^{-\lambda^2 t}+(1-\gamma^2)\cos^2\varphi(\mathrm{e}^{-\lambda^2 t}+\lambda^2 t-1)]\}}{\sqrt{1-\mathrm{e}^{-\lambda^2 t}+(1-\gamma^2)\cos^2\varphi(\mathrm{e}^{-\lambda^2 t}+\lambda^2 t-1)}}. \tag{56}$$

To describe cyclotron resonance experiments on QWWs it is important to know $\Delta E_0(0)$ and $\Delta E_1(0)$, derived firstly in Ref. [29], which are given by

$$\Delta E_0(0) = -\alpha_\mathrm{p}\frac{\lambda}{\sqrt{\pi}}\int_0^\infty \mathrm{d}t\, \mathrm{e}^{-(1-\Delta_0(0))t}\frac{1}{\sqrt{\gamma^2(1-\mathrm{e}^{-\lambda^2 t})+(1-\gamma^2)\lambda^2 t}}\boldsymbol{K}\left(\sqrt{A(t)}\right) \tag{57}$$

and

$$\Delta E_1(0) = -\alpha_\mathrm{p}\frac{\lambda}{\sqrt{\pi}}\int_0^\infty \mathrm{d}t\, \mathrm{e}^{-(1-\Delta_1(0))t}\frac{1}{\sqrt{\gamma^2(1-\mathrm{e}^{-\lambda^2 t})+(1-\gamma^2)\lambda^2 t}} \times\left\{\boldsymbol{K}\left(\sqrt{A(t)}\right)+\frac{2\sinh^2(\lambda^2 t/2)}{\gamma^2(1-\mathrm{e}^{-\lambda^2 t})+(1-\gamma^2)\lambda^2 t)}\left[\gamma^2\boldsymbol{K}\left(\sqrt{A(t)}\right)+\lambda^2 t\left(\frac{1-\gamma^2}{[\gamma^2(1-\mathrm{e}^{-\lambda^2 t})+(1-\gamma^2)\lambda^2 t](\mathrm{e}^{-\lambda^2 t}+\lambda^2 t-1)}\right)^{1/2}\boldsymbol{K}'\left(\sqrt{A(t)}\right)\right]\right\}, \tag{58}$$

where

$$A(t) = \frac{(1-\gamma^2)(\mathrm{e}^{-\lambda^2 t}+\lambda^2 t-1)}{1-\mathrm{e}^{-\lambda^2 t}+(1-\gamma^2)(\mathrm{e}^{-\lambda^2 t}+\lambda^2 t-1)}, \tag{59}$$

$\boldsymbol{K}(x)$ is the complete elliptical integral of the first kind and $\boldsymbol{K}'(x) = \boldsymbol{E}(x)/[x(1-x^2)] - \boldsymbol{K}(x)/x$ is its first derivative, with $\boldsymbol{E}(x)$ the complete elliptical integral of the second kind.

If the lateral confinement potential vanishes, i.e. for $\Omega = 0$, which corresponds to $\gamma = 1$ and $\gamma^2 = \omega_\mathrm{c}/\omega_\mathrm{L}$, we obtain from Eq. (55) the 2D magnetopolaron self-energy in the form

$$\Delta E_N^{2\mathrm{D}}(k_x) = -\alpha_\mathrm{p}\int_0^\infty \mathrm{d}q_{||}\mathrm{e}^{-q_{||}/\lambda^2}\int_0^\infty \mathrm{d}t \exp\{-[1-\lambda^2 N - \Delta_N(k_x)]t\} \times\sum_{N'=0}^{\infty}\frac{N_2!}{N_1!}\left(\frac{q_{||}}{\lambda}\right)^{2(N1-N2)}\left[L_{N2}^{N1-N2}\left(\frac{q_{||}}{\lambda}\right)^2\right]^2\mathrm{e}^{-\lambda^2 N' t}. \tag{60}$$

The same expression follows from Eq. (55) in the limit $B \to \infty$. It becomes obvious that this expression is independent of k_x: $\Delta E_N^{2D}(k_x) \equiv \Delta E_N^{2D}$. This is true because electrons quantum confined in the x–y plane in the presence of a quantizing magnetic field are totally quantized in Landau levels. In Eq. (60) we can perform the integral over $q_{||}$, which gives with [61]

$$\Delta E_N^{2D} = -\alpha_p \frac{\lambda\sqrt{\pi}}{2}\int_0^\infty dt \exp\{-[1-\lambda^2 N - \Delta_N]t\} \sum_{N'=0}^{\infty} \frac{(2N_2)!(2(N_1-N_2))!}{(2^{N_1}(N_1-N_2)!N_2!)^2}$$

$$\times {}_3F_2\left(-N_2,\ N_1-N_2+\frac{1}{2},\ \frac{1}{2};\ 1+N_1-N_2,\ \frac{1}{2}-N_2;\ 1\right) e^{-\lambda^2 N' t}, \tag{61}$$

where ${}_3F_2(a_1, a_2, a_3; b_1, b_2; x)$ is a generalized hypergeometric function (or series). Please note that in Eq. (61) the integral over t may be resubstituted if one is interested in calculating the branch inside the phonon continuum. Similar expressions were found in Refs. [12,40]. With the help of the integral [62] one obtains directly from Eq. (60) (or alternatively from Eq. (61) by calculating the generalized hypergeometric function) the analytical result for the lowest Landau level

$$\Delta E_0^{2D} = -\alpha_p \frac{\sqrt{\pi}}{2\lambda} B\left(\frac{1-\Delta_0}{\lambda^2}, \frac{1}{2}\right), \tag{62}$$

where $B(x, y)$ is the beta function. In terms of the gamma function, $\Gamma(x)$, Eq. (62) reads

$$\Delta E_0^{2D} = -\alpha_p \frac{\pi}{2\lambda} \frac{\Gamma((1-\Delta_0)/\lambda^2)}{\Gamma((1-\Delta_0)/(\lambda^2+1/2))}. \tag{63}$$

This result was firstly obtained by Larsen [38]. It should be noted that the RSPT and IWBPT results for the energy correction ΔE_0^{2D} are identical because in both cases $\Delta_0 = 0$ is valid.

For the special case of a vanishing magnetic field ($B = 0$), Eqs. (55)–(58) are valid with $\gamma = 0$, $\lambda^2 = \Omega/\omega_L$ and $a = (q_{||}/\lambda)^2 \sin^2\varphi$:[2]

$$\Delta E_N(k_x) = -\frac{\alpha_p}{2\pi}\int_0^\infty dq_{||}\int_{-\pi}^{\pi} d\varphi\, e^{-a}\int_0^\infty dt \exp\{-[1-\lambda^2 N + q_{||}^2\cos^2\varphi - 2k_x q_{||}\cos\varphi - \Delta_N(k_x)]t\}$$

$$\times \sum_{N'=0}^{\infty} \frac{N_2!}{N_1!} a^{N1-N2}[L_{N2}^{N1-N2}(a)]^2\, e^{-\lambda^2 N' t}, \tag{64}$$

$$\Delta E_0(k_x) = -\frac{\alpha_p}{\sqrt{\pi}}\int_0^\infty dt \frac{e^{-(1-\Delta_0(k_x))t}}{\sqrt{t}}\int_0^{\pi/2} d\varphi \frac{\exp\{t k_x^2\cos^2\varphi/[1-A(t)|_{\gamma=0}\sin^2\varphi]\}}{\sqrt{1-A(t)|_{\gamma=0}\sin^2\varphi}}, \tag{65}$$

$$\Delta E_0(0) = -\frac{\alpha_p}{\sqrt{\pi}}\int_0^\infty dt \frac{e^{-(1-\Delta_0(0))t}}{\sqrt{t}} K\left(\sqrt{A(t)|_{\gamma=0}}\right), \tag{66}$$

$$\Delta E_1(0) = -\frac{\alpha_p}{\sqrt{\pi}}\int_0^\infty dt \frac{e^{-(1-\Delta_1(0))t}}{\sqrt{t}}\left\{K\left(\sqrt{A(t)|_{\gamma=0}}\right) + \frac{2\sinh^2(\lambda^2 t/2)}{\lambda^2 t\sqrt{A(t)|_{\gamma=0}}} K'\left(\sqrt{A(t)|_{\gamma=0}}\right)\right\}, \tag{67}$$

[2] We profit by this occasion to correct a misprint in Eq. (12) of our earlier paper [31].

where

$$A(t)|_{\gamma=0} = \frac{e^{-\lambda^2 t} + \lambda^2 t - 1}{\lambda^2 t}. \tag{68}$$

These equations were discussed in detail in Ref. [31]. Performing now the 2D limit (e.g. from Eq. (64) with [63]) one obtains the polaron correction to the 2D energy–momentum relation $\mathscr{E}_{2D}(k_x) = (1-\gamma^2)k_x^2$:

$$\Delta E_{2D}(k_x) = -\frac{\alpha_p}{\sqrt{1-\Delta_{2D}(k_x)}} \boldsymbol{K}\left(\frac{k_x}{\sqrt{1-\Delta_{2D}(k_x)}}\right). \tag{69}$$

This result was firstly discussed by Peeters et al. [42], who showed that $|\Delta E_{2D}(k_x)| \to \infty$ if $E_{2D}(k_x) - E_{2D}(0) \to 1$ and thus the 2D energy–momentum relation is pinned at this line. The RSPT result [20] is obtained with $\Delta_{2D}(k_x) = 0$ and is only valid for $k_x \ll k_L$. In the case of a vanishing wave vector component k_x, from Eq. (69) and with $\boldsymbol{K}(0) = \pi/2$ the result

$$\Delta E_{2D}(0) = -\frac{\alpha_p \pi}{2} \frac{1}{\sqrt{1-\Delta_{2D}(0)}} \tag{70}$$

follows. The RSPT and IWBPT energy corrections for the ground-state renormalization at $k_x = 0$ are identical and given by

$$\Delta E_{2D}(0) = -\alpha_p \frac{\pi}{2}, \tag{71}$$

and differ from that of the WBPT. The result of Eq. (71) was obtained originally in Ref. [64].

Before analyzing the Q1D magnetopolaron dispersion relations, obtained with the different standard quantum-mechanical perturbation theories in detail by numerical calculations, Green's function technique applied to QWWs is developed in the relevant Hilbert space, the subband space, to calculate the quasi-particle properties and compare it with the results of the standard quantum-mechanical perturbation theories.

4. Green's function technique: Feynman–Dyson perturbation theory

4.1. Dyson's equation for subband electrons

The *single-particle temperature* (*Matsubara*) *Green's function* of an electron in a many-particle system is defined as (see e.g. Refs. [65–67])

$$\begin{aligned}\mathscr{G}_{\alpha\beta}(\boldsymbol{x}, \boldsymbol{x}'|\tau, \tau') &= -\frac{1}{\hbar} \mathrm{Tr}\{\hat{\rho}_G T_\tau \hat{\Psi}_\alpha(\boldsymbol{x}, \tau)\hat{\Psi}^\dagger_\beta(\boldsymbol{x}', \tau')\} \\ &= -\frac{1}{\hbar}\langle T_\tau \hat{\Psi}_\alpha(\boldsymbol{x}, \tau)\hat{\Psi}^\dagger_\beta(\boldsymbol{x}', \tau')\rangle,\end{aligned} \tag{72}$$

where $\boldsymbol{x}$ or $\boldsymbol{x}'$ denote the spatial coordinates and α or β the spin coordinates. In Eq. (72), $\hat{\Psi}_\alpha(\boldsymbol{x}, \tau)$ is the electron field operator ($\hat{\Psi}_\alpha$ denotes the destruction and $\hat{\Psi}^\dagger_\alpha$ denotes the creation operator) in the (modified) Heisenberg picture, satisfying the anticommutation relations $[\hat{\Psi}_\alpha(\boldsymbol{x}), \hat{\Psi}^\dagger_\beta(\boldsymbol{x})']_+ = \delta_{\alpha\beta}\delta(\boldsymbol{x}-\boldsymbol{x}')$ and $[\hat{\Psi}^\dagger_\alpha(\boldsymbol{x}), \hat{\Psi}^\dagger_\beta(\boldsymbol{x})']_+ = [\hat{\Psi}_\alpha(\boldsymbol{x}), \hat{\Psi}_\beta(\boldsymbol{x}')]_+ = 0$, where $[\ldots]_+$ denotes the anticommutator. The symbol Tr denotes the trace, i.e. a sum

over a complete set of states in the Hilbert space, each contribution beeing weighted with the operator $\hat{\rho}_G$ and T_τ is the Wick time-order symbol, which orders the operators according to their value of τ (the "*imaginary time*") with the smallest one at the right-hand side. It includes the signature factor $(-1)^P$, where P is the number of permutations of Fermion operators needed to restore the original ordering. Further, $\hat{\rho}_G$ is the *statistical operator* of a grand canonical ensemble

$$\hat{\rho}_G = \frac{e^{-\beta(\hat{H}_p - \mu\hat{N})}}{\mathrm{Tr}\{e^{-\beta(\hat{H}_p - \mu\hat{N})}\}} \tag{73}$$

with $\beta = 1/(k_B T)$ and μ is the chemical potential. Herein, $\hat{H}_p$ is the magnetopolaron Hamiltonian and $\hat{N}$ is the total electron number operator. In this chapter all operators are used in the representation of the second quantization (denoted by the symbol " $\hat{}$ "). Thus, the statistical effects of the many-magnetopolaron problem are incorporated automatically. The magnetopolaron Hamiltonian $\hat{H}_p$ in the representation of the second quantization reads

$$\hat{H}_p = \sum_\alpha \int d^3x \hat{\Psi}^\dagger_\alpha(\boldsymbol{x}) H_p \hat{\Psi}_\alpha(\boldsymbol{x}). \tag{74}$$

The *particle-density operator* is

$$\hat{n}(\boldsymbol{x}) = \sum_\alpha \hat{\Psi}^\dagger_\alpha(\boldsymbol{x})\hat{\Psi}_\alpha(\boldsymbol{x}) \tag{75}$$

and the *spin-density operator* reads

$$\hat{\boldsymbol{\sigma}}(\boldsymbol{x}) = \sum_{\alpha,\beta} \hat{\Psi}^\dagger_\alpha(\boldsymbol{x})\boldsymbol{\sigma}_{\alpha\beta}\hat{\Psi}^\dagger_\beta(\boldsymbol{x}), \tag{76}$$

where $\boldsymbol{\sigma}_{\alpha\beta} = (\sigma_x^{\alpha\beta}, \sigma_y^{\alpha\beta}, \sigma_z^{\alpha\beta})$ stands for the matrix elements of the Pauli spin operator. Then, the *total electron number operator* is

$$\hat{N} = \sum_\alpha \int d^3x \hat{\Psi}^\dagger_\alpha(\boldsymbol{x})\hat{\Psi}_\alpha(\boldsymbol{x}), \tag{77}$$

with which one can write

$$\begin{aligned} \hat{K}_p &= \hat{H}_p - \mu\hat{N}, \\ \hat{\rho}_G &= \frac{e^{-\beta\hat{K}_p}}{Z_G} = e^{\beta(\Omega - \hat{K}_p)}, \\ Z_G &= \mathrm{Tr}\{e^{-\beta\hat{K}_p}\} = e^{-\beta\Omega}, \end{aligned} \tag{78}$$

where here, $\Omega = \Omega(T, V, \mu)$ denotes the *thermodynamical potential* and Z_G is the *grand partition function*. The electron field operator can be represented by the closed set of single-particle electronic states $\{|N, k_x, m_s\rangle\}$ of the QWW:

$$\hat{\Psi}_\alpha(\boldsymbol{x}) = \sum_{N,k_x,m_s} \Psi_{Nk_xm_s}(\boldsymbol{x}, \alpha)\hat{c}_{Nk_xm_s}, \tag{79}$$

$$\hat{\Psi}^\dagger_\alpha(\boldsymbol{x}) = \sum_{N,k_x,m_s} \Psi^*_{Nk_xm_s}(\boldsymbol{x}, \alpha)\hat{c}^\dagger_{Nk_xm_s}, \tag{80}$$

where $\hat{c}_{Nk_xm_s}(\hat{c}^{\dagger}_{Nk_xm_s})$ is the destruction (creation) operator of an electron of the QWW with the quantum numbers $\{N, k_x, m_s\}$, satisfying

$$[\hat{c}_{Nk_xm_s}, \hat{c}^{\dagger}_{N'k'_xm'_s}]_+ = \delta_{NN'}\delta_{k_xk'_x}\delta_{m_sm'_s},$$
$$[\hat{c}^{\dagger}_{Nk_xm_s}, \hat{c}^{\dagger}_{N'k'_xm'_s}]_+ = [\hat{c}_{Nk_xm_s}, \hat{c}_{N'k'_xm'_s}]_+ = 0. \tag{81}$$

As usual the time dependence in the (modified) Heisenberg picture is given by

$$\hat{\Psi}_{\alpha}(\boldsymbol{x}, \tau) = \mathrm{e}^{(\hat{H}_{\mathrm{p}} - \mu\hat{N})\tau/\hbar}\hat{\Psi}_{\alpha}(\boldsymbol{x})\mathrm{e}^{-(\hat{H}_{\mathrm{p}} - \mu\hat{N})\tau/\hbar}. \tag{82}$$

In the here considered case $\hat{H}_{\mathrm{p}}$ is time independent and hence, $\mathscr{G}_{\alpha\beta}(\boldsymbol{x}, \boldsymbol{x}' \,|\, \tau, \tau')$ only depends on the difference $\tau - \tau'$. Using the periodicity of $\mathscr{G}_{\alpha\beta}(\boldsymbol{x}, \boldsymbol{x}' \,|\, \tau) = \mathscr{G}_{\alpha\beta}(\boldsymbol{x}, \boldsymbol{x}' \,|\, \tau + 2\beta\hbar)$ in the time variable, it follows

$$\mathscr{G}_{\alpha\beta}(\boldsymbol{x}, \boldsymbol{x}'|\tau) = \frac{1}{\beta\hbar}\sum_n \mathrm{e}^{-\mathrm{i}\nu_n\tau}\mathscr{G}_{\alpha\beta}(\boldsymbol{x}, \boldsymbol{x}'|\mathrm{i}\nu_n), \tag{83}$$

$$\mathscr{G}_{\alpha\beta}(\boldsymbol{x}, \boldsymbol{x}'|\mathrm{i}\nu_n) = \int_0^{\beta\hbar} \mathrm{d}\tau\, \mathrm{e}^{\mathrm{i}\nu_n\tau}\mathscr{G}_{\alpha\beta}(\boldsymbol{x}, \boldsymbol{x}'|\tau), \tag{84}$$

where the frequency ν_n, called *Matsubara frequency* of the electron, is $\nu_n = (2n + 1)\pi/(\beta\hbar)$ with $n = 0, \pm 1, \pm 2, \ldots$. Using the field operators of the Q1D electrons in Eq. (72) it follows

$$\mathscr{G}_{\alpha\beta}(\boldsymbol{x}, \boldsymbol{x}'|\mathrm{i}\nu_n) = \frac{1}{L_x}\sum_{k_x} \mathrm{e}^{\mathrm{i}k_x(x-x')} \sum_{N,N'} \sum_{m_s,m'_s} \Phi_N(y - Y_{k_x})\, \Phi^*_{N'}(y' - Y_{k_x})\, \delta(z)\, \chi_{m_s}(\alpha)\, \chi^*_{m'_s}(\beta)\, \mathscr{G}_{\substack{N \\ m_s}\ \substack{N' \\ m'_s}}(k_x, \mathrm{i}\nu_n), \tag{85}$$

where

$$\mathscr{G}_{\substack{N \\ m_s}\ \substack{N' \\ m'_s}}(k_x, \mathrm{i}\nu_n) = \int_0^{\beta\hbar} \mathrm{d}\tau\, \mathrm{e}^{\mathrm{i}\nu_n\tau}\left[-\frac{1}{\hbar}\mathrm{Tr}\{\hat{\rho}_G T_\tau \hat{c}_{k_xNm_s}(\tau)\hat{c}^{\dagger}_{k_xN'm'_s}(0)\}\right] \tag{86}$$

is the *electron matrix Green's function* in the *subband space* [68]. Because of the property $\chi_{m_s}(\alpha) = \delta_{\alpha m_s}$ the spin summation can be performed with the result $\mathscr{G}_{\substack{N \\ m_s}\ \substack{N' \\ m'_s}} \Rightarrow \mathscr{G}_{\substack{N \\ \alpha}\ \substack{N' \\ \beta}}$ in Eq. (85). Thus, α,β are used in the following as spin indices quite generally. The *unperturbed* or *non-interacting* matrix Green's function results for $\hat{H}_{\mathrm{p}} \to \hat{H}_{\mathrm{e}}$ and is given by

$$\mathscr{G}^{(0)}_{\substack{N \\ \alpha}\ \substack{N' \\ \beta}}(k_x, \mathrm{i}\nu_n) = \frac{\delta_{\alpha\beta}\delta_{NN'}}{\mathrm{i}\hbar\nu_n - [\mathscr{E}_{N\alpha}(k_x) - \mu]} \equiv \delta_{\alpha\beta}\delta_{NN'}\mathscr{G}_{NN;\alpha}(k_x, \mathrm{i}\nu_n). \tag{87}$$

From the spectral representation of the Matsubara Green's function

$$\mathscr{G}_{\alpha\beta}(\boldsymbol{x}, \boldsymbol{x}'|\mathrm{i}\nu_n) = \int_{-\infty}^{\infty} \mathrm{d}E \frac{A_{\alpha\beta}(\boldsymbol{x}, \boldsymbol{x}'|E)}{\mathrm{i}\hbar\nu_n - E}, \tag{88}$$

where for the *spectral function* $A_{\alpha\beta}(\boldsymbol{x}, \boldsymbol{x}'|E)$

$$\int_{-\infty}^{\infty} \mathrm{d}E\, A_{\alpha\beta}(\boldsymbol{x}, \boldsymbol{x}'|E) = \delta_{\alpha\beta}\delta(\boldsymbol{x} - \boldsymbol{x}') \tag{89}$$

is valid, it follows with

$$A_{\alpha\beta}(\boldsymbol{x}, \boldsymbol{x}'|E) = \frac{1}{L_x}\sum_{k_x} \mathrm{e}^{\mathrm{i}k_x(x-x')} \sum_{N,N'} \Phi_N(y - Y_{k_x})\, \Phi^*_{N'}(y' - Y_{k_x})\, \delta(z)\, A_{\substack{N \\ \alpha}\ \substack{N' \\ \beta}}(k_x, E) \tag{90}$$

the spectral representation of the matrix Green's function in subband space

$$\mathscr{G}_{\substack{N\\ \alpha}\ \substack{N'\\ \beta}}(k_x, \mathrm{i}\nu_n) = \int_{-\infty}^{\infty} \mathrm{d}E \frac{A_{\substack{N\\ \alpha}\ \substack{N'\\ \beta}}(k_x, E)}{\mathrm{i}\hbar\nu_n - E}. \tag{91}$$

The matrix spectral function obeys the equation

$$\int_{-\infty}^{\infty} \mathrm{d}E\, A_{\substack{N\\ \alpha}\ \substack{N'\\ \beta}}(k_x, E) = \delta_{\alpha\beta}\delta_{NN'}. \tag{92}$$

The matrix spectral function $A_{\substack{N\\ \alpha}\ \substack{N'\\ \beta}}(k_x, E)$ is the probability that an electron moves from the state $|N', \beta\rangle$ to the state $|N,\alpha\rangle$ with momentum $p_x = \hbar k_x$ and energy E. Obviously, the free electron matrix spectral function is

$$A^{(0)}_{\substack{N\\ \alpha}\ \substack{N'\\ \beta}}(k_x, E) = \delta_{\alpha\beta}\ \delta_{NN'}\ \delta(E - \mathscr{E}_{N\alpha}(k_x) + \mu). \tag{93}$$

The *dressed* or *exact Green's function* of a single electron in the QWW in the presence of a quantizing magnetic field interacting with LO phonons obeys the *Dyson equation*

$$\begin{aligned}\mathscr{G}_{\alpha\beta}(\boldsymbol{x}, \boldsymbol{x}'|\tau, \tau') = \mathscr{G}^{(0)}_{\alpha\beta}(\boldsymbol{x}, \boldsymbol{x}'|\tau, \tau') + \sum_{\sigma,\sigma'} \int \mathrm{d}^3x'' \int \mathrm{d}^3x''' \int_0^{\beta\hbar} \mathrm{d}\tau'' \int_0^{\beta\hbar} \mathrm{d}\tau'''\mathscr{G}^{(0)}_{\alpha\sigma}(\boldsymbol{x}, \boldsymbol{x}''|\tau, \tau'')\\ \times \Sigma_{\sigma\sigma'}(\boldsymbol{x}'', \boldsymbol{x}'''|\tau'', \tau''')\mathscr{G}_{\sigma'\beta}(\boldsymbol{x}''', \boldsymbol{x}'|\tau''', \tau'),\end{aligned} \tag{94}$$

where $\Sigma_{\alpha\beta}(\boldsymbol{x}, \boldsymbol{x}'|\tau, \tau')$ is the *irreducible* or *proper* (Matsubara) *self-energy*. In the subband space Dyson's equation reads [68]

$$\mathscr{G}_{\substack{N\\ \alpha}\ \substack{N'\\ \beta}}(k_x, \mathrm{i}\nu_n) = \mathscr{G}^{(0)}_{\substack{N\\ \alpha}\ \substack{N'\\ \beta}}(k_x, \mathrm{i}\nu_n) + \sum_{N_1,N_1'} \sum_{\sigma,\sigma'} \mathscr{G}^{(0)}_{\substack{N\\ \alpha}\ \substack{N_1\\ \sigma}}(k_x, \mathrm{i}\nu_n)\Sigma_{\substack{N_1\\ \sigma}\ \substack{N_1'\\ \sigma'}}(k_x, \mathrm{i}\nu_n)\mathscr{G}_{\substack{N_1'\\ \sigma'}\ \substack{N'\\ \beta}}(k_x, \mathrm{i}\nu_n). \tag{95}$$

This equation represents a very complicated system of algebraic equations. The different elements of this equation and Dyson's equation itself are graphically shown in Figs. 3 and 4, respectively.

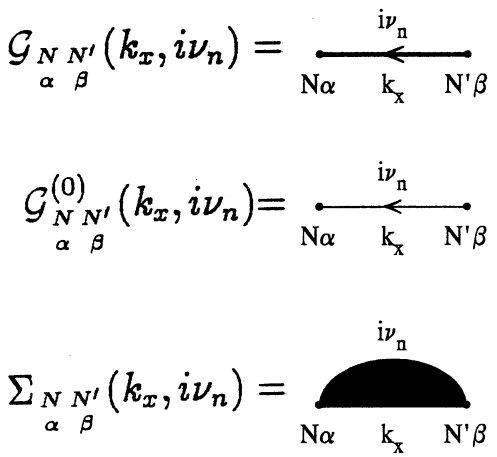

Fig. 3. Diagrammatic representation of the matrix Green's function and of the irreducible matrix self-energy in the subband space.

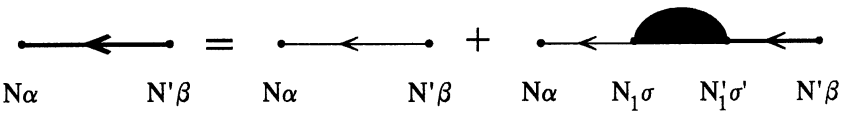

Fig. 4. Diagrammatic representation of the Dyson equation for $\mathscr{G}_{\substack{N \\ \alpha}\ \substack{N' \\ \beta}}(k_x, \mathrm{i}\nu_n)$ in the subband space.

4.2. Quasi-particles in the subband space

In the here considered case the spin is a good quantum number and thus, $\mathscr{G}_{\substack{N \\ \alpha}\ \substack{N' \\ \beta}}(k_x, \mathrm{i}\nu_n) = \delta_{\alpha\beta}\mathscr{G}_{NN';\alpha}(k_x, \mathrm{i}\nu_n)$ is valid. After performing the frequency sum, when calculating the Green's function $\mathscr{G}_{NN';\alpha}(k_x,\mathrm{i}\nu_n)$, one has to perform the analytic continuation to the *retarded* Green's function $G^{\mathrm{R}}_{NN';\alpha}(k_x, E)$ by performing the change $\mathrm{i}\hbar\nu_n \to E + \mathrm{i}\delta$ for an electron in the Fermi sea or by $\mathrm{i}\hbar\nu_n \to E - \mu + \mathrm{i}\delta$ for a single electron in the QWW and subsequently let $\delta \to 0^+$. Using Eq. (87) in Eq. (95) we obtain

$$\sum_{N_1} \{E\delta_{NN_1} - [(\mathscr{E}_{N\alpha}(k_x) - \mu)\delta_{NN_1} + \Sigma^{\mathrm{R}}_{NN_1;\alpha}(k_x, E)]\} G^{\mathrm{R}}_{N_1N';\alpha}(k_x, E) = \delta_{NN'}. \tag{96}$$

For further work it is useful to introduce the abbreviation

$$M_{NN_1;\alpha}(k_x, E) = E\delta_{NN_1} - [(\mathscr{E}_{N\alpha}(k_x) - \mu)\delta_{NN_1} + \Sigma^{\mathrm{R}}_{NN_1;\alpha}(k_x, E)]. \tag{97}$$

To solve the algebraic system of equations, Eq. (96), one further approximation is necessary. In principle for this there are two different possibilities:

1. *diagonal approximation*: $\Sigma^{\mathrm{R}}_{NN';\alpha}(k_x, E) = \delta_{NN'}\Sigma^{\mathrm{R}}_{NN;\alpha}(k_x, E)$,
2. *multi-subband model*: $N = 0, 1, 2, \ldots, M-1$.

It is obvious that the diagonal approximation can only be applied if the *intersubband coupling* (ISC) due to electron motion between different subbands, induced by the EPI, is weak. In many cases however, the diagonal approximation is well justified because the non-diagonal matrix elements of the self-energy are usually only 1–10% in magnitude of the diagonal one. Using the *diagonal approximation* we obtain from Eq. (96)

$$G^{\mathrm{R}}_{NN';\alpha}(k_x, E) = \frac{\delta_{NN'}}{E - \mathscr{E}_{N\alpha}(k_x) + \mu - \Sigma^{\mathrm{R}}_{NN;\alpha}(k_x, E)}. \tag{98}$$

With

$$G^{\mathrm{R}}_{NN';\alpha}(k_x, E) = \int_{-\infty}^{\infty} \mathrm{d}E' \frac{A_{NN';\alpha}(k_x, E')}{E - E' + \mathrm{i}\delta} \tag{99}$$

and

$$A_{NN';\alpha}(k_x, E') = -\frac{1}{\pi} \mathrm{Im}\, G^{\mathrm{R}}_{NN';\alpha}(k_x, E), \tag{100}$$

one obtains

$$A_{NN';\alpha}(k_x, E) = -\frac{1}{\pi} \frac{\mathrm{Im}\, \Sigma^{\mathrm{R}}_{NN;\alpha}(k_x, E)}{[E - \mathscr{E}_{N\alpha}(k_x) - \mathrm{Re}\, \Sigma^{\mathrm{R}}_{NN;\alpha}(k_x, E)]^2 + [\mathrm{Im}\, \Sigma^{\mathrm{R}}_{NN;\alpha}(k_x, E)]^2}, \tag{101}$$

where Re means real part and Im imaginary part.

On the other hand, for a *multi-subband model*, from Eqs. (96) and (97) it follows

$$\boldsymbol{G}^{\mathrm{R}}(k_x, E) = \boldsymbol{M}^{-1}(k_x, E), \tag{102}$$

which gives, e.g. for a two-subband model the following matrix elements $G^{\mathrm{R}}_{NN';\alpha}(k_x, E)$ of the Green's function $\boldsymbol{G}^{\mathrm{R}}(k_x, E) = (G^{\mathrm{R}}_{NN';\alpha}(k_x, E))$ in subband space:

$$G^{\mathrm{R}}_{00;\alpha}(k_x, E) = \frac{E - \mathscr{E}_{1\alpha}(k_x) + \mu - \Sigma^{\mathrm{R}}_{11;\alpha}(k_x, E)}{\Lambda_\alpha(k_x, E)}, \tag{103}$$

$$G^{\mathrm{R}}_{01;\alpha}(k_x, E) = \frac{\Sigma^{\mathrm{R}}_{01;\alpha}(k_x, E)}{\Lambda_\alpha(k_x, E)}, \tag{104}$$

$$G^{\mathrm{R}}_{10;\alpha}(k_x, E) = \frac{\Sigma^{\mathrm{R}}_{10;\alpha}(k_x, E)}{\Lambda_\alpha(k_x, E)}, \tag{105}$$

$$G^{\mathrm{R}}_{11;\alpha}(k_x, E) = \frac{E - \mathscr{E}_{0\alpha}(k_x) + \mu - \Sigma^{\mathrm{R}}_{00;\alpha}(k_x, E)}{\Lambda_\alpha(k_x, E)}, \tag{106}$$

where the denominator is given by

$$\begin{aligned}\Lambda_\alpha(k_x, E) = {} & (E - \mathscr{E}_{0\alpha}(k_x) + \mu - \Sigma^{\mathrm{R}}_{00;\alpha}(k_x, E))\,(E - \mathscr{E}_{1\alpha}(k_x) + \mu - \Sigma^{\mathrm{R}}_{11;\alpha}(k_x, E)) \\ & - \Sigma^{\mathrm{R}}_{01;\alpha}(k_x, E)\Sigma^{\mathrm{R}}_{10;\alpha}(k_x, E).\end{aligned} \tag{107}$$

The Q1D magnetopolaron is a quasi-particle and thus, we have to look to the quasi-particle poles of the Green's function in subband space. For obvious reasons the Green's function $\boldsymbol{G}^{\mathrm{R}}(k_x, E)$ using a M-subband model has $2M$ *isolated single poles* at the complex energies $E_\eta(k_x) - \mu - \mathrm{i}\Gamma_\eta(k_x)$; $\eta = 1, 2, \ldots, 2M$ connected with subband ($N = 0, 1, \ldots, M-1$) and spin index ($\alpha = \pm\frac{1}{2}$). From the theory of complex functions it follows that the Green's function can be represented in the following form:[3]

$$G^{\mathrm{R}}_{NN';\alpha}(k_x, E) = \sum_{\eta=1}^{2M} \frac{z^{NN';\alpha}_\eta(k_x)}{E - E_\eta(k_x) + \mu + \mathrm{i}\Gamma_\eta(k_x)} + g^{\mathrm{inc}}_{NN';\alpha}(k_x, E), \tag{108}$$

where $z^{NN';\alpha}_\eta(k_x)$ is the residue of $G^{\mathrm{R}}_{NN';\alpha}(k_x,E)$ at the pole $E = E_\eta - \mu - \mathrm{i}\Gamma_\eta$. The so-called incoherent part $g^{\mathrm{inc}}_{NN';\alpha}(k_x, E)$, describing the background, is a slowly varying function and is finite at the poles. Thus, it is usually neglected for energies close to the poles. If, and only if $\Gamma_\eta(k_x) \ll |E_\eta(k_x) - \mu|$ is valid, i.e. the poles occur very close to the real axis, the states are *true quasi-particle states*. In this case Q1D magnetopolarons are formed with large *life-times* $\tau_\eta(k_x) = (2\Gamma_\eta(k_x))^{-1}$. Their energies and damping functions are determined from the equation[4]

$$\det[M_{NN';\alpha}(k_x, E_\eta(k_x) - \mu - \mathrm{i}\Gamma_\eta(k_x))|_{\Sigma^{\mathrm{R}}_{NN';\alpha}(k_x, E_\eta(k_x)-\mu)}] = 0 \tag{109}$$

and

$$z^{NN';\alpha}_\eta(k_x) = \operatorname*{Res}_{E = E_\eta(k_x) - \mu} \{(\boldsymbol{M}^{-1}(k_x, E))_{NN';\alpha}\}, \tag{110}$$

[3] This representation is true because the function $f(z) = G^{\mathrm{R}}_{NN';\alpha}(k_x,z) - g^{\mathrm{inc}}_{NN';\alpha}(k_x,z)$ with $z \in \mathbb{C}$ is in general a meromorphic function, or more specific a rational function, if the number of poles is finite. A meromorphic function $f(z)$ with only single poles at $z = z_\nu$ can be represented as $f(z) = \sum_\nu \mathrm{Res}_{z=z_\nu} f(z)/(z - z_\nu) + g(z)$, where $g(z)$ is an entire function, which is assumed to be incorporated into $g^{\mathrm{inc}}_{NN';\alpha}(k_x, E)$ in Eq. (108).

[4] Please note $(M^{-1})_{ij}$ = cofactor of $M_{ji}/\det[M_{ij}]$, where the cofactor of M_{ji} equals $(-1)^{i+j}$ times the determinant of the matrix which $\boldsymbol{M}$ becomes if its jth row and ith column are deleted.

where $(\boldsymbol{M}^{-1})_{NN';\alpha}$ denotes the $(NN';\alpha)$th element of $\boldsymbol{M}^{-1}$, Res means the residue at the pole and in the self-energy $\Gamma_\eta \to 0$ is assumed. Then, it follows for the spectral function

$$A_{NN';\alpha}(k_x, E) \approx \frac{1}{\pi} \sum_{\eta=1}^{2M} \frac{z_\eta^{NN';\alpha}(k_x)\Gamma_\eta(k_x)}{[E - E_\eta(k_x) + \mu]^2 + \Gamma_\eta^2(k_x)}, \tag{111}$$

where the " $\approx$ " sign results from the fact that the incoherent part is neglected. If the quasi-particle damping is vanishingly small, the Lorentz profile becomes a sharp delta peak:

$$A_{NN';\alpha}(k_x, E) \approx \sum_{\eta=1}^{2M} z_\eta^{NN';\alpha}(k_x)\ \delta(E - E_\eta(k_x) + \mu). \tag{112}$$

Here, $z_\eta^{NN';\alpha}(k_x)$ is called the *renormalization factor* of the quasi-particle. For a free, or non-interacting particle, we have $E = \mathscr{E}_{N\alpha}(k_x)$ so that the probability distribution is a delta function and hence, there is only one value E for each $\mathscr{E}_{N\alpha}(k_x)$ and vice versa (see Eq. (93). For interacting systems, however, there is a band of E values for each k_x, described by Eq. (111). For a weakly interacting system the quasi-particle energy becomes sharp and Eq. (112) is valid. In the *quasi-particle approximation* (QPA) one uses the matrix spectral function, given by Eq. (112), in the whole spectrum, i.e. with Eq. (92) the *sum rule*

$$\sum_{\eta=1}^{2M} z_\eta^{NN';\alpha}(k_x) = \delta_{NN'} \tag{113}$$

becomes valid.

Let us consider the special case of a two-subband model. The quasi-particle energies and damping functions follow from the equation:

$$\begin{aligned}&[E_\eta - \mathrm{i}\Gamma_\eta(k_x) - \mathscr{E}_{0\alpha}(k_x) - \mathrm{Re}\,\Sigma^{\mathrm{R}}_{00;\alpha}(k_x, E_\eta - \mu) - \mathrm{i}\ \mathrm{Im}\,\Sigma^{\mathrm{R}}_{00;\alpha}(k_x, E_\eta - \mu)]\\ &\quad\times[E_\eta - \mathrm{i}\Gamma_\eta(k_x) - \mathscr{E}_{1\alpha}(k_x) - \mathrm{Re}\,\Sigma^{\mathrm{R}}_{11;\alpha}(k_x, E_\eta - \mu) - \mathrm{i}\ \mathrm{Im}\,\Sigma^{\mathrm{R}}_{11;\alpha}(k_x, E_\eta - \mu)] - [\mathrm{Re}\,\Sigma^{\mathrm{R}}_{01;\alpha}(k_x, E_\eta - \mu)\\ &\quad+ \mathrm{i}\ \mathrm{Im}\,\Sigma^{\mathrm{R}}_{01;\alpha}(k_x, E_\eta - \mu)][\mathrm{Re}\,\Sigma^{\mathrm{R}}_{10;\alpha}(k_x, E_\eta - \mu) + \mathrm{i}\ \mathrm{Im}\,\Sigma^{\mathrm{R}}_{10;\alpha}(k_x, E_\eta - \mu)] = 0\end{aligned} \tag{114}$$

and the residues at these poles follow from Eqs. (103)–(106) with standard technique.

In the case of the diagonal approximation we obtain for the energy–momentum relation

$$E_{N\alpha}(k_x) = \mathscr{E}_{N\alpha}(k_x) + \mathrm{Re}\,\Sigma^{\mathrm{R}}_{NN;\alpha}(k_x, E_{N\alpha}(k_x) - \mu) \tag{115}$$

and for the damping function

$$\Gamma_{N\alpha}(k_x) = -\mathrm{Im}\,\Sigma^{\mathrm{R}}_{NN;\alpha}(k_x, E_{N\alpha}(k_x) - \mu). \tag{116}$$

Thus, in this case we have

$$G^{\mathrm{R}}_{NN;\alpha}(k_x, E) = \frac{z_{N\alpha}(k_x)}{E - E_{N\alpha}(k_x) + \mu + \mathrm{i}\Gamma_{N\alpha}(k_x)}, \tag{117}$$

$$A_{NN;\alpha}(k_x, E) = \frac{1}{\pi}\frac{z_{N\alpha}(k_x)\Gamma_{N\alpha}(k_x)}{[E - E_{N\alpha}(k_x) + \mu]^2 + \Gamma^2_{N\alpha}(k_x)}, \tag{118}$$

with

$$z_{N\alpha}(k_x) = \frac{1}{1 - (\partial/\partial E)\Sigma^{\mathrm{R}}_{NN;\alpha}(k_x, E)|_{E = E_{N\alpha}(k_x) - \mu}}. \tag{119}$$

It is obvious that the quasi-particle picture is only valid if $|\mathscr{E}_{N\alpha} - \mu + \mathrm{Re}\,\Sigma^{\mathrm{R}}_{NN;\alpha}| \gg |\mathrm{Im}\,\Sigma^{\mathrm{R}}_{NN;\alpha}|$. In the QPA, $z_{N\alpha}(k_x) = 1$ and henceforth, we obtain

$$A_{NN;\alpha}(k_x, E) = \delta(E - E_{N\alpha}(k_x) + \mu). \tag{120}$$

The above results for the diagonal approximation follow from that of the general case with $z^{NN';\alpha}_{\eta}(k_x) = \delta_{NN'}\delta_{\eta N} z_{N\alpha}(k_x)$.

From the energy–momentum relation $E_\eta(k_x)$ one can calculate the magnetopolaron effective mass of subband η:

$$\frac{1}{\tilde{m}^*_\eta} = \lim_{k_x\to 0} \frac{1}{k_x\hbar^2}\frac{\mathrm{d}}{\mathrm{d}k_x} E_\eta(k_x), \tag{121}$$

which gives in the diagonal approximation

$$\begin{aligned}\frac{\tilde{m}_\mathrm{e}}{\tilde{m}^*_{N\alpha}} &= \lim_{k_x\to 0}\left\{\frac{1 + \tilde{m}_\mathrm{e}/(k_x\hbar^2)\,(\partial/\partial k_x)\,\mathrm{Re}\,\Sigma^{\mathrm{R}}_{NN;\alpha}(k_x,\, E_{N\alpha}(0))}{1 - (\partial/\partial E)\,\mathrm{Re}\,\Sigma^{\mathrm{R}}_{NN;\alpha}(k_x,\, E)|_{E=E_{N\alpha}(0)-\mu}}\right\}\\ &= \lim_{k_x\to 0} z_{n\alpha}(k_x)\left\{1 + \frac{\tilde{m}_\mathrm{e}}{k_x\hbar^2}\frac{\partial}{\partial k_x}\mathrm{Re}\,\Sigma^{\mathrm{R}}_{NN;\alpha}(k_x,\, E_{N\alpha}(0))\right\}.\end{aligned} \tag{122}$$

One further approach in calculating the magnetopolaronic renormalization of the electronic subbands is the *on-mass-shell approximation* (OMS). Energy E and canonical momentum $p_{\mathrm{e}_x} = \hbar k_x$ of the self-energy $\Sigma^{\mathrm{R}}_{NN;\alpha}(k_x,E)$ are no longer considered as separate variables. In evaluating $\Sigma^{\mathrm{R}}_{NN;\alpha}(k_x,\, E)$ the energy E is set equal to $\mathscr{E}_{N\alpha}(k_x)$ with the result $\Sigma^{\mathrm{R}}_{NN;\alpha}(k_x,\, E) \Rightarrow \Sigma^{\mathrm{OMS}}_{NN;\alpha}(k_x)$. Of course, if $\mathrm{Im}\,\Sigma^{\mathrm{R}}_{NN;\alpha}(k_x,\, E) = 0$, the energy and momentum are always uniquely related by Eq. (115). In the on-mass-shell approximation the magnetopolaron effective mass using the diagonal approximation is given by

$$\frac{\tilde{m}_\mathrm{e}}{\tilde{m}^*_{N\alpha}} = 1 + \frac{\tilde{m}_\mathrm{e}}{k_x\hbar^2}\frac{\mathrm{d}}{\mathrm{d}k_x}\mathrm{Re}\,\Sigma^{\mathrm{OMS}}_{NN;\alpha}(k_x)|_{k_x=0}. \tag{123}$$

4.3. Tamm–Dancoff approximation for the self-energy in subband space

The irreducible self-energy contains an infinite number of different Feynman diagrams. In the Feynman–Dyson perturbation theory a finite number of irreducible Feynman graphs is used in Dyson's equation. This equation arises from the S-matrix expansion of $\mathscr{G}_{\alpha\beta}(\boldsymbol{x}, \boldsymbol{x}'|\tau)$ in powers of the interaction Hamiltonian. If one uses the electron–phonon interaction Hamiltonian in this expansion we can average the electron and phonon operators separately. Only those terms with an even number of H_{ep} are non-vanishing and thus, the Feynman diagrams for the electron Green's function turn out to be the same as for a two-particle interaction between electrons. The only difference is that here the two-particle interaction potential is

$$V^{\mathrm{ph}}_{\gamma\gamma'\delta\delta'}(\boldsymbol{x}_1, \boldsymbol{x}_2|\tau_1, \tau_2) = \delta_{\gamma\gamma'}\delta_{\delta\delta'}\left\{-\frac{1}{\hbar}\,{}_0\langle \mathrm{T}_\tau \hat{H}_{\mathrm{ep}}(\boldsymbol{x}_1, \tau_1)\hat{H}_{\mathrm{ep}}(\boldsymbol{x}_2, \tau_2)\rangle\right\}, \tag{124}$$

i.e. a *phonon-mediated electron–electron interaction potential*, where ${}_0\langle \cdots \rangle \equiv \mathrm{Tr}\{\hat{\rho}^{(0)}_{\mathrm{G}} \ldots\}$ means averaging over the unperturbed system $\hat{H}_{\mathrm{p}} \to \hat{H}_0 = \hat{H}_{\mathrm{e}} + \hat{H}_{\mathrm{ph}}$. Herein, $\hat{H}_{\mathrm{ep}}(\boldsymbol{x}, \tau)$ is the EPI Hamiltonian, given by Eq. (19) for the here considered case with phonon operators in the (modified) interaction picture. Using this Hamiltonian in Eq. (124) we obtain

$$V^{\mathrm{ph}}_{\gamma\gamma'\delta\delta'}(\boldsymbol{x}_1, \boldsymbol{x}_2|\tau_1, \tau_2) = \delta_{\gamma\gamma'}\delta_{\delta\delta'}\frac{1}{V_{\mathrm{G}}}\sum_{\boldsymbol{q}} \mathrm{e}^{\mathrm{i}\boldsymbol{q}\cdot(\boldsymbol{x}_1 - \boldsymbol{x}_2)} V^{\mathrm{ph}}(\boldsymbol{q}|\tau_1, \tau_2), \tag{125}$$

where

$$V^{\mathrm{ph}}(\boldsymbol{q}|\tau_1,\,\tau_2) = M(\boldsymbol{q})M(-\boldsymbol{q})\mathscr{D}_{\mathrm{L}}^{(0)}(\boldsymbol{q}|\tau_1,\,\tau_2). \tag{126}$$

Herein, $\mathscr{D}_{\mathrm{L}}^{(0)}(\boldsymbol{q}|\tau_1,\,\tau_2)$ is the unperturbed LO phonon Green's function:

$$\mathscr{D}_{\mathrm{L}}^{(0)}(\boldsymbol{q}|\tau_1,\,\tau_2) = -\frac{1}{\hbar}\,{}_0\langle \mathrm{T}_\tau \hat{A}_{\mathrm{L}}(\boldsymbol{q},\,\tau_1)\hat{A}_{\mathrm{L}}(-\boldsymbol{q},\,\tau_2)\rangle \tag{127}$$

with

$$\hat{A}_{\mathrm{L}}(\boldsymbol{q},\,\tau) = \hat{a}_{\mathrm{L}}(\boldsymbol{q},\,\tau) + \hat{a}_{\mathrm{L}}^{\dagger}(\boldsymbol{q},\,\tau), \tag{128}$$

which gives after Fourier transformation according Eqs. (83) and (84)

$$\mathscr{D}_{\mathrm{L}}^{(0)}(\boldsymbol{q},\,\mathrm{i}\omega_n) = \frac{2}{\hbar}\frac{\omega_{\mathrm{L}}}{(\mathrm{i}\omega_n - \omega_{\mathrm{L}})(\mathrm{i}\omega_n + \omega_{\mathrm{L}})}. \tag{129}$$

The (Matsubara) frequency of the phonons is $\omega_n = 2n\pi/(\beta\hbar)$, $n = 0, \pm 1, \pm 2, \ldots$. It is obvious that $\mathscr{D}_{\mathrm{L}}^{(0)}(\boldsymbol{q},\,\mathrm{i}\omega_n)$ is independent of the phonon wave vector $\boldsymbol{q}$ because the long-wavelength LO phonons are dispersionless. Transforming Dyson's equation for $\mathscr{G}_{\alpha\beta}(\boldsymbol{x},\,\boldsymbol{x}'|\mathrm{i}\nu_n)$ in the subband space, each phonon line is associated with [68,69]

$$V^{\mathrm{ph}}_{\substack{N_1 \\ k_x+q_x}\;\substack{N_2 \\ k_x}\;\substack{N_3 \\ k_x'-q_x}\;\substack{N_4 \\ k_x'}}(q_x,\,\mathrm{i}\omega_n) = f^{\mathrm{LO}}_{4N_1N_2N_3N_4}{}^{k_x+q_xk_xk_x'-q_xk_x'}(q_x)\mathscr{D}_{\mathrm{L}}^{(0)}(q_x,\,\mathrm{i}\omega_n), \tag{130}$$

where

$$f^{\mathrm{LO}}_{\substack{N_1 \\ k_x+q_x}\;\substack{N_2 \\ k_x}\;\substack{N_3 \\ k_x'-q_x}\;\substack{N_4 \\ k_x'}}(q_x) = 2\alpha_p r_p(\hbar\omega_{\mathrm{L}})^2 f^{\mathrm{C}}_{\substack{N_1 \\ k_x+q_x}\;\substack{N_2 \\ k_x}\;\substack{N_3 \\ k_x'-q_x}\;\substack{N_4 \\ k_x'}}(q_x) \tag{131}$$

with

$$f^{\mathrm{C}}_{\substack{N_1 \\ k_x+q_x}\;\substack{N_2 \\ k_x}\;\substack{N_3 \\ k_x'-q_x}\;\substack{N_4 \\ k_x'}}(q_x) = \frac{1}{2}\int_{-\infty}^{\infty}\mathrm{d}q_y\frac{1}{\sqrt{q_x^2+q_y^2}}\int_{-\infty}^{\infty}\mathrm{d}y\int_{-\infty}^{\infty}\mathrm{d}y'\;\Phi_{N_1}^{*}(y - Y_{k_x+q_x})\Phi_{N_2}(y - Y_{k_x})$$

$$\times\,\mathrm{e}^{\mathrm{i}q_y(y-y')}\Phi_{N_3}^{*}(y' - Y_{k_x'-q_x})\Phi_{N_4}(y' - Y_{k'_x}). \tag{132}$$

With the integral given in Ref. [57] it is possible to represent this form factor analogous to that in Eq. (49). Explicit calculation of $f^{\mathrm{C}}_{\substack{N_1 \\ k_x+q_x}\;\substack{N_2 \\ k_x}\;\substack{N_3 \\ k_x'-q_x}\;\substack{N_4 \\ k_x'}}(q_x)$ shows that this form factor is independent of the wave vector components k_x and k_x'. The phonon-mediated electron–electron interaction potential $V^{\mathrm{ph}}_{\substack{N_1 \\ k_{x1}}\;\substack{N_2 \\ k_{x2}}\;\substack{N_3 \\ k_{x3}}\;\substack{N_4 \\ k_{x4}}}(q_x,\,\mathrm{i}\omega_n)$ signifies the scattering of an electron from subband N_2 to N_1 by another electron which becomes scattered from subband N_4 to N_3 by exchanging a LO phonon (see Fig. 5). The leading-order self-energy Feynman diagram (one-phonon self-energy) is plotted in Fig. 6. It results in the *Tamm–Dancoff approximation* (TDA) of the matrix self-energy $\Sigma^{(1)}_{NN';\alpha}(k_x,\,\mathrm{i}\nu_n) \equiv \Sigma^{\mathrm{TD}}_{NN';\alpha}(k_x,\,\mathrm{i}\nu_n)$:

$$\Sigma^{(1)}_{NN';\alpha}(k_x,\,\mathrm{i}\nu_n) = \frac{1}{L_x}\sum_{q_x}\sum_{N_1,N_1'}\left(-\frac{1}{\beta}\right)\sum_{\mathrm{i}\omega_n} V^{\mathrm{ph}}_{\substack{N \\ k_x}\;\substack{N_1 \\ k_x-q_x}\;\substack{N_1' \\ k_x-q_x}\;\substack{N' \\ k_x}}(q_x,\,\mathrm{i}\omega_n)\mathscr{G}^{(0)}_{N_1N_1';\alpha}(k_x - q_x,\,\mathrm{i}\nu_n - \mathrm{i}\omega_n). \tag{133}$$

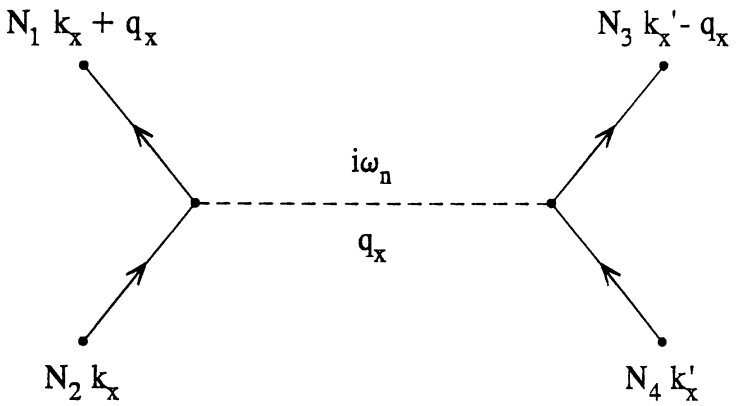

$$V^{ph}_{\substack{N_1 \\ k_x+q_x}\ \substack{N_2 \\ k_x}\ \substack{N_3 \\ k'_x-q_x}\ \substack{N_4 \\ k'_x}}(q_x, i\omega_n) = f^{LO}_{\substack{N_1 \\ k_x+q_x}\ \substack{N_2 \\ k_x}\ \substack{N_3 \\ k'_x-q_x}\ \substack{N_4 \\ k'_x}}(q_x)\mathcal{D}^{(0)}_L(q_x, i\omega_n)$$

Fig. 5. Feynman diagram of the electron–phonon interaction potential (phonon mediated electron–electron interaction potential) $V^{\mathrm{ph}}_{\substack{N_1 \\ k_x+q_x}\ \substack{N_2 \\ k_x}\ \substack{N_3 \\ k'_x-q_x}\ \substack{N_4 \\ k'_x}}(q_x, \mathrm{i}\omega_n)$ in the subband space.

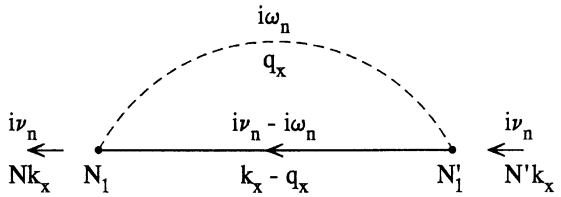

Fig. 6. Feynman diagram of the one-phonon (first-order) irreducible matrix self-energy $\sum^{(1)}_{NN';\alpha}(k_x, \mathrm{i}\nu_n)$.

Performing the frequency sum and assuming now a single electron in the QWW by changing $\mathrm{i}\hbar\nu_n \to E - \mu + \mathrm{i}\delta$; $\delta \to 0^+$, one obtains the *retarded matrix self-energy* in TDA

$$\Sigma^{(1)R}_{NN';\alpha}(k_x, E) = \frac{1}{L_x}\sum_{q_x}\sum_{N_1} f^{\mathrm{LO}}_{\substack{N \\ k_x}\ \substack{N_1 \\ k_x-q_x}\ \substack{N_1 \\ k_x-q_x}\ \substack{N' \\ k_x}}(q_x)$$

$$\times\left\{\frac{n_B(\omega_L)+1}{E - \mathscr{E}_{N_1\alpha}(k_x - q_x) - \hbar\omega_L + \mathrm{i}\delta} + \frac{n_B(\omega_L)}{E - \mathscr{E}_{N_1\alpha}(k_x - q_x) + \hbar\omega_L + \mathrm{i}\delta}\right\}, \tag{134}$$

where $n_B(\omega_L) = [\mathrm{e}^{\beta\hbar\omega_L} - 1]^{-1}$ is the Bose occupancy factor of the LO phonons. From Eq. (134) it becomes obvious that the spin dependence of the self-energy consists only in a scaling of the energy, i.e. it can be droped if one redefines the energy E. Using Eq. (42) in the definition of the EPI form factor, we obtain

$$f^{\mathrm{LO}}_{\substack{N \\ k_x}\ \substack{N_1 \\ k_x-q_x}\ \substack{N_1 \\ k_x-q_x}\ \substack{N' \\ k_x}}(q_x) = \alpha_p r_p(\hbar\omega_L)^2\int_{-\infty}^{\infty} \mathrm{d}q_y \frac{2^{\frac{L_1-L_2+L_3-L_4}{2}}\,\mathrm{e}^{-a}}{\sqrt{q_x^2+q_y^2}}$$

$$\times\sqrt{\frac{L_2!L_4!}{L_1!L_3!}}\left(\frac{1}{2\tilde{l}_0}\left[\mathrm{sgn}(N_1-N)Y_{q_x}+\mathrm{i}\tilde{l}_0^2 q_y\right]\right)^{L_1-L_2}$$

$$\times\left(\frac{1}{2\tilde{l}_0}\left[\mathrm{sgn}(N_1-N')Y_{q_x}+\mathrm{i}\tilde{l}_0^2 q_y\right]\right)^{L_3-L_4} L_{L_2}^{L_1-L_2}(a)L_{L_4}^{L_3-L_4}(a), \tag{135}$$

where $L_1=\max\{N, N_1\}$, $L_2=\min\{N, N_1\}$, $L_3=\max\{N', N_1\}$, $L_4=\min\{N', N_1\}$ and we have defined $\mathrm{sgn}(x)=+1$ for $x\geqslant 0$ and $\mathrm{sgn}(x)=-1$ for $x<0$. Note that for vanishing magnetic field the result is still given by Eq. (51). Splitting explicitly the self-energy $\Sigma^{(1)}_{NN';\alpha}(k_x, E)$ into real and imaginary parts, we obtain

$$\mathrm{Re}\,\Sigma^{(1)\mathrm{R}}_{NN';\alpha}(k_x, E)=\frac{1}{2\pi}\sum_{N_1}\mathscr{P}\int_{-\infty}^{\infty}\mathrm{d}q_x\, f^{\mathrm{LO}}_{\substack{N\\k_x}\ \substack{N_1\\k_x-q_x}\ \substack{N_1\\k_x-q_x}\ \substack{N'\\k_x}}(q_x)$$

$$\times\left\{\frac{n_{\mathrm{B}}(\omega_{\mathrm{L}})+1}{E-\mathscr{E}_{N_1\alpha}(k_x-q_x)-\hbar\omega_{\mathrm{L}}}+\frac{n_{\mathrm{B}}(\omega_{\mathrm{L}})}{E-\mathscr{E}_{N_1\alpha}(k_x-q_x)+\hbar\omega_{\mathrm{L}}}\right\}, \tag{136}$$

where $\mathscr{P}\int\mathrm{d}q_x$ denotes the principal value integral and

$$\mathrm{Im}\,\Sigma^{(1)\mathrm{R}}_{NN';\alpha}(k_x, E)=-\frac{1}{2}\sum_{N_1}\int_{-\infty}^{\infty}\mathrm{d}q_x\, f^{\mathrm{LO}}_{\substack{N\\k_x}\ \substack{N_1\\k_x-q_x}\ \substack{N_1\\k_x-q_x}\ \substack{N'\\k_x}}(q_x)\{(n_{\mathrm{B}}(\omega_{\mathrm{L}})+1)\delta(E-\mathscr{E}_{N_1\alpha}(k_x-q_x)-\hbar\omega_{\mathrm{L}})$$

$$+n_{\mathrm{B}}(\omega_{\mathrm{L}})\delta(E-\mathscr{E}_{N_1\alpha}(k_x-q_x)+\hbar\omega_{\mathrm{L}})\}. \tag{137}$$

This self-energy determines via Eq. (109) the magnetopolaron energy–momentum relation $E_\eta=E_\eta(k_x^{\mathrm{pol}})$ and damping $\Gamma_\eta=\Gamma_\eta(k_x^{\mathrm{pol}})$ and the ket $|\eta, k_x^{\mathrm{pol}}; \{n_q\}\rangle$ describes the eigenstates of the interacting electron–phonon system. The expression for the magnetopolaron self-energy is valid for energies below and above the threshold E_{th} of the phonon continuum in difference to Eq. (55), which is only valid for energies below E_{th}. Below the phonon continuum the denominator of the real part of the self-energy does not have a zero for $T=0$ and hence, the principal value integral becomes a simple integral. But for $T\neq 0$ and also above the threshold E_{th} of the phonon continuum for $T=0$, the denominator has a zero and the integral must be calculated as a principal value integral. Thus, Green's function technique gives the unique way to calculate the magnetopolaron dispersion relation also within the phonon continuum in difference to the orthodox quantum-mechanical perturbation theories: RSPT, WBPT and IWBPT. The non-vanishing imaginary part results from the emission and absorption of real optical phonons. The first term comes from the emission of a phonon by the magnetopolaron. This term is finite even at $T=0$. However, this term is finite only if $E>\hbar\omega_{\mathrm{L}}$, i.e. for energies above the threshold of the phonon continuum, and is zero when $E<\hbar\omega_{\mathrm{L}}$. The second term corresponds to the absorption of a phonon by the electron. Because this term is proportional to the phonon distribution function $n_{\mathrm{B}}(\omega_{\mathrm{L}})$, it vanishes at zero temperature. For vanishing imaginary part of the self-energy the renormalization of the subbands is due to virtual emission and reabsorption processes of LO phonons. It is important to note that for energies above the threshold E_{th} of the one-phonon continuum we can only speak from the quasi-particle magnetopolaron as long as $\mathrm{Im}\,\Sigma^{(1)\mathrm{R}}_{NN';\alpha}$ is small at the quasi-particle pol of $G^{\mathrm{R}}_{NN';\alpha}$. Following, if one is interested in the properties of the interacting electron–phonon system for $E>E_{\mathrm{th}}$ one has at first to calculate $\mathrm{Re}\,\Sigma^{(1)\mathrm{R}}_{NN';\alpha}(k_x, E)$ and $\mathrm{Im}\,\Sigma^{(1)\mathrm{R}}_{NN';\alpha}(k_x, E)$ and only if the imaginary part is small enough one can proceed to calculate the quasi-particle properties by setting $E=E_\eta-\mathrm{i}\Gamma_\eta$ in the Green's function. Then, including ISC the magnetopolaron energies and damping functions are given by Eq. (109). Because the electron–phonon interaction is spin-independent the problem entirely separates for spin up and down electrons. Thus, one may consider the problem for $\boldsymbol{G}^{\mathrm{R}}_{\uparrow}(k_x, E)$ separately from that of $\boldsymbol{G}^{\mathrm{R}}_{\downarrow}(k_x, E)$. In this case η runs from 1 to M for each Greens' function. Also, two threshold energies, $E_{\mathrm{th}}^{(\uparrow)}$ and $E_{\mathrm{th}}^{(\downarrow)}$ appear.

In the diagonal approximation the renormalized energy levels are given by Eq. (115) and the magnetopolaron damping by Eq. (116), both used for $\mu = 0$. We have sharp definite levels below $E_{\mathrm{th}}^{(\alpha)}$, but broadened levels inside the phonon continuum. Below the phonon continuum the spectral function shows delta-like peaks and inside the phonon continuum Lorentzian-shaped peaks as long as the quasi-particle picture is valid. The self-energy at the quasi-particle poles at $T = 0$ in diagonal approximation is given by

$$\mathrm{Re}\,\Sigma_{NN;\alpha}^{(1)\mathrm{R}}(k_x,\, E_{N\alpha}(k_x)) = \frac{1}{2\pi}\sum_{N_1} \mathscr{P}\int_{-\infty}^{\infty} \mathrm{d}q_x \frac{f^{\mathrm{LO}}_{\substack{N\\k_x}\;\substack{N_1\\k_x-q_x}\;\substack{N_1\\k_x-q_x}\;\substack{N\\k_x}}(q_x)}{E_{N\alpha}(k_x) - \mathscr{E}_{N_1\alpha}(k_x - q_x) - \hbar\omega_{\mathrm{L}}}, \tag{138}$$

$$\mathrm{Im}\,\Sigma_{NN;\alpha}^{(1)\mathrm{R}}(k_x,\, E_{N\alpha}(k_x)) = -\frac{1}{2}\sum_{N_1} \int_{-\infty}^{\infty} \mathrm{d}q_x f^{\mathrm{LO}}_{\substack{N\\k_x}\;\substack{N_1\\k_x-q_x}\;\substack{N_1\\k_x-q_x}\;\substack{N\\k_x}}(q_x)\; \delta(E_{N\alpha}(k_x) - \mathscr{E}_{N_1\alpha}(k_x - q_x) - \hbar\omega_{\mathrm{L}}) \tag{139}$$

and thus, the renormalized levels follow from

$$E_{N\alpha}(k_x) = \mathscr{E}_{N\alpha}(k_x) + \mathrm{Re}\,\Sigma_{NN;\alpha}^{(1)\mathrm{R}}(k_x,\, E_{N\alpha}(k_x)) \tag{140}$$

and the associated damping function from

$$\Gamma_{N\alpha}(k_x) = -\,\mathrm{Im}\,\Sigma_{NN;\alpha}^{(1)\mathrm{R}}(k_x,\, E_{N\alpha}(k_x)). \tag{141}$$

Performing the on-mass-shell approximation, the matrix self-energy reads

$$\mathrm{Re}\,\Sigma_{NN;\alpha}^{(1)\mathrm{OMS}}(k_x) = \frac{1}{2\pi}\sum_{N_1} \mathscr{P}\int_{-\infty}^{\infty} \mathrm{d}q_x \frac{f^{\mathrm{LO}}_{\substack{N\\k_x}\;\substack{N_1\\k_x-q_x}\;\substack{N_1\\k_x-q_x}\;\substack{N\\k_x}}(q_x)}{\mathscr{E}_{N\alpha}(k_x) - \mathscr{E}_{N_1\alpha}(k_x - q_x) - \hbar\omega_{\mathrm{L}}} \tag{142}$$

and

$$\mathrm{Im}\,\Sigma_{NN;\alpha}^{(1)\mathrm{OMS}}(k_x) = -\frac{1}{2}\sum_{N_1} \mathscr{P}\int_{-\infty}^{\infty} \mathrm{d}q_x\, f^{\mathrm{LO}}_{\substack{N\\k_x}\;\substack{N_1\\k_x-q_x}\;\substack{N_1\\k_x-q_x}\;\substack{N\\k_x}}(q_x)\; \delta(\mathscr{E}_{N\alpha}(k_x) - \mathscr{E}_{N_1\alpha}(k_x - q_x) - \hbar\omega_{\mathrm{L}}). \tag{143}$$

In the last two equations the renormalized energy levels are given by

$$E_{N\alpha}(k_x) = \mathscr{E}_{N\alpha}(k_x) + \mathrm{Re}\,\Sigma_{NN;\alpha}^{(1)\mathrm{OMS}}(k_x) \tag{144}$$

and the damping function reads

$$\Gamma_{N\alpha}(k_x) = -\,\mathrm{Im}\,\Sigma_{NN;\alpha}^{(1)\mathrm{OMS}}(k_x). \tag{145}$$

Here, it becomes explicitly obvious that the self-energy is independent of the spin index because the Zeeman energy subtracts from the energy difference. From Eqs. (138) and (139) it is seen that the renormalization of the subband $E_{N\alpha}(k_x)$ due to EPI results within the TDA from the scattering of an electron from an unrenormalized level to a renormalized level, but within the scheme of the TDA on-mass-shell between two unshifted levels. As seen from the corresponding Feynman graph, Fig. 6, in both approaches only one LO phonon is present.

If one compares the energy correction $\Delta E_\eta(k_x)$ due to the matrix self-energy $\Sigma_{NN';\alpha}^{(1)\mathrm{R}}(k_x,\, E)$, Eqs. (136)–(143), of Green's function technique with the energy correction $\Delta E_N(k_x)$ of orthodox quantum mechanics, Eq. (53), the following becomes obvious:

1. The Feynman–Dyson perturbation theory gives real and imaginary self-energy contributions for intra- and intersubband processes, while the old-fashioned perturbation theories (RSPT, WBPT, IWBPT) give only real self-energy contributions for intra- and some intersubband processes.

2. The matrix self-energy calculated with Green's function technique contains scattering processes of two electrons from subbands N_1 to N and from N' to N_1, whereas RSPT, WBPT and IWBPT include only the symmetric processes of scattering from N_1 to N and from N to N_1. The asymmetric scattering of the two electrons by exchanging an optical phonon give rise to the non-diagonal elements of the matrix self-energy.
3. Neglecting these asymmetric scattering processes, the diagonal elements of the real part of the matrix self-energy $\mathrm{Re}\,\Sigma^{(1)\mathrm{R}}_{NN}(k_x, E_N(k_x))$ in TDA at $T = 0$ become equivalent to the second-order WBPT.
4. The diagonal elements of the TDA matrix self-energy in mass-shell approximation, $\mathrm{Re}\,\Sigma^{(1)\mathrm{OMS}}_{NN}(k_x)$, become the same as in second-order RSPT.

As discussed above in the 3D bulk case the orthodox RSPT gives the best result for the ground state ($k_x \to 0$, $\omega_c \to 0$), where it fails near possible resonances of the levels. Hence, we can conclude that the self-energy in TDA calculated on-mass shell is the best choice for the ground-state renormalization. But, unfortunately the TDA does not result in a magnetopolaron dispersion relation with the correct pinning behaviour because of the same reasons as WBPT fails in this question. Thus, further improvement are necessary.

4.4. Hartree–Fock approximation for the self-energy in subband space

To improve the TDA one has to include in the irreducible self-energy further Feynman diagrams containing more than one LO phonon. One standard approach in many-particle theory is the *Hartree–Fock approximation* [68], developed for the electron–electron interaction problem. It consists in replacing the unperturbed electron Green's function $\mathscr{G}^{(0)}_{NN';\alpha}(k_x, \mathrm{i}\nu_n)$ in the one-phonon electron self-energy $\Sigma^{(1)}_{NN';\alpha}(k_x, \mathrm{i}\nu_n)$ (see Fig. 6) by the dressed Green's function $\mathscr{G}_{NN';\alpha}(k_x, \mathrm{i}\nu_n)$, as shown in Fig. 7(a) and Fig 7(b). The Hartree–Fock (HF) magnetopolaron self-energy is given by

$$\Sigma^{\mathrm{HF}}_{NN';\alpha}(k_x, \mathrm{i}\nu_n) = \frac{1}{L_x}\sum_{q_x}\sum_{N_1,N'_1}\left(-\frac{1}{\beta}\right)\sum_{\mathrm{i}\omega_n} V^{\mathrm{ph}}_{\substack{N\\k_x}\ \substack{N_1\\k_x-q_x}\ \substack{N'_1\\k_x-q_x}\ \substack{N'\\k_x}}(q_x, \mathrm{i}\omega_n)\mathscr{G}_{N_1N'_1;\alpha}(k_x - q_x, \mathrm{i}\nu_n - \mathrm{i}\omega_n). \tag{146}$$

The EPI potential depends on the Matsubara frequency ω_n and thus, the calculation of the HF self-energy of the EPI is much more complicated than in the case of the electron–electron interaction because the electron–electron interaction potential is independent of the frequency. In order to perform the frequency sum over $\mathrm{i}\omega_n$ in Eq. (146), we represent the dressed Green's function by its spectral representation, Eq. (91), with the result

$$\Sigma^{\mathrm{HF}}_{NN';\alpha}(k_x, \mathrm{i}\nu_n) = \frac{1}{L_x}\sum_{q_x}\sum_{N_1,N'_1} f^{\mathrm{LO}}_{\substack{N\\k_x}\ \substack{N_1\\k_x-q_x}\ \substack{N'_1\\k_x-q_x}\ \substack{N'\\k_x}}(q_x)\int_{-\infty}^{\infty} \mathrm{d}E' A_{N_1N'_1;\alpha}(k_x - q_x, E')$$

$$\times\left(-\frac{1}{\beta}\right)\sum_{\mathrm{i}\omega_n}\frac{1}{\mathrm{i}\hbar\nu_n - \mathrm{i}\hbar\omega_n - E'}\mathscr{D}^{(0)}_{\mathrm{L}}(q_x, \mathrm{i}\omega_n). \tag{147}$$

Note that the form factor $f^{\mathrm{LO}}_{\substack{N\\k_x}\ \substack{N_1\\k_x-q_x}\ \substack{N'_1\\k_x-q_x}\ \substack{N'\\k_x}}(q_x)$ is still given by Eq. (135) if one replaces L_3 and L_4 by $L_3 = \max\{N'_1, N\}$ and $L_4 = \min\{N'_1, N'\}$, respectively. The frequency sum is trivially performed and one

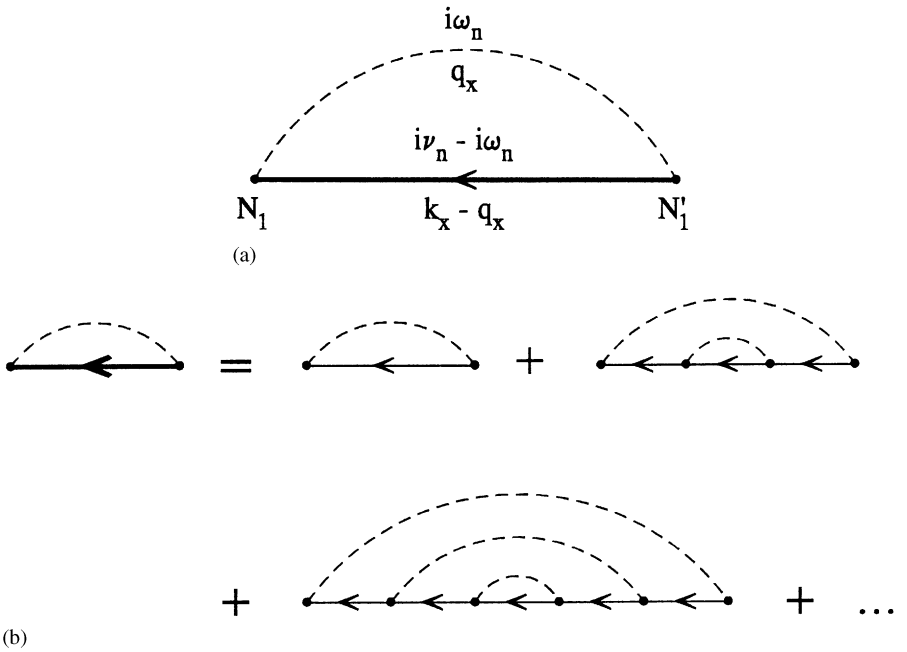

Fig. 7. (a) Feynman diagram of the irreducible Hartree–Fock matrix self-energy $\sum^{\mathrm{HF}}_{NN';\alpha}(k_x, \mathrm{i}\nu_n)$. (b) The self-energy Feynman diagrams which are included in the irreducible Hartree–Fock matrix self-energy $\sum^{\mathrm{HF}}_{NN';\alpha}(k_x, \mathrm{i}\nu_n)$ of the interacting electron–phonon system.

obtains for the retarded HF self-energy

$$\Sigma^{\mathrm{HF}}_{NN';\alpha}(k_x, E) = \frac{1}{L_x}\sum_{q_x}\sum_{N_1,N'_1} f^{\mathrm{LO}}_{N\ k_x\ k_x-q_x\ k_x-q_x\ k_x} (q_x)\int_{-\infty}^{\infty} \mathrm{d}E' A_{N_1N'_1;\alpha}(k_x - q_x, E')$$

$$\times\left\{\frac{n_{\mathrm{B}}(\omega_{\mathrm{L}})+1}{E-E'-\hbar\omega_{\mathrm{L}}+\mathrm{i}\delta} + \frac{n_{\mathrm{B}}(\omega_{\mathrm{L}})}{E-E'+\hbar\omega_{\mathrm{L}}+\mathrm{i}\delta}\right\}. \tag{148}$$

Resubstituting the spectral function with the help of Eq. (91), Eq. (148) may be written as

$$\Sigma^{\mathrm{HF}}_{NN';\alpha}(k_x, E) = \frac{1}{L_x}\sum_{q_x}\sum_{N_1,N'_1} f^{\mathrm{LO}}_{N\ k_x\ k_x-q_x\ k_x-q_x\ k_x} (q_x)\{[n_{\mathrm{B}}(\omega_{\mathrm{L}})+1]G^{\mathrm{R}}_{N_1N'_1;\alpha}(k_x - q_x, E-\hbar\omega_{\mathrm{L}})$$

$$+ n_{\mathrm{B}}(\omega_{\mathrm{L}})G^{\mathrm{R}}_{N_1N'_1;\alpha}(k_x - q_x, E+\hbar\omega_{\mathrm{L}})\}, \tag{149}$$

where $\boldsymbol{G}^{\mathrm{R}}(k_x, E)$ is the *dressed retarded HF Green's function*. The HF matrix self-energy $\Sigma^{\mathrm{HF}}_{NN';\alpha}(k_x, E)$, with $G^{\mathrm{R}}_{NN';\alpha}(k_x, E)$ in terms of $\Sigma^{\mathrm{HF}}_{NN';\alpha}(k_x, E)$ via Dyson's equation, Eq. (95), is then given by a very complicated *matrix equation*, including an *integral equation* for q_x and a *difference equation* in frequency.

If one uses for the Green's function, appearing inside of the matrix self-energy of Eq. (149), a diagonal approximation according Eq. (98), which I call an *internal diagonal approximation*, Eq. (149) takes

on the form

$$\Sigma^{\mathrm{HF}}_{NN';\alpha}(k_x,\,E)=\frac{1}{L_x}\sum_{q_x}\sum_{N_1} f^{\mathrm{LO}}{}^{\;N_1\;\;N_1\;\;N'}_{k_x\;k_x-q_x\;k_x-q_x\;k_x}(q_x)$$

$$\times\left\{\frac{n_{\mathrm{B}}(\omega_{\mathrm{L}})+1}{E-\mathscr{E}_{N_1\alpha}(k_x-q_x)-\Sigma^{\mathrm{HF}}_{N_1N_1;\alpha}(k_x-q_x,\,E-\hbar\omega_{\mathrm{L}})-\hbar\omega_{\mathrm{L}}}\right.$$

$$\left.+\frac{n_{\mathrm{B}}(\omega_{\mathrm{L}})}{E-\mathscr{E}_{N_1\alpha}(k_x-q_x)-\Sigma^{\mathrm{HF}}_{N_1N_1;\alpha}(k_x-q_x,\,E+\hbar\omega_{\mathrm{L}})+\hbar\omega_{\mathrm{L}}}\right\}. \tag{150}$$

It becomes obvious that the self-energy remains a *non-diagonal* matrix if the internal diagonal approximation is performed and via Dyson's equation the dressed Green's function too.

On the other hand, if one applies the QPA for the spectral function appearing in Eq. (148) by using Eq. (112), i.e. performing an *internal* QPA, it follows

$$\Sigma^{\mathrm{HF}}_{NN';\alpha}(k_x,\,E)=\frac{1}{L_x}\sum_{q_x}\sum_{N_1,N'_1} f^{\mathrm{LO}}{}^{\;N_1\;\;N'_1\;\;N'}_{k_x\;k_x-q_x\;k_x-q_x\;k_x}(q_x)\sum_{\eta=0}^{2M} z_\eta^{N_1N'_1;\alpha}(k_x-q_x)$$

$$\times\left\{\frac{n_{\mathrm{B}}(\omega_{\mathrm{L}})+1}{E-E_\eta(k_x-q_x)-\hbar\omega_{\mathrm{L}}+\mathrm{i}\delta}+\frac{n_{\mathrm{B}}(\omega_{\mathrm{L}})}{E-E_\eta(k_x-q_x)+\hbar\omega_{\mathrm{L}}+\mathrm{i}\delta}\right\}, \tag{151}$$

where $E_\eta(k_x-q_x)$ is a solution of Eq. (109), $z^{N_1N'_1;\alpha}(k_x-q_x)$ is given by Eq. (110) and fulfills the sum rule (113). Eq. (151) generalizes our earlier result [32] to the case that in the matrix self-energy all possible intersubband processes are included.

In general, the numerical calculation of the self-energy in the forms of Eqs. (149)–(151) is possible but very cumbersome. Thus, we will look for further suitable approximations. If one assumes additionally to the internal QPA an internal diagonal approximation for the dressed Green's function, with Eq. (120), Eq. (148) takes on the form

$$\Sigma^{\mathrm{HF}}_{NN';\alpha}(k_x,\,E)=\frac{1}{L_x}\sum_{q_x}\sum_{N_1} f^{\mathrm{LO}}{}^{\;N_1\;\;N_1\;\;N'}_{k_x\;k_x-q_x\;k_x-q_x\;k_x}(q_x)$$

$$\times\left\{\frac{n_{\mathrm{B}}(\omega_{\mathrm{L}})+1}{E-\mathscr{E}_{N_1\alpha}(k_x-q_x)-\mathrm{Re}\,\Sigma^{\mathrm{HF}}_{N_1N_1;\alpha}(k_x-q_x,\,E_{N_1\alpha}(k_x-q_x))-\hbar\omega_{\mathrm{L}}+\mathrm{i}\delta}\right.$$

$$\left.+\frac{n_{\mathrm{B}}(\omega_{\mathrm{L}})}{E-\mathscr{E}_{N_1\alpha}(k_x-q_x)-\mathrm{Re}\,\Sigma^{\mathrm{HF}}_{N_1N_1;\alpha}(k_x-q_x,\,E_{N_1\alpha}(k_x-q_x))+\hbar\omega_{\mathrm{L}}+\mathrm{i}\delta}\right\}. \tag{152}$$

Introducing polaronic units and cylindrical coordinates in the q_x–q_y plane, this equation reads

$$\Sigma^{\mathrm{HF}}_{NN';\alpha}(k_x,\,E)=\frac{\alpha_{\mathrm{p}}}{2\pi}\sum_{N_1}\int_0^\infty \mathrm{d}q_{||}\int_{-\pi}^{\pi}\mathrm{d}\varphi\,2^{L_1-L_2+L_3-L_4}\,\mathrm{e}^{-a}\sqrt{\frac{L_2!L_4!}{L_1!L_3!}}$$

$$\times\left(\frac{q_{||}}{2\lambda}[\mathrm{sgn}(N_1-N)\gamma\cos\varphi+\mathrm{i}\sin\varphi]\right)^{L_1-L_2}\left(\frac{q_{||}}{2\lambda}[\mathrm{sgn}(N_1-N')\gamma\cos\varphi-\mathrm{i}\sin\varphi]\right)^{L_3-L_4}$$

$$\times L_{L_2}^{L_1-L_2}(a)\;L_{L_4}^{L_3-L_4}(a)$$

$$\times\left\{\frac{n_{\mathrm{B}}(\omega_{\mathrm{L}})+1}{E-\lambda^2(N_1+\frac{1}{2})-\frac{g^*\mu_{\mathrm{B}}}{\hbar\omega_{\mathrm{L}}}B\alpha-(1-\gamma^2)(k_x-q_{||}\cos\varphi)^2-\mathrm{Re}\,\Sigma^{\mathrm{HF}}_{N_1N_1;\alpha}(k_x-q_{||}\cos\varphi|E_{N_1\alpha}(k_x-q_{||}\cos\varphi))-1+\mathrm{i}\delta}\right.$$

$$\left.+\frac{n_{\mathrm{B}}(\omega_{\mathrm{L}})}{E-\lambda^2(N_1+\frac{1}{2})-\frac{g^*\mu_{\mathrm{B}}}{\hbar\omega_{\mathrm{L}}}B\alpha-(1-\gamma^2)(k_x-q_{||}\cos\varphi)^2-\mathrm{Re}\,\Sigma^{\mathrm{HF}}_{N_1N_1;\alpha}(k_x-q_{||}\cos\varphi|E_{N_1\alpha}(k_x-q_{||}\cos\varphi))+1+\mathrm{i}\delta}\right\}. \tag{153}$$

Comparing the HFA, Eqs. (152) and (153), with the TDA, Eq. (134), it becomes obvious that the HF matrix self-energy contains the same scattering processes as in the Tamm–Dancoff case but between the renormalized subband energies. Thus, from the point of view of the EPI, the HF approach given by Eqs. (152) and (153) is an *improved Tamm–Dancoff approximation* (ITDA).

In principle, the HF matrix self-energy of Eqs. (152) and (153) may be calculated numerically. However, this is a very complex and cumbersome procedure because for the calculation of a certain matrix element all the other matrix elements of the self-energy of the chosen multi-subband model must be known from the foregoing step of the self-consistent procedure. Thus, it is profitable to look for a further simplifying approximation. However, for this simplifying approximation of the HF self-energy, given by Eqs. (152) and (153), we have to demand that the resulting self-energy shall remain an improved TDA and, therefore, it has to fulfill two requirements. From the discussion of the orthodox perturbation theories it becomes obvious that, firstly, for $k_x \to 0$ the matrix self-energy of the ground state should approach the corresponding matrix self-energy calculated on-mass shell ($\mathrm{Re}\,\Sigma^{\mathrm{HF}}_{00;\alpha}(k_x\to 0,\,E)\Rightarrow \mathrm{Re}\,\Sigma^{(1)\mathrm{OMS}}_{00;\alpha}(k_x\to 0)$). Secondly, for large k_x the matrix self-energy should give the correct pinning behaviour of the zero-phonon magnetopolaron energy–momentum relations at the one-phonon energy $\hbar\omega_{\mathrm{L}}$ above the renormalized ground state $E_0(0;B)$. From Eq. (152) it becomes obvious that the real part of the HF self-energy at the quasi-particle energies shows the energetically lowest resonance at $E_\eta(k_x)=\mathscr{E}_{0\alpha}(0)+\mathrm{Re}\,\Sigma^{\mathrm{HF}}_{00;\alpha}(0,\,E_{0\alpha}((0))+\hbar\omega_{\mathrm{L}}$ because the phonon wave vector component q_x is a "free" parameter which can take all possible values. Therefore, to reduce numerical expense it should be a reasonable approach to set $\mathrm{Re}\,\Sigma^{\mathrm{HF}}_{N_1N_1;\alpha}(k_x-q_x,\;E_{N_1\alpha}(k_x-q_x))\Rightarrow \mathrm{Re}\,\Sigma^{\mathrm{HF}}_{00;\alpha}(0,\,E_{0\alpha}(0))\equiv \mathrm{Re}\,\Sigma^{(1)\mathrm{OMS}}_{00;\alpha}(0)$ in the denominator of the HF matrix self-energy of Eqs. (152) and (153). Then, Eq. (153) takes on the form:

$$\begin{aligned}\Sigma^{\mathrm{MHF}}_{NN';\alpha}(k_x,\,E)=&\frac{\alpha_{\mathrm{p}}}{2\pi}\sum_{N_1}\int_0^\infty \mathrm{d}q_{||}\int_{-\pi}^{\pi}\mathrm{d}\varphi\,2^{L_1-L_2+L_3-L_4}\,\mathrm{e}^{-a}\sqrt{\frac{L_2!L_4!}{L_1!L_3!}}\\
&\times\left(\frac{q_{||}}{2\lambda}[\mathrm{sgn}(N_1-N)\gamma\cos\varphi+\mathrm{i}\sin\varphi]\right)^{L_1-L_2}\left(\frac{q_{||}}{2\lambda}[\mathrm{sgn}(N_1-N')\gamma\cos\varphi-\mathrm{i}\sin\varphi]\right)^{L_3-L_4}\\
&\times L_{L_2}^{L_1-L_2}(a)L_{L_4}^{L_3-L_4}(a)\\
&\times\left\{\frac{n_{\mathrm{B}}(\omega_{\mathrm{L}})+1}{E-\lambda^2(N_1+\frac{1}{2})-\frac{g^*\mu_{\mathrm{B}}}{\hbar\omega_{\mathrm{L}}}B\alpha-(1-\gamma^2)(k_x-q_{||}\cos\varphi)^2-\mathrm{Re}\,\Sigma^{(1)\mathrm{OMS}}_{00;\alpha}(0)-1+\mathrm{i}\delta}\right.\\
&\left.+\frac{n_{\mathrm{B}}(\omega_{\mathrm{L}})}{E-\lambda^2(N_1+\frac{1}{2})-\frac{g^*\mu_{\mathrm{B}}}{\hbar\omega_{\mathrm{L}}}B\alpha-(1-\gamma^2)(k_x-q_{||}\cos\varphi)^2-\mathrm{Re}\,\Sigma^{(1)\mathrm{OMS}}_{00;\alpha}(0)+1+\mathrm{i}\delta}\right\}.\end{aligned} \tag{154}$$

I call Eq. (154) together with Eq. (109) (for $\mu=0$) *the modified Hartree–Fock approximation* (MHFA) for the interacting electron–phonon system in the subband space.

Let us discuss the physical meaning of this approach in detail. In the MHFA we use in the calculation of the matrix self-energy, when starting from Eq. (149), instead of the exact dressed HF Green's function $G^{R}_{NN';\alpha}(k_x, E)$ an approximated one: $G^{R}_{NN';\alpha}(k_x,E) = \delta_{NN'}/[E - \mathscr{E}_{N\alpha}(k_x) - \Sigma^{HF}_{00;\alpha}(0,E_0(0))]$. It becomes obvious that the MHFA exactly fulfills the first requirement, i.e. that for $k_x \to 0$ the matrix self-energy of the ground state should approach the corresponding matrix self-energy calculated on-mass shell (see also discussion below). The MHF self-energy simplifies the HF self-energy, Eq. (152), twofold: (i) At first it is assumed as the starting point of the self-consistent calculation of the matrix self-energy that the renormalization is the same for all levels. (ii) Secondly, for the *reference levels* $E_{N_1\alpha}(k_x - q_x) + \hbar\omega_L = \mathscr{E}_{N_1\alpha}(k_x - q_x) + \mathrm{Re}\,\Sigma^{HF}_{N_1N_1;\alpha}(k_x - q_x, E_{N_1\alpha}(k_x - q_x)) + \hbar\omega_L \approx \mathscr{E}_{N_1\alpha}(k_x - q_x) + \mathrm{Re}\,\Sigma^{HF}_{00;\alpha}(0,E_{0\alpha}(0)) + \hbar\omega_L$ the pinning at $E_{N_1\alpha}(0) + 2\hbar\omega_L$ is neglected. As described above the denominator of the fraction $1/\{E_\eta(k_x) - [E_{N_1\alpha}(k_x - q_x) + \hbar\omega_L]\}$ is responsible for electron scattering between E_η and $E_{N_1\alpha} + \hbar\omega_L$. Assuming for the moment E_η and k_x to be fixed, the most important contributions to the self-energy $\Sigma^{HF}_{NN';\alpha}$ result from the electron scattering between E_η and the energetically lowest reference levels, i.e. the reference levels $E_{0\alpha}(k_x - q_x) + \hbar\omega_L$. As shown above, $E_{0\alpha}(k_x - q_x) + \hbar\omega_L$ bends over at $E_{0\alpha}(0) + 2\hbar\omega_L$. Because the self-energy is nearly independent of the wave vector, $\mathrm{Re}\,\Sigma^{HF}_{00;\alpha}(k_x - q_x, E_{0\alpha}(k_x - q_x)) \simeq \mathrm{Re}\,\Sigma^{HF}_{00;\alpha}(0,E_{0\alpha}(0))$, as long as the energy is below the bend-over region (see e.g. Fig. 16(a) below), the sum over all quasi-continuous values of q_x gives a sum of fractions $1/\{E_\eta(k_x) - [E_{0\alpha}(k_x - q_x) + \hbar\omega_L]\}$, in which the most important large terms, arising from energies below of $E_{0\alpha}(0) + 2\hbar\omega_L$, are *correct* in the MHFA. Only the unimportant smallest terms, i.e. the smallest fractions in the sum over q_x, arising for energies in the bend-over region of the reference levels, $E_{0\alpha}(k_x - q_x) + \hbar\omega_L \approx E_{0\alpha}(0) + 2\hbar\omega_L$, are in the MHFA smaller than in the HFA. Thus, compared with the HFA, the MHFA for the self-energy *slightly underestimates* the EPI. It is noteworthy that this is a negligibly small effect. This result is true because of the quasi-continuum of states according to the different q_x, we have for a given k_x a quasi-infinite number of correct states, which have the largest contribution to the self-energy. For this reason, the energetically higher states, $N_1 > 0$, give only minor contributions to the self-energy, so that part (i) of the simplifications on the HF self-energy has practical no consequence for the numerical value of the matrix self-energy.

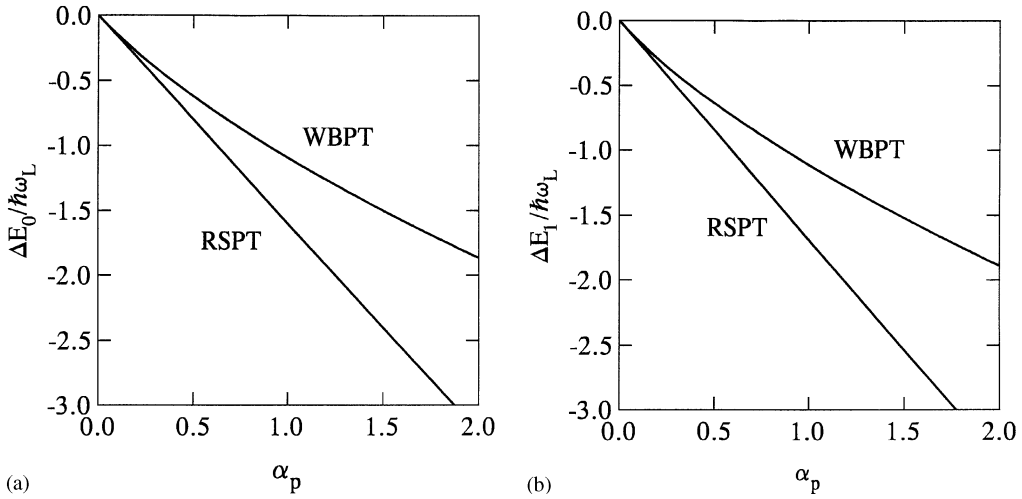

Fig. 8. The energy renormalizations ΔE_0 (a) and ΔE_1 (b) of the Q1D subbands $\mathscr{E}_0$ and $\mathscr{E}_1$, respectively, for $k_x = 0$ and $B = 0$ as a function of the polaron coupling constant α_p calculated in RSPT, WBPT and IWBPT. Please note that in (a) $\Delta E_0^{RSPT} = \Delta E_0^{IWBPT} \neq \Delta E_0^{WBPT}$ and in (b) $\Delta E_1^{RSPT} \neq \Delta E_1^{IWBPT} \neq \Delta E_1^{WBPT}$, but the difference between the RSPT and IWBPT results is not to be drawn.

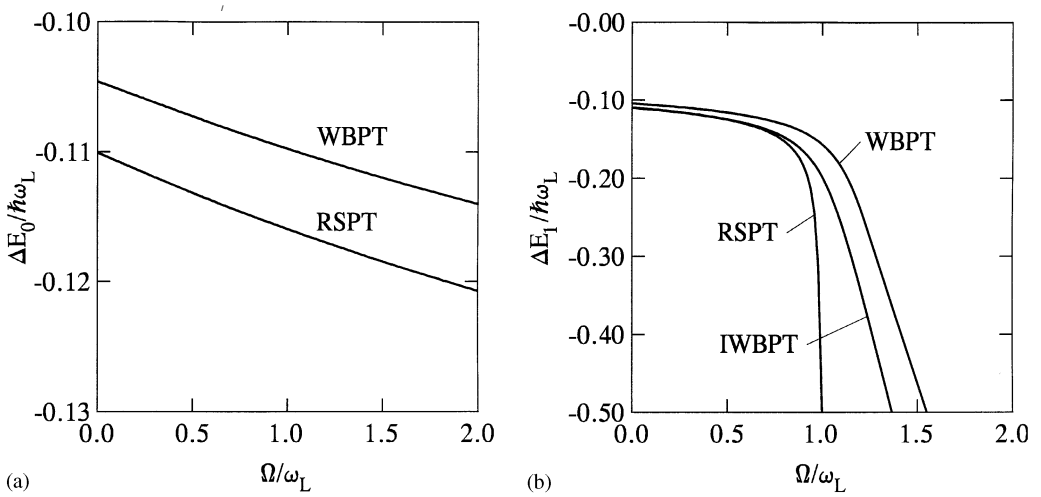

Fig. 9. The energy renormalizations ΔE_0 (a) and ΔE_1 (b) of the Q1D subbands $\mathscr{E}_0$ and $\mathscr{E}_1$, respectively, for $k_x = 0$ and $B = 0$ as a function of the confining frequency Ω of the lateral confining potential of the QWW calculated in RSPT, WBPT and IWBPT. Please note that in (a) $\Delta E_0^{\mathrm{RSPT}} = \Delta E_0^{\mathrm{IWBPT}} \neq \Delta E_0^{\mathrm{WBPT}}$.

Table 1
Polaron self-energies of the two lowest subbands for a GaAs–$Ga_{1-x}Al_xAs$ QWW with $\hbar\Omega = 2\,\mathrm{meV}$

Approximation	ΔE_0 (meV)	ΔE_1 (meV)
RSPT	3.992	4.023
WBPT	3.796	3.822
IWBPT	3.992	4.036

Table 2
Polaron self-energies of the two lowest subbands for a GaAs–$Ga_{1-x}Al_xAs$ QWW with $\hbar\Omega = 12\,\mathrm{meV}$

Approximation	ΔE_0 (meV)	ΔE_1 (meV)
RSPT	4.057	4.516
WBPT	3.850	4.206
IWBPT	4.057	4.482

Thus, we can conclude that the MHFA drastically simplifies the calculation of the matrix self-energy but still gives highly accurate results. This is especially true for the lower subbands. But the most important result of the MHFA is that it results in the correct pinning behaviour of the zero-phonon magnetopolaron dispersion relations. Compared with the exact HFA, the MHFA is computinally much simpler and highly efficient.

Note that at $T = 0$ the diagonal elements of the MHF matrix self-energy of Eq. (154) at the quasi-particle energies become equivalent to the IWBPT, but only for energies below the phonon continuum. Nevertheless, the discussion above demonstrates the refinement (accuracy and computinality) of the IWBPT of orthodox perturbation theory, developed by Lindemann et al. [52] perturbation theory.

5. Results and discussion

Most of the numerical calculations we have applied to a GaAs–$Ga_{1-x}Al_xAs$ QWW. If not explicitely indicated otherwise in the caption, we have used the following material parameters for GaAs, where the electrons are confined: $\alpha_p = 0.07$, $r_p = 3.987\,\text{nm}$, $\hbar\omega_L = 36.17\,\text{meV}$, $m_e = 0.06624m_0$ and for the confinement energy $\hbar\Omega = 12\,\text{meV}$ is used. The calculations are done for the zero-phonon magnetopolaron states of the lowest subband ($N = 0$) and the first excited subband ($N = 1$) in RSPT, WBPT and modified IWBPT, which correspond to the diagonal approximation for the TDA on-mass shell (OMS), the TDA and MHFA, respectively. For the chosen parameters the non-diagonal elements of the matrix self-energy are small compared to the diagonal elements and thus, the diagonal approximation is a suitable approach. In this case the MHF quasi-particle properties follow from Eq. (154) with Eqs. (140), (141) and (122). But in general, with

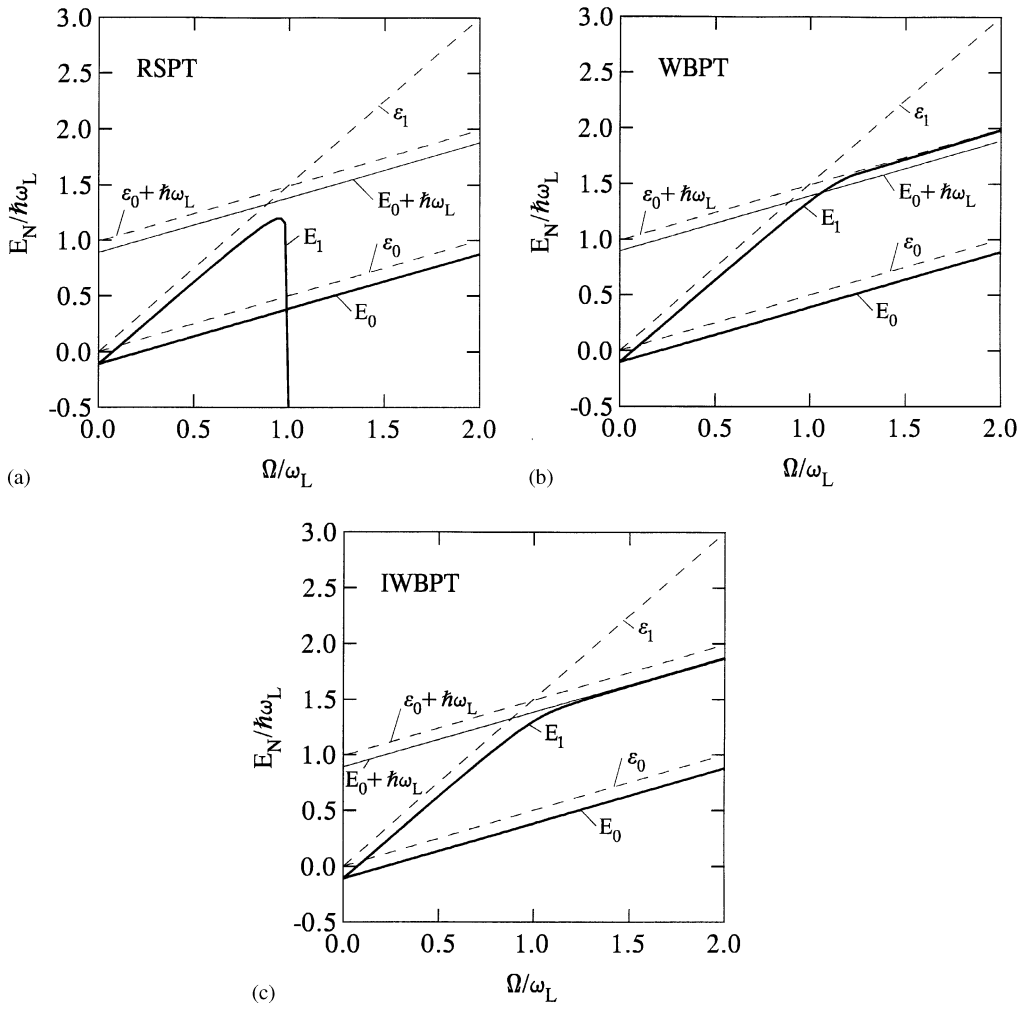

Fig. 10. Dependence of the renormalized levels E_0, E_1 (heavy solid lines) and $E_0 + \hbar\omega_L$ (thin solid line) and of the unenormalized levels $\mathscr{E}_0$, $\mathscr{E}_1$ and $\mathscr{E}_1 + \hbar\omega_L$ (dashed lines) on the confining frequency Ω of the lateral confining potential of the QWW: (a) calculated in RSPT; (b) in WBPT and (c) in IWBPT.

decreasing confining energy the contribution of the non-diagonal elements to the quasi-particle properties of the coupled electron–phonon system increases.

In Fig. 8(a) and Fig. 8(b) we show, respectively, the variations of ΔE_0 and ΔE_1 as functions of the polaron coupling constant α_p for the case $B = 0$ and $k_x = 0$ calculated with the three different perturbation theories. Obviously, for the RSPT this dependence is linear, while for the self-consistent WBPT the renormalization deviates from this line. This deviation is mainly caused by the α_p^2 term, which has, as mentioned above, the wrong sign. Please note that $\Delta E_0^{\mathrm{RSPT}} = \Delta E_0^{\mathrm{IWBPT}}$ and $\Delta E_1^{\mathrm{RSPT}} \neq \Delta E_1^{\mathrm{IWBPT}}$, but this difference is very small and not to be drawn in Fig. 8(b). Fig. 8(a) and Fig. 8(b) show that the here applied perturbation theories are valid for QWWs with $\alpha_p < 0.1$, i.e. especially for GaAs based QWWs.

The dependence of ΔE_0 and ΔE_1 on the confining frequency Ω of the QWW ($\alpha_p = 0.07$) is plotted in Fig. 9(a) and Fig. 9(b) for the three different weak-coupling perturbation theories under consideration for the case $B = 0$ and $k_x = 0$. The absolute value of the self-energies ΔE_0 and ΔE_1, i.e. the polaron binding energy, increases with increasing confining frequency. For vanishing confining frequency the 2D limit is realized with $\Delta E_{2D}^{\mathrm{RSPT}} = -3.977$ meV for RSPT and IWBPT and $\Delta E_{2D}^{\mathrm{WBPT}} = -3.850$ meV for WBPT. In the case of a finite lateral confining potential the results for the energy renormalization are given for $\hbar\Omega = 2$ meV in Table 1 and for $\hbar\Omega = 12$ meV the corresponding results are given in Table 2. For comparison, the 3D ground-state renormalization is $\Delta E_{3D}^{\mathrm{RSPT}} = -2.532$ meV, i.e. the energy renormalization increases with decreasing dimensionality. It is seen that the energy correction of the first excited level $\Delta E_1^{\mathrm{RSPT}}$, calculated with RSPT, diverges negatively at the resonance of $\mathscr{E}_1(\Omega)$ with $\mathscr{E}_0(\Omega) + 1$ appearing if $\Omega = \omega_L$.

The lowest two energy levels, both renormalized and unrenormalized, are shown in Fig. 10 as a function of the confining frequency Ω of the QWW. It is seen that for all three perturbation theories the renormalized levels E_0 are slightly below the unrenormalized one, $\mathscr{E}_0$. Further, the first excited level E_1 diverges negatively at $\Omega = \omega_L$ in the case of RSPT, approaches $\mathscr{E}_0 + 1$ for large Ω in WBPT, which is obviously above the threshold of the phonon continuum at $E_{th} = E_0 + 1$, but approaches the correct result $E_0 + 1$ for large Ω in IWBPT. This means that E_1 calculated in WBPT lies inside the phonon continuum, i.e. an obviously wrong result. Thus, we come to the conclusion that even for $B = 0$ and $k_x = 0$, RSPT and WBPT are only useful for QWWs with weak lateral confinement, i.e. for $\Omega \ll \omega_L$. Only IWBPT and its analogon, the MHFA, give the correct polaronic behaviour of the excited states for larger confining frequencies.

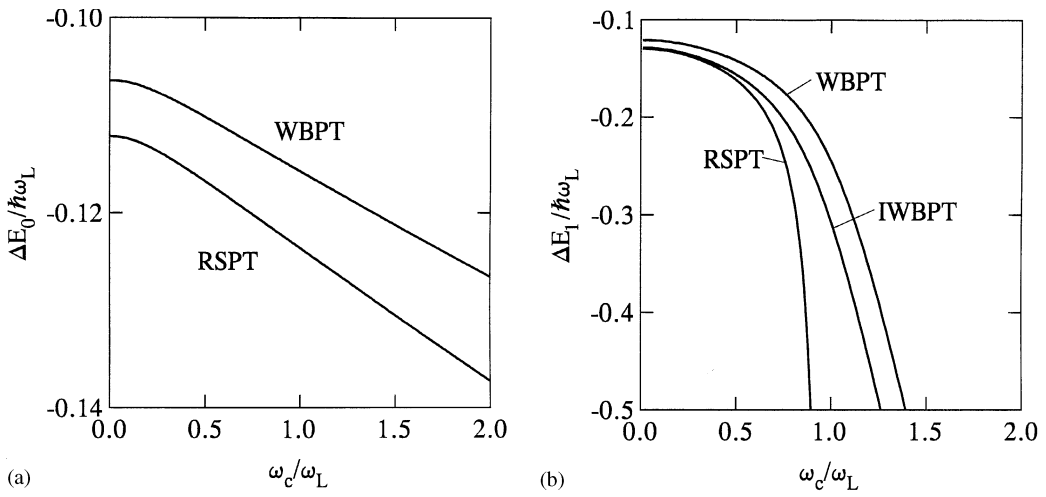

Fig. 11. The energy renormalizations ΔE_0 (a) and ΔE_1 (b) of the Q1D subbands $\mathscr{E}_0$ and $\mathscr{E}_1$, respectively, for $k_x = 0$ as a function of the magnetic field calculated in RSPT, WBPT and IWBPT. Please note that in (a) $\Delta E_0^{\mathrm{RSPT}} = \Delta E_0^{\mathrm{IWBPT}} \neq \Delta E_0^{\mathrm{WBPT}}$.

The dependence of the polaronic properties of QWWs on the magnetic field is investigated in Figs. 11–15. Here, and in the following the energy-momentum relations are plotted without the Zeeman energy. If it is necessary to include the spin, two different figures appear, one for spin up and the other for spin down electrons, i.e. one figure with energies all shifted down by the Zeeman energy and the other figure with energies all shifted up by the Zeeman energy. Note further that the spin splitting of the levels is very small compared to the subband separation of 12 meV under consideration, e.g. for $B_L = 20.7$ T, where $\omega_c = \omega_L$, we have $|g^*\mu_B B| = 0.527$ meV for GaAs, where $g^* = -0.44$.

In Fig. 11(a) and Fig. 11(b) are depicted the energy renormalization of the ground-state level and of the first excited level, ΔE_0 and ΔE_1, respectively, as functions of the magnetic field in the case of vanishing wave vector component $k_x = 0$. The behaviour of these quantities on the magnetic field is very similar but not identical to that on the confining frequency (cp. Fig. 9(a) and Fig. 9(b)). It is seen that the divergency of $\Delta E_1^{\mathrm{RSPT}}$ is slightly below $\omega_c = \omega_L$.

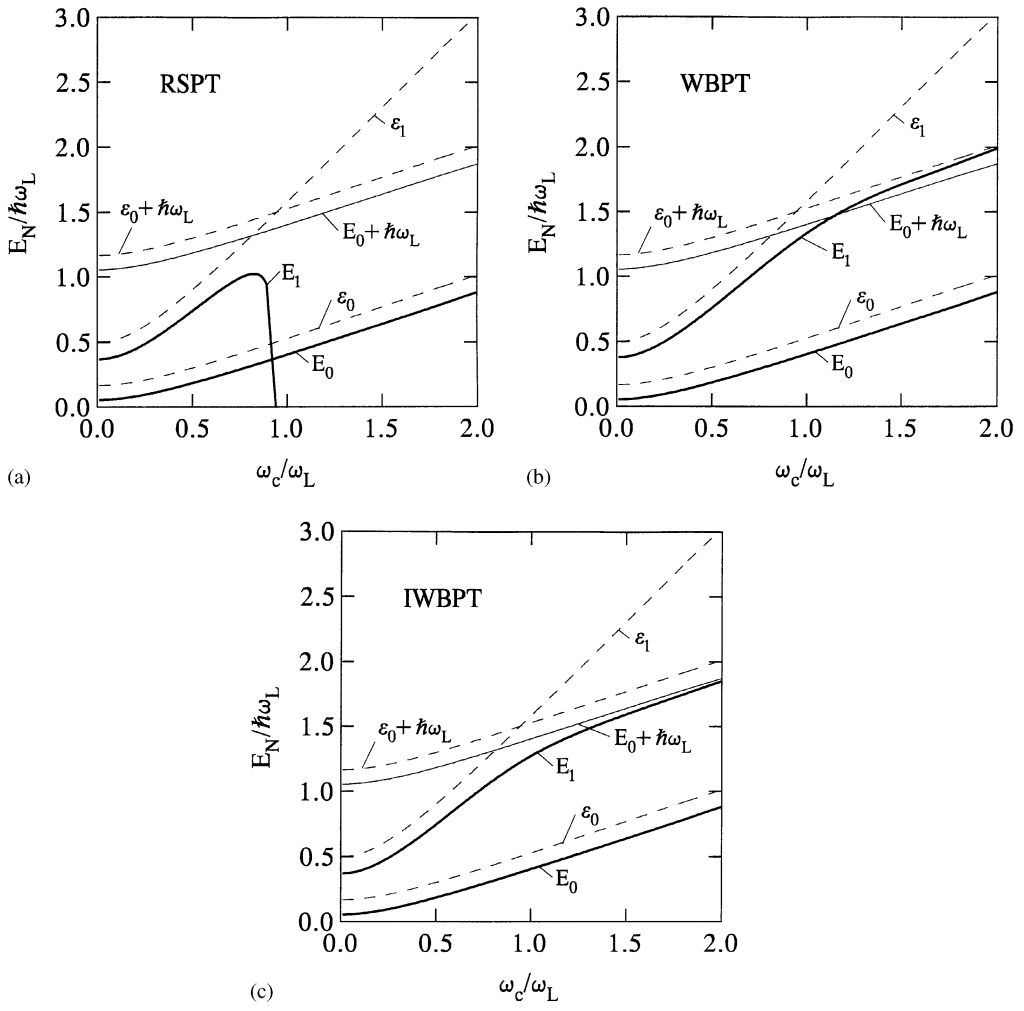

Fig. 12. Dependence of the renormalized levels E_0, E_1 (heavy solid lines) and $E_0 + \hbar\omega_L$ (thin solid line) and of the unrenormalized levels $\mathscr{E}_0$, $\mathscr{E}_1$ and $\mathscr{E}_1 + \hbar\omega_L$ (dashed lines) on the magnetic field: (a) calculated in RSPT; (b) in WBPT and (c) in IWBPT.

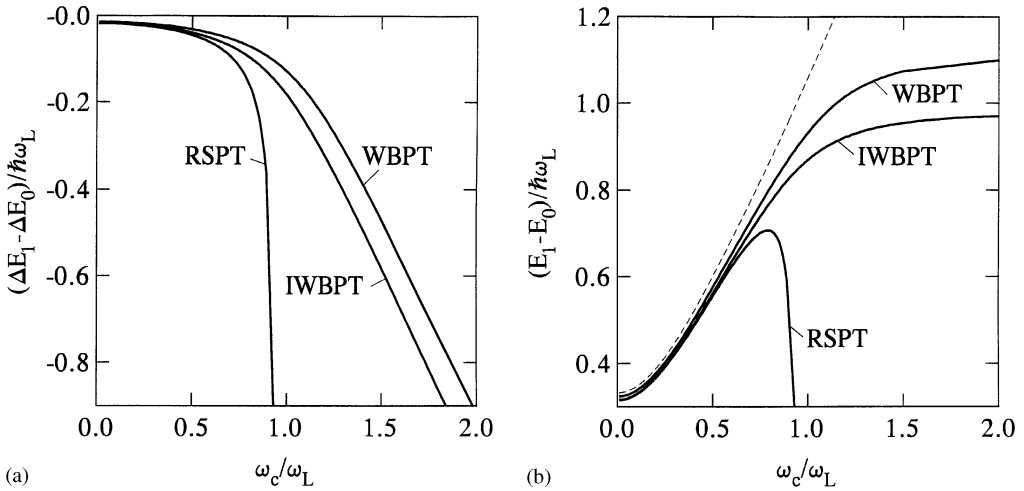

Fig. 13. Energy difference between the subband renormalization $\Delta E_1 - \Delta E_0$ (a), the energy levels $E_1 - E_0$ (heavy solid line) and $\mathscr{E}_1 - \mathscr{E}_0$ (thin dashed line) (b) of a QWW as a function of the magnetic field calculated in RSPT, WBPT and in IWBPT for $k_x = 0$.

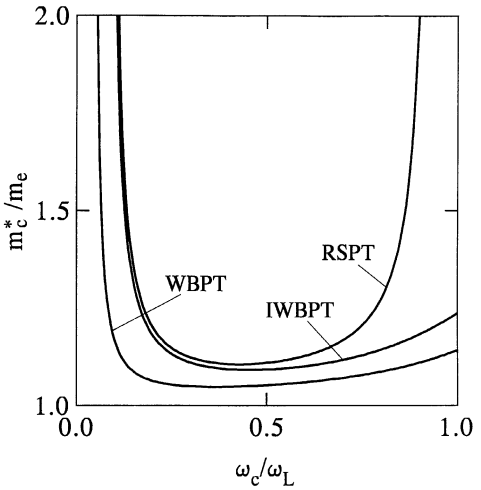

Fig. 14. Polaron cyclotron mass m_c^* of the Q1D magnetopolaron as a function of the magnetic field calculated from Eq. (34) for $N = 1$ using RSPT, WBPT and modified IWBPT.

The dependence of the first two renormalized and unrenormalized levels on the magnetic field is plotted in Fig. 12 for $k_x = 0$. Again E_0 is slightly below the unrenormalized ground-state energy $\mathscr{E}_0$. If calculated in RSPT, E_1 diverges negatively at the resonance, which appears in dependence on the confining frequency below $\omega_c = \omega_L$ and E_1 approaches for large magnetic fields $\mathscr{E}_0 + 1$ if calculated in WBPT, i.e. the pinning appears at the wrong energy inside the phonon continuum. Only the IWBPT gives the correct pinning of E_1 for large magnetic fields at the threshold of the one-phonon continuum, i.e. at the correct ground state plus one LO phonon: $E_0 + 1$.

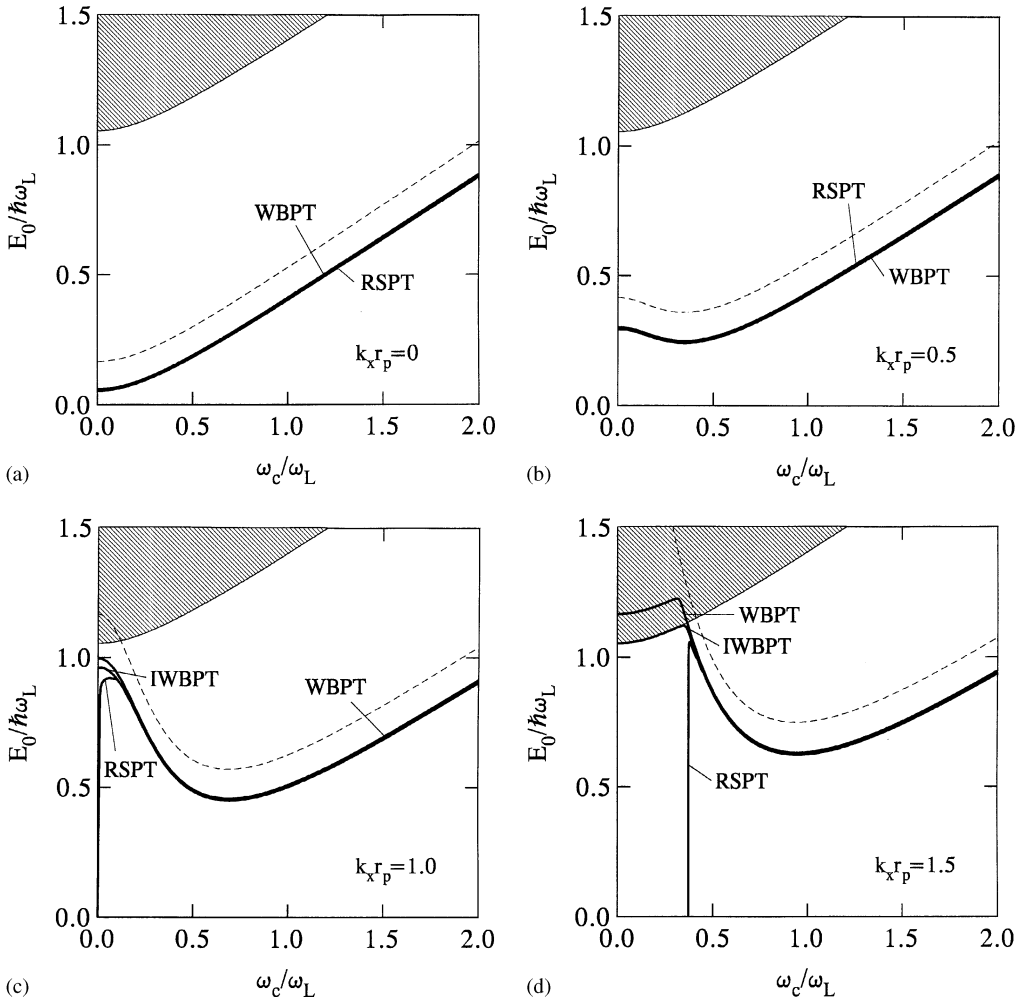

Fig. 15. The lowest Q1D magnetopolaron level $E_0(k_x;B)$ (heavy solid line) as a function of the magnetic field for different magnetopolaron momenta ($k_x^{pol} = k_x$): (a) $k_xr_p = 0$; (b) $k_xr_p = 0.5$; (c) $k_xr_p = 1.0$ and (d) $k_xr_p = 1.5$. The corresponding unperturbed dispersion relation $\mathscr{E}_0(k_x;B)$ is plotted by the dashed line. Please note that in (a) $\Delta E_0^{RSPT} = \Delta E_0^{IWBPT} \neq \Delta E_0^{WBPT}$, but in (b)–(d) $\Delta E_0^{RSPT} \neq \Delta E_0^{IWBPT} \neq \Delta E_0^{WBPT}$ (difference in (a) and (b) not to be drawn). The renormalized one-phonon continuum is shown by the hatched area.

From these figures we can extract the differences $\Delta E_1 - \Delta E_0$ and $E_1 - E_0$, important for the calculation of the polaron cyclotron mass m_c^* defined in Eq. (34). It becomes obvious from Fig. 13(a) that the difference $\Delta E_1(0) - \Delta E_0(0)$ becomes a negative constant for $B \to 0$ and the absolute value of this quantity increases with increasing magnetic field. Fig. 13(b) shows the difference $E_1(0) - E_0(0)$ of the renormalized levels for $k_x = 0$ as a function of the magnetic field. While for RSPT this quantity diverges negatively at the resonance of the first excited level with the ground state plus one LO phonon, the energy differences of the WBPT and IWBPT are increasing functions with increasing magnetic field.

It was shown [29] that for QWWs the polaron cyclotron mass m_c^* increases with decreasing magnetic field for small magnetic fields due to the geometrical confinement and has a minimum at a finite value of the magnetic field. For larger magnetic fields, m_c^* increases with increasing magnetic field. This behaviour is shown in Fig. 14. The unusual increase of the polaron cyclotron mass m_c^* with decreasing magnetic field for

small magnetic fields can be understood from Eq. (34), which reads in polaronic units

$$\frac{m_c^*}{m_e} = \frac{\lambda^2\gamma}{\sqrt{(\lambda^2\gamma)^2 + 2\lambda^2[\Delta E_1(0) - \Delta E_0(0) + [\Delta E_1(0) - \Delta E_0(0)]^2}}, \tag{155}$$

if we expand $\Delta E_1(0) - \Delta E_0(0)$ in a power series of ω_c/ω_L. In RSPT it follows:

$$\Delta E_1^{\mathrm{RSPT}}(0) - \Delta E_0^{\mathrm{RSPT}}(0) = -\alpha_p \frac{2}{\sqrt{\pi\eta}}\left[\int_0^\infty \mathrm{d}t\, \frac{\mathrm{e}^{-t/\eta}}{t} \frac{\sinh^2(t/2)}{\sqrt{\mathrm{e}^{-t}+t-1}} \boldsymbol{K}'\left(\sqrt{\frac{\mathrm{e}^{-t}+t-1}{t}}\right) + \mathcal{O}\left(\left(\frac{\omega_c}{\omega_L}\right)^2\right)\right], \tag{156}$$

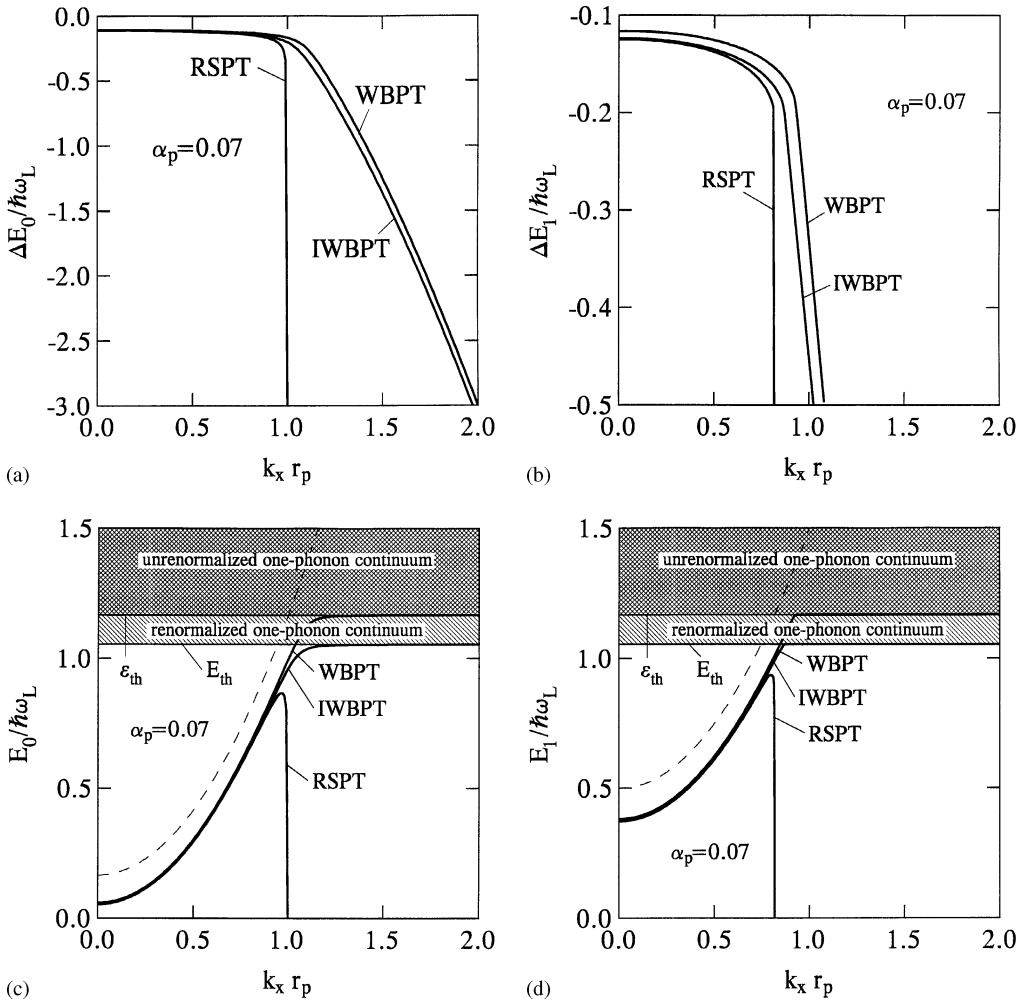

Fig. 16. The energy renormalizations ΔE_0 (a) and ΔE_1 (b) of the Q1D subbands $\mathscr{E}_0$ and $\mathscr{E}_1$, respectively, for $B = 0$ and $\alpha_p = 0.07$ as a function of wave vector component k_x calculated in RSPT, WBPT and IWBPT. In (c) is plotted the energy–momentum relation of the lowest renormalized level E_0 (heavy solid line) and in (d) is shown that of the first excited renormalized level E_1 (heavy solid line). The corresponding unperturbed dispersion relations $\mathscr{E}_0(k_x; B)$ and $\mathscr{E}_1(k_x; B)$ are plotted by the dashed lines. The hatched areas are the renormalized and the unrenormalized phonon continua.

where $\eta = \Omega/\omega_L$. Because $\Delta E_1(0) - \Delta E_0(0)$ approaches a negative constant for $\gamma \to 0$, $\lambda^2 \to \Omega/\omega_L$ (cp. Fig. 13(a)), the polaron cyclotron mass diverges in this limit. Quite generally, if one measures the transition between two levels of a semiconductor nanostructure having for vanishing magnetic field different level shifts, the corresponding polaron cyclotron mass diverges in this limit [37]. A similar behaviour of the polaron cyclotron mass was found for heterostructures with triangular QWs, when including the conduction-band nonparabolicity [70]. In both cases the polaron cyclotron mass itself is not a very convenient measure of the polaronic effects for small magnetic fields.

The magnetic field dependence of the lowest subband including the magnetopolaronic corrections is plotted in Fig. 15 for different magnetopolaron momenta $\hbar k_x^{pol} = \hbar k_x$. The hatched area in this figure is the

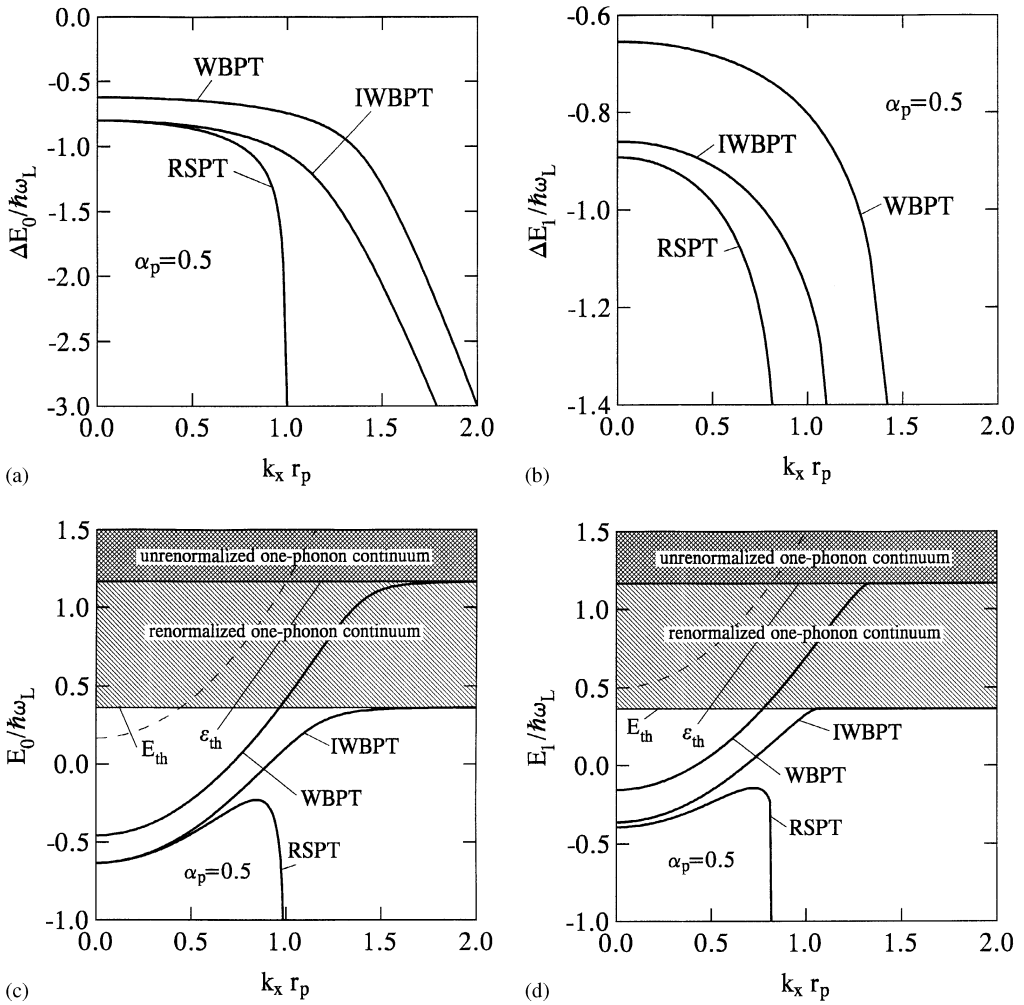

Fig. 17. The energy renormalizations ΔE_0 (a) and ΔE_1 (b) of the Q1D subbands $\mathscr{E}_0$ and $\mathscr{E}_1$, respectively, for $B = 0$ and $\alpha_p = 0.5$ as a function of wave vector component k_x calculated in RSPT, WBPT and IWBPT. In (c) is plotted the energy–momentum relation of the lowest renormalized level E_0 (heavy solid line) and in (d) is shown that of the first excited renormalized level E_1 (heavy solid line). The corresponding unperturbed dispersion relations $\mathscr{E}_0(k_x;B)$ and $\mathscr{E}_1(k_x;B)$ are plotted by the dashed lines. The hatched areas are the renormalized and the unrenormalized phonon continua.

renormalized phonon continuum. It is seen from Fig. 15 that for vanishing magnetopolaron momentum the energy $E_0 = E_0(k_x = 0; B)$ increases with increasing magnetic field (Fig. 15(a)), but the self-energy (cp. Fig. 11(a)) only weakly depends on the magnetic field. For a finite magnetopolaron momentum the curves $E_0(k_x \neq 0;B)$ have a minimum at $B \neq 0$ (Fig. 15(b)). This minimum results from the fact that with increasing magnetic field the effective mass $\tilde{m}_e$ increases, $\tilde{m}_e \to \infty$ for $B \to \infty$, and thus, the kinetic energy *decreases*, whereas the confining energy $\hbar\tilde{\omega}_c$ *increases*. Please note that in Fig. 15(a) $\Delta E_0^{RSPT} = \Delta E_0^{IWBPT} \neq \Delta E_0^{WBPT}$, but in Fig. 15(b)–Fig. 15(d) $\Delta E_0^{RSPT} \neq \Delta E_0^{IWBPT} \neq \Delta E_0^{WBPT}$ (difference in (a) and (b) not to be drawn). Further, in Fig. 15(c) and Fig. 15(d) it is assumed that the kinetic energy of the unperturbed electron in subband $N = 0$ is so large that $\mathscr{E}_0(k_x;B = 0)$ lies within the phonon continuum. As mentioned above a resonance of $\mathscr{E}_0(k_x;B)$ with

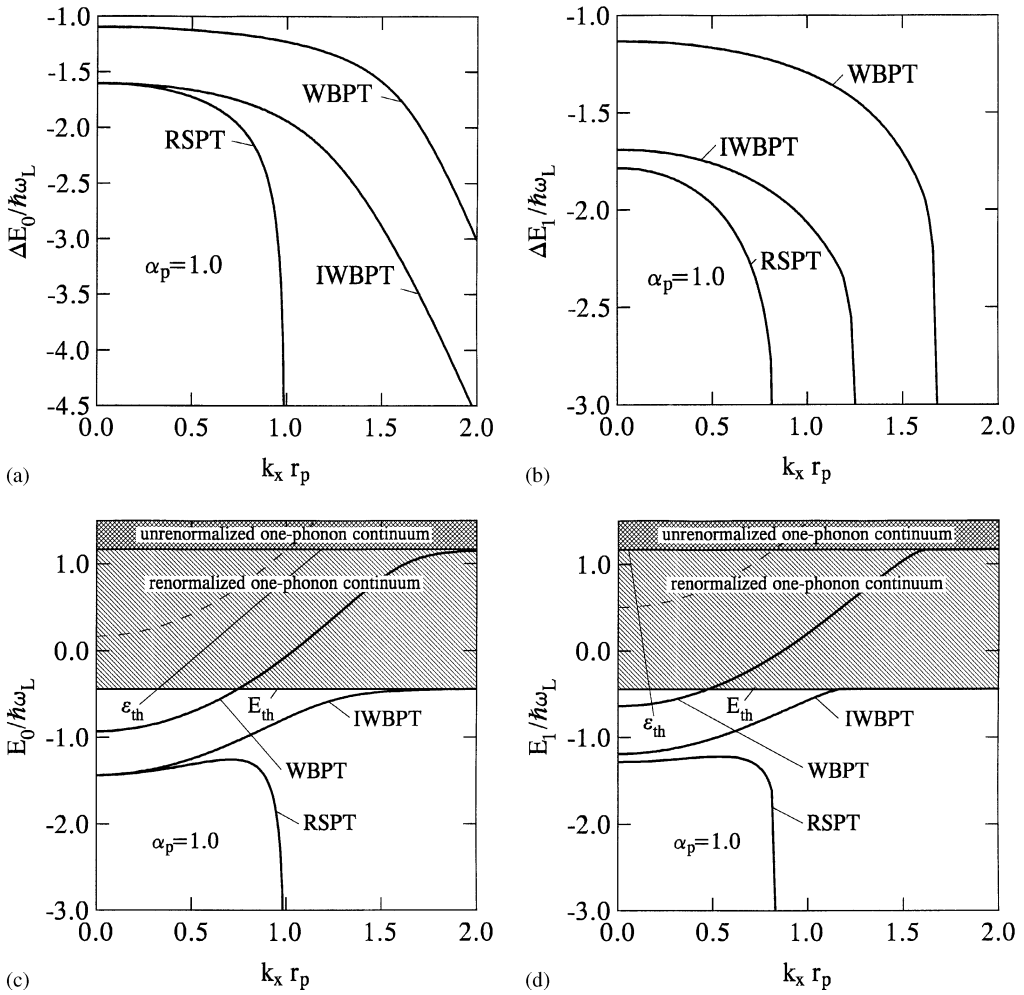

Fig. 18. The energy renormalizations ΔE_0 (a) and ΔE_1 (b) of the Q1D subbands $\mathscr{E}_0$ and $\mathscr{E}_1$, respectively, for $B = 0$ and $\alpha_p = 1.0$ as a function of wave vector component k_x calculated in RSPT, WBPT and IWBPT. In (c) is plotted the energy–momentum relation of the lowest renormalized level E_0 (heavy solid line) and in (d) is shown that of the first renormalized excited level E_1 (heavy solid line). The corresponding unperturbed dispersion relations $\mathscr{E}_0(k_x; B)$ and $\mathscr{E}_1(k_x; B)$ are plotted by the dashed lines. The hatched areas are the renormalized and the unrenormalized phonon continua.

$\mathscr{E}_0(0; B) + 1$ is only possible for $k_x \geqslant 1$ and occurs at $\omega_c = \omega^{(0)} = \Omega\sqrt{k_x^2 - 1}$. Thus, for the chosen values of k_x this resonance occurs at $B = 0$ in Fig. 15(c) and at $B > 0$ in Fig. 15(d). The EPI will result in a shift of the magnetopolaron dispersion curve below the phonon continuum. This is valid for all polaron coupling strengths and thus, is a special feature of the resonance of a discrete state with a continuum of states. It is seen that for larger magnetic fields the RSPT result exists and approaches the value for the energy of the renormalized ground state of the two other perturbation theories. This is true because the resonant wave vector $k_L^{(0)} = 1/(1 - \gamma^2)$ is 1 for $B = 0$ but becomes infinite for large magnetic fields. Thus, for a given wave vector $k_x \geqslant 1$ and magnetic fields $\omega_c > \omega_c^{(0)}$ one is below the resonance.

In Fig. 16(a) and Fig. 16(b) we show the wave-vector dependence of the self-energies $\Delta E_0(k_x)$ and $\Delta E_1(k_x)$ for $B = 0$ and $\alpha_p = 0.07$. It is seen that with increasing momentum the absolute values of the self-energies increase, $\Delta E_0^{\mathrm{RSPT}}(k_x)$ and $\Delta E_1^{\mathrm{RSPT}}(k_x)$ diverge negatively at $k_x = k_L^{(0)} = 1$ and $k_x = k_L^{(1)} = \sqrt{1 - \Omega/\omega_L}$, respectively. The energy–momentum relation of the Q1D polarons in subbands $N = 0$ and $N = 1$ is plotted in Fig. 16(c) and Fig. 16(d) for $B = 0$ and $\alpha_p = 0.07$. It is seen that the RSPT dispersion curves diverge negatively at $k_x = k^{(N)}$, the WBPT dispersion curves bend over and become pinned at the threshold of the unrenormalized one-phonon continuum, $\mathscr{E}_{th} = \mathscr{E}_0(0) + 1$ and only the IWBPT dispersion curves show the correct pinning at the threshold of the renormalized one-phonon continuum $E_{th} = E_0(0) + 1$. The same quantities are plotted in Fig. 17 for $\alpha_p = 0.5$ and in Fig. 18 for $\alpha_p = 1.0$. Obviously, with increasing polaron coupling constant the renormalization of the energy levels increases, which "smoothens" the dispersion curves, i.e. the dispersion decreases. Further, the WBPT becomes more and more incorrect with increasing α_p even for small momenta.

The energy–momentum relation of the Q1D magnetopolarons in the lowest subband $E_0 = E_0(k_x; B)$ is plotted in Fig. 19(a) and Fig. 19(b) for different magnetic field strengths (cp. Fig. 16(c) for $B = 0$). It can be seen from these figures that the magnetopolaron dispersion curve $E_0(k_x)$ bends over at the threshold $E_{th} = E_0(0) + 1$. The bend-over region shifts to higher magnetopolaron momenta with increasing magnetic field (Figs. 16(c), 19(a) and (b)). A magnetopolaron with energy–momentum relation $E_0(k_x)$ calculated in IWBPT as plotted in Figs. 16–19 cannot emit at $T = 0$ a real LO phonon, because of the finite energy difference between $E_0(k_x)$ and E_{th}. In real systems, however, the energy levels are broadened due to impurity

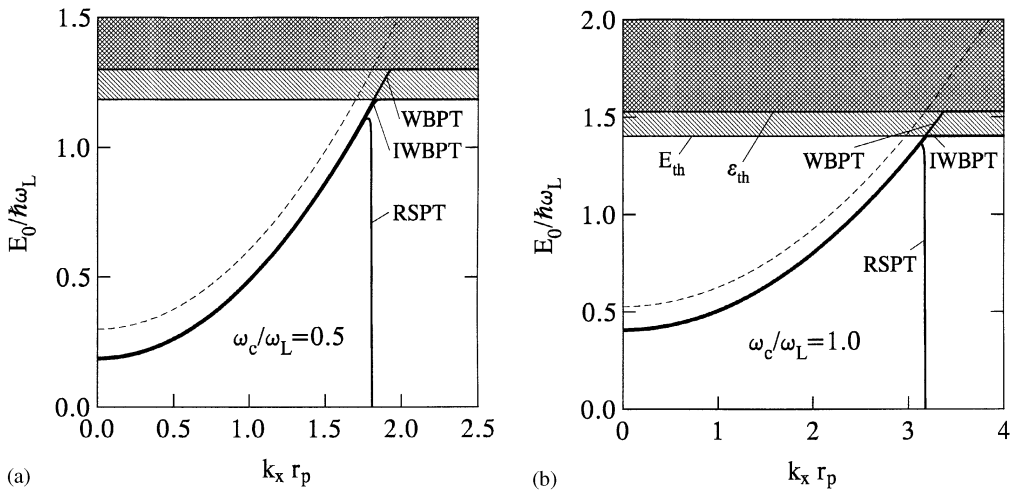

Fig. 19. Energy–momentum relation for Q1D magnetopolarons $E_0(k_x; B)$ in the lowest level (heavy solid line) calculated for different magnet-field strengths: (a) $\omega_c/\omega_L = 0.5$ and (b) $\omega_c/\omega_L = 1.0$. The corresponding unperturbed dispersion relation $\mathscr{E}_0(k_x; B)$ is plotted by the dashed line. The renormalized and the unrenormalized one-phonon continua are shown by the hatched areas above E_{th} and $\mathscr{E}_{th}$, respectively.

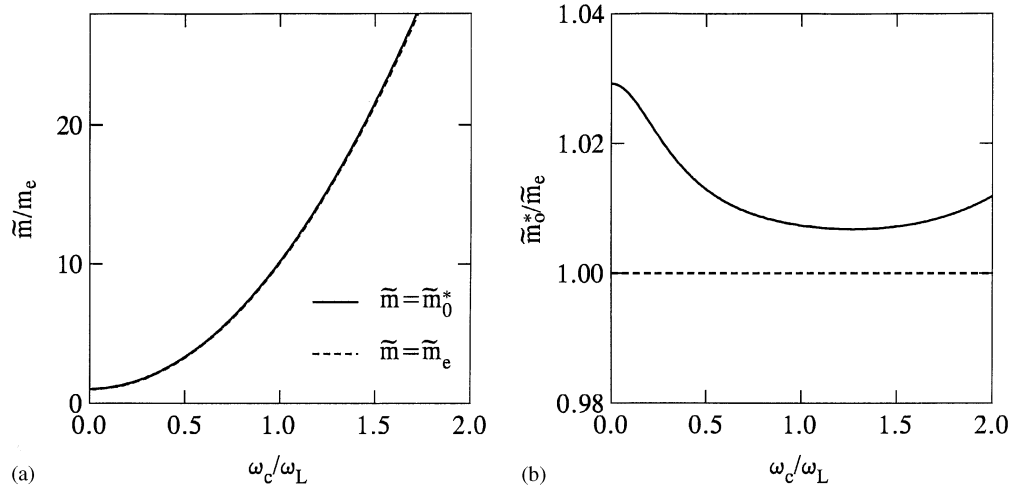

Fig. 20. Magnetopolaron effective mass of the lowest subband $\tilde{m}_0^*$ as a function of the magnetic field (heavy solid line) calculated in IWBPT: (a) $\tilde{m}_0^*/m_e$ and (b) $\tilde{m}_0^*/\tilde{m}_e$. The magnetic-field dependent non-interacting effective mass $\tilde{m}_e$ is shown by the dashed line.

scattering processes also below the phonon continuum. Then, it could be possible that the magnetopolaron emits a real LO phonon if the energy is large enough. After emitting this phonon the magnetopolaron relaxes to the subband minimum. It was shown for the case $B = 0$ [31] that this process results in an oscillation of the electron group velocity if an electric field is applied along the wire. In the high-field magnetotransport, which is essentially ballistic in GaAs–$Ga_{1-x}Al_xAs$ QWWs, these electron velocity oscillations should be measurable.

The magnetopolaron effective mass of the lower subband, calculated from Eq. (33) or equivalently from Eq. (122), is plotted in Fig. 20(a). For smaller magnetic fields this mass has nearly the same dependence on the magnetic field as $\tilde{m}_e$. The effective mass $\tilde{m}_N^*$ defined in Eq. (33) is quite different from the polaron cyclotron mass m_c^* defined in Eq. (34). In polaronic units Eq. (33) takes on the form

$$\frac{\tilde{m}_0^*}{m_e} = \frac{1}{1-\gamma^2 + (1/(2k_x))(\mathrm{d}/\mathrm{d}k_x)\Delta E_0(k_x)|_{k_x\to 0}} \tag{157}$$

and obviously, we have $\tilde{m}_e/m_e = 1/(1-\gamma^2)$. The second summand in the denominator is negative for $B = 0$ and approaches zero for large magnetic fields. Because $1-\gamma^2 = 1$ for $B = 0$ and 0 for $B = \infty$, $\tilde{m}_0^*/m_e$ grows with magnetic field somewhat slower than $\tilde{m}_e/m_e$. In Fig. 20(b) the quotient $\tilde{m}_0^*/\tilde{m}_e$ is plotted. This quotient decreases for smaller magnetic fields with increasing magnetic field because in this range $1-\gamma^2$ tends to zero more slowly than $\frac{1}{2k_x}\frac{\mathrm{d}}{\mathrm{d}k_x}\Delta E_0(k_x)|_{k_x\to 0}$. For larger magnetic fields this mass quotient increases with increasing magnetic field.

6. Summary and conclusions

We have presented a theory of the quasi-particle properties of the coupled electron–phonon system in QWWs in the presence of a quantizing magnetic field. The energy–momentum relation (dispersion relation) for magnetopolarons is calculated in detail in the subband space. Three different "old-fashioned"

perturbation theories, RSPT, WBPT and the modified IWBPT are investigated and compared with different results of the diagrammatic approach of Green's function theory, TDA, TDA on mass-shell and the MHFA. It is shown that the Green's function technique results in additional contributions from intersubband processes, not described by the standard perturbation theories. Whereas RSPT and TDA on mass-shell well describe the ground-state renormalization, these approaches fail to describe the pinning of the dispersion curves at the boundary of the one-phonon continuum. This behaviour is only well described by the modified IWBPT and HFA. Again, the last approach contains intersubband contributions absent in modified IWBPT. Further, TDA and TDA on-mass shell fail for the calculation of the renormalization of the excited subband energies in QWWs with strong lateral confining potential even for vanishing magnetic field and polaron momentum. Thus, it becomes obvious that the modified IWBPT and especially the MHFA are the simplest procedures to obtain in a suitable way the correct results for the magnetopolaronic properties below E_{th} for all B, k_x and confining potentials of the QWW. Green's function technique applied to the magnetopolaron problem in QWWs has some advantages over the orthodox perturbation theories:

1. In low-dimensional electron systems Green's function technique includes in a natural way all the real and virtual scattering processes within one and between different subbands.
2. It simply allows the calculation of damping (energy broadening) by calculating the imaginary part of the self-energy, e.g. important when calculating the magnetopolaron levels inside the phonon continuum.
3. The modified HFA allows to calculate the magnetopolaron energy–momentum relation $E_N(k_x; B)$ for all subbands, momenta and magnetic fields for QWWs with any strong lateral confinement, where all intersubband scattering processes become important.

The here developed theory generalizes our earlier work on Q1D polarons [31] to magnetopolarons described in the framework of Green's function technique. The analytic results are valid for all temperatures and arbitrary magnetic field strength. The here developed theory modifies both IWBPT and HFA to the Q1D magnetopolaron problem and gives the correct bend-over and pinning behaviour of the dispersion curves for all subbands at the boundary of the one-phonon continuum. It is shown that compared with the exact HFA the MHFA drastically simplifies the calculation and gives highly accurate results, which slightly underestimate the EPI self-energy.

Possible improvements on these results for future work would be:

1. To use the correct spectrum of the long-wavelength optical phonons, i.e. modified LO phonons and interface phonons.
2. To consider the different intersubband processes, i.e. go beyond the diagonal approximation.
3. To include the conduction-band nonparabolicity (*band-structure effect*).
4. To include a possible nonparabolicity of the lateral confining potential.
5. To include the finite width of the QWW in growth direction (*wave-function* and *subband effect*).
6. If many electrons are present, to include *occupation* and *screening effects*.

Further, in future work, special attention should be directed to the magnetopolaron states above the threshold of the one-phonon continuum. The here developed theory can be successfully applied to the above mentioned problems.

References

[1] L.D. Landau, Z. Phys. Sowj. 3 (1933) 644.
[2] H. Fröhlich, Proc. Roy. Soc. A 160 (1937) 230.
[3] S. Pekar, Zh. Eksp. Teor. Fiz. 16 (1946) 335.
[4] L.D. Landau, S. Pekar, Zh. Eksp. Teor. Fiz. 16 (1946) 341.

[5] S. Pekar, Untersuchungen über die Elektronentheorie der Kristalle, Akademie Verlag, Berlin, 1954.
[6] H. Fröhlich, H. Pelzer, S. Zienau, Phil. Mag. 41 (1950) 221.
[7] H. Fröhlich, Adv. Phys. 3 (1954) 325.
[8] C. Kuper, G. Whitfield (Eds.), Polarons and Excitons, Oliver & Boyd, Edinburgh, 1963.
[9] J.T. Devreese (Ed.), Polarons in Ionic Crystals and Polar Semiconductors, North-Holland, Amsterdam, 1972.
[10] G. Whitfield, R. Puff, Phys. Rev. 139 (1965) A338.
[11] D.M. Larsen, Phys. Rev. 144 (1966) 697.
[12] F.M. Peeters, J.T. Devreese, Phys. Rev. B 31 (1985) 3689.
[13] D.M. Larsen, in: J.T. Devreese (Ed.), Polarons in Ionic Crystals and Polar Semiconductors, North-Holland, Amsterdam, 1972, p. 237.
[14] I.B. Levinson, E.I. Rashba, Usp. Fiz. Nauk. 111 (1973) 683 [Sov. Phys. Usp. 16 (1974) 892].
[15] R. Haupt, L. Wendler, Solid State Commun. 89 (1994) 741.
[16] E.S. Hellman, J.S. Harris, Phys. Rev. B 33 (1986) 8284.
[17] S. Das Sarma, A. Madhukar, Phys. Rev. B 22 (1980) 2823.
[18] D. Larsen, Phys. Rev. B 30 (1984) 4595.
[19] R. Lassnig, W. Zawadzki, Surf. Sci. 142 (1984) 388.
[20] S. Das Sarma, D. Mason, Ann. Phys. (NY) 163 (1985) 78.
[21] R. Haupt, L. Wendler, Ann. Phys. (NY) 233 (1994) 214.
[22] R. Haupt, L. Wendler, Z. Phys. B 94 (1994) 49.
[23] R. Haupt, L. Wendler, Semicond. Sci. Technol. 9 (1994) 803.
[24] J.-J. Shi, X.-Q. Zhu, Z.-X. Liu, S.-H. Pan, X.-Y. Li, Phys. Rev. 55 (1997) 4670.
[25] Y.J. Wang, H.A. Nickel, B.D. McCombe, F.M. Peeters, J.M. Shi, G.Q. Hai, X.-G. Wu, T.J. Eustis, W. Schaff, Phys. Rev. Lett. 79 (1997) 3226.
[26] M.H. Degani, O. Hipólito, Phys. Rev. 35 (1987) 9345.
[27] M.H. Degani, O. Hipólito, Solid State Commun. 65 (1988) 1185.
[28] H.Y. Zhou, K.-D. Zhu, S.-W. Gu, J. Phys.: Condens. Matter 4 (1992) 4613.
[29] L. Wendler, A.V. Chaplik, R. Haupt, O. Hipólito, J. Phys.: Condens. Matter 5 (1993) 4817.
[30] G.Q. Hai, T.M. Peeters, J.T. Devreese, L. Wendler, Phys. Rev. B 48 (1993) 12 016.
[31] L. Wendler, R. Kügler, J. Phys.: Condens. Matter 6 (1994) 7857.
[32] L. Wendler, R. Kügler, R. Haupt, in: D. Heiman (Ed.), Proc. 11th Int. Conf. on High Magnetic Fields in the Physics of Semiconductors, World Scientific, Singapore, 1995, p. 520.
[33] E.P. Pokatilov, S.N. Klimin, S.N. Balaban, V.M. Fomin, Phys. Stat. Sol. (b) 189 (1995) 433.
[34] C. Ammann, M.A. Dupertuis, U. Bockelmann, B. Deveaud, Phys. Rev. B 55 (1997) 2420.
[35] C.R. Bennett, K. Güven, B. Tanatar, Phys. Rev. B 57 (1998) 3994.
[36] L. Wendler, Phys. Rev. B 57 (1998) 9214.
[37] L. Wendler, A.V. Chaplik, R. Haupt, O. Hipólito, J. Phys.: Condens. Matter 5 (1993) 8031.
[38] D. Larsen, Phys. Rev. B 30 (1984) 4807.
[39] S. Das Sarma, Phys. Rev. Lett. 52 (1984) 895.
[40] F.M. Peeters, W. Xiaoguang, J.T. Devreese, Phys. Rev. B 33 (1986) 4338.
[41] S. Das Sarma, Phys. Rev. B 27 (1983) 2590.
[42] F.M. Peeters, P. Warmenbol, J.T. Devreese, Europhys. Lett. 3 (1987) 1219.
[43] L. Wendler, Phys. Stat. Sol. (b) 129 (1985) 513.
[44] M.A. Stroscio, Phys. Rev. B 40 (1989) 6428.
[45] N.C. Constantinou, B.K. Ridley, Phys. Rev. B 41 (1990) 10 627.
[46] M.A. Stroscio, K.W. Kim, M.A. Littlejohn, H. Chuang, Phys. Rev. B 42 (1990) 1488.
[47] K.-D. Zhu, S.-W. Gu, J. Phys.: Condens. Matter 4 (1992) 1291.
[48] D.A. Knipp, T.L. Reinecke, Phys. Rev. B 45 (1992) 9091.
[49] D.A. Knipp, T.L. Reinecke, in: G. Abstreiter (Ed.), Proc. 6th Int. Conf. on Modulated Semiconductor Structures (MSS-6), Garmisch-Partenkirchen, Germany, 1993, p. 783.
[50] B. Tanatar, K. Güven, C.R. Bennett, N.C. Constantinou, Phys. Rev. B 53 (1996) 10 866.
[51] D. Childes, P. Pincus, Phys. Rev. 177 (1969) 1036.
[52] G. Lindemann, R. Lassnig, W. Seidenbusch, E. Gornik, Phys. Rev. B 28 (1983) 4693.
[53] D.M. Larsen, E.J. Johnson, J. Phys. Soc. Japan 21 (Suppl.) (1966) 443.
[54] F.M. Peeters, Wu Xiaoguang, J.T. Devreese, Phys. Rev. B 34 (1986) 1160.
[55] J.T. Devreese, F.M. Peeters, Solid State Commun. 58 (1986) 861.
[56] I.S. Gradshteyn, I.M. Ryzhik, Table of Integrals, Series, and Products, Academic Press, New York, 1980, No. 7.377.
[57] I.S. Gradshteyn, I.M. Ryzhik, Table of Integrals, Series, and Products, Academic Press, New York, 1980, No. 3.754(2).

[58] L. Wendler, V.G. Grigoryan, Phys. Rev. B 54 (1996) 8652.
[59] D.M. Larsen, Phys. Rev. 142 (1966) 428.
[60] I.S. Gradshteyn, I.M. Ryzhik, Table of Integrals, Series, and Products, Academic Press, New York, 1980, No. 3.323(2).
[61] A.P. Prudnikov, Yu.A. Brychkov, O.I. Marishev, Integrals and Series: Special Functions, Nauka, Moscow, 1983, No. 2.19.14(8) (in Russian).
[62] I.S. Gradshteyn, I.M. Ryzhik, Table of Integrals, Series, and Products, Academic Press, New York, 1980, No. 3.312(1).
[63] I.S. Gradshteyn, I.M. Ryzhik, Table of Integrals, Series, and Products, Academic Press, New York, 1980, No. 3.361(2) and No. 2.612(1).
[64] J. Sak, Phys. Rev. B 6 (1972) 3981.
[65] A.A. Abrikosov, L.P. Gorkov, I.E. Dzyaloshinski, Methods of Quantum Field Theory in Statistical Physics, Dover, New York, 1963.
[66] A.L. Fetter, J.D. Walecka, Quantum Theory of Many Particle Systems, McGraw-Hill, New York, 1971.
[67] G.D. Mahan, Many-Particle Physics, Plenum Press, New York, 1981.
[68] L. Wendler, R. Pechstedt, Phys. Stat. Sol. (b) 138 (1986) 197.
[69] L. Wendler, R. Haupt, R. Pechstedt, Phys. Rev. B 43 (1991) 14 669.
[70] W. Zawadzki, Solid State Commun. 56 (1985) 43.